CHA1 in Management of Triple-Negative Breast Cancer

A thesis submitted by

Mariam Alamoudi

in partial fulfillment of the requirements for the degree of

PhD

in

Pharmacology and Experimental Therapeutics

Tufts University

Graduate School of Biomedical Sciences

May 2022

Advisor: Amy S. Yee, PhD

Abstract

Triple negative breast cancer (TNBC) is an aggressive subtype of breast cancer that is defined by the markers that it lacks. Specifically, TNBC does not express estrogen (ER) receptors, progesterone (PR) receptors, and does not have overexpressed HER2 receptors. TNBC is associated with poor prognosis and metastasis. Wnt/β-catenin signaling promotes many cancer processes such as maintenance of cancer stem cells, the epithelial-mesenchymal transition (EMT), and more recently escape from immune surveillance. Wnt signaling is active in TNBC, contributing to high rates of relapse and resistance to immune therapy. Based on molecular mechanisms of Wnt signaling, we designed a combinatorial therapy (termed CHA1) comprised of epigallocatechin-gallate (EGCG) and decitabine (DAC) to inhibit Wnt signaling. As predicted, CHA1 was effective at inhibiting Wnt signaling and growth in TNBC human xenograft and TNBC syngeneic models. However, upon investigation of the CHA1 mechanism, we also discovered that CHA1 reversed tumor EMT, increased tumor antigen presentation, activated interferon signaling, including induction of viral mimicry, JAK phosphorylation of STAT3, and upregulation of interferon-stimulated genes. In addition, CHA1 elevated tumor PD-L1 expression and induced a gene signature characteristic of T-cell inflammation. These broad tumor responses were fully dependent on the combination of the two compounds, as either of them alone was less effective than in combination. Furthermore, we observed alterations in tumor-infiltrating immune cells such as decreased Treg cells, as well as increased infiltration of IFNγ-secreting $Ki67^{+}CD8^{+}$ T cells, macrophages and NK cell activation including perforin and granzyme B expression. Finally, CHA1 in combination with anti-PD-L1 was significantly more effective at

inhibiting tumor growth and prolonged tumor-bearing mouse survival. These results demonstrate that CHA1, by inhibiting Wnt signaling, broadly reprograms tumors and alters the immune landscape. A clinical application of our findings is an opportunity to enhance susceptibility to immunotherapies and open up new treatment options for patients with breast and other cancers.

Acknowledgements

First of all, I would like to thank God for giving me the strength during my weak moments and for giving me the understanding to reach this goal, without God help none of this would have been possible.

Second, I would like to thank my advisor Dr. Amy Yee for the trust placed in me and in this project and for sharing her knowledge with me. Special thanks to Dr. Amy Yee for help me to participate and attend scientific conferences. Also, I would like to thank my co-advisor Dr. Eric Paulson for all his endless help, support, advice, and assistance to run the experiments.

Thank you to my committee chair Dr. James Baleja and my committee member Dr. David Greenblatt for their all guidance and support during my PhD study. Special thanks to Dr. Alain Charest for accepting to be my external examiner.

Also, thank you to the program director of Pharmacology and Experimental Therapeutics (PPET) Dr. Emanuel Pothos for his help and support during this journey. I also would like to thank all PPET faculty for their effort to help whenever I need assistance. My thanks are extended to the Dean Dr. Daniel Jay and the Associate Dean Dr. Daniel Volchok for their help and assistance during my stay at Tufts.

I would like to express my gratitude to breast cancer project team for their valuable help and input in the project. Special thanks to Francesca DeIeso-Frechette who worked with me for 3 years in the project. I also would like to thank Mollie Chipman for her help in bioinformatic analysis and for help in design and validate the human primers. My thanks also to Kaiqi Li who helped in the project specially in conducting the animal experiment of human xenograft and syngeneic QOD treatment models. In addition, I

would like to thank Rui Zhang and Zixu Wang (William) for their assistance in design and validate mouse primers and running the experiments in the syngeneic QOD treatment models. Special thanks to Kyle Gillani who helped in the project and for his endless support and motivation. I also would like to thank Maricel Castener and Helen Uong for performing in vitro experiments and conducting the animal experiment of human xenograft. My thanks are extended to George Triantafillou, Roaya Alqurashi, Ahlam Bogis, and Mohammed Alshagawi for conducting QD treatment and ICIs animal experiment. I also would like to thank Christoper Herbosa for his help in running QD treatment experiment. Finally, special thanks to Corinne Carland, Anise Applebaum, Eileen Liu, Salwa Hafez, Ashley Besch, Lama Hassan, and Ismail Shakir for their help and efforts in the project.

In addition, special thanks to the current and former Yee's lab members for sharing knowledge and for their assistance. I would like to express my appreciation and thanks to the former PPET students, Mona Bawazeer and Haifa, and the former PDD student, Kulood Almhmadi, for sharing advice, knowledge and for endless help and support whenever I need. They always being beside me especially during my hard time.

I am grateful to my great friend and the former PDD student Dalal Alkhelb for her kindness and for those endless talks about science and her advice throughout the journey and for sharing with me not only my happy moments, but also the sad ones. Thank you for taking care of my daughter, especially during the pandemic.

My deepest gratitude to my mom, Laila Alamoudi, my dad, Khalid Alamoudi, and my sisters, Balqees, Fawziah and Sufana, for supporting me in my dreams and teaching me that everything is possible with effort and dedication. Special thanks to my dad and

my aunt, Huda Alamoudi, for their infinite financial support during my studies. Thanks for everything.

Special thanks to my lovely daughter, Jana Alamoudi, for being my inspiration and for always giving me reasons to smile and never give up. I am grateful to my husband, Ahmed Alamoudi, for all his endless support, patience and for always taking care of our daughter. It was challenging for both my husband and I as international PhD students to take care of our child especially during the pandemic. I could not success without his infinite assistance and support. From the bottom of my heart, thank you.

Special thanks and appreciation for my government and my sponsors Prince Sattam bin Abdulaziz University and Saudi Arabian Cultural Mission to the U.S.(SACM) for their financial support. I could not achieve my dream and purse my PhD without their assistance.

Table of Contents

List of Tables

List of Figures

List of Copyrighted materials

Harbeck, N., et al., Breast cancer. Nature Reviews Disease Primers, 2019. 5(1): p. 66.

Janin, M. and M. Esteller, Epigenetic Awakening of Viral Mimicry in Cancer. Cancer Discovery, 2020. 10(9): p. 1258-1260.

Li, C.-J., et al., Pathogenesis and Potential Therapeutic Targets for Triple-Negative Breast Cancer. Cancers, 2021. 13(12): p. 2978.

Luo, J., et al., Wnt Signaling and Human Diseases: What are the Therapeutic Implications? Laboratory Investigation, 2007. 87(2): p. 97-103.

Nagarsheth, N., M.S. Wicha, and W. Zou, Chemokines in the Cancer Microenvironment and their Relevance in Cancer Immunotherapy. Nat Rev Immunol, 2017. 17(9): p. 559-572.

Namal Senanayake, S.P.J., Green tea extract: Chemistry, antioxidant properties and food applications – A review. Journal of Functional Foods, 2013. 5(4): p. 1529-1541.

Neefjes, J., et al., Towards a Systems Understanding of MHC Class I and MHC Class II Antigen Presentation. Nature Reviews Immunology, 2011. 11(12): P. 823-836.

Oki, Y., E. Aoki, and J.-P.J. Issa, Decitabine-Bedside to bench. Critical Reviews in Oncology/Hematology, 2007. 61(2): p. 140-152.

Parker, B.S., J. Rautela, and P.J. Hertzog, Antitumour actions of interferons: implications for cancer therapy. Nature Reviews Cancer, 2016. 16(3): p. 131-144.

Wright, J.J., A.C. Powers, and D.B. Johnson, Endocrine toxicities of immune checkpoint inhibitors. Nature Reviews Endocrinology, 2021. 17(7): p. 389-399.

List of Abbreviations

aDCs	Activated Dendritic Cells
AML	Acute Myeloid Leukemia
AMPK	AMP-Activated Protein Kinase
ANOVA	Analysis of Variance
AP1	Activating Protein 1
APAF1	Apoptotic Peptidase Activating Factor 1
APC	Adenomatous Polyposis Coli
APH1B	Aph-1 Homolog B, Gamma-Secretase Subunit
AZA	Azacytidine
β2M	Beta-2-Microglobulin
BAX	Bcl-2 Associated X-protein
BBB	Blood-Brain Barrier
BCL-2	B-Cell Lymphoma 2
BHLHE41	Basic Helix-Loop-Helix Family Member E41
BL1	Basal Cell-Like Type 1
BL2	Basal Cell Like Type 2
BM	Brain Metastases
BRCA1	Breast Cancer gene 1
BSA	Bovine Serum Albumin
CAR T	Chimeric Antigen Receptor T Cells
CaMKK	Ca^{2+}/Calmodulin-Dependent Protein Kinase Kinase
CCL	C-C Motif Chemokine Ligand
CCR	Conventional Care Regimens
CD	Cluster of Differentiation
CDA	Cytidine Deaminase
CDAi	Cytidine Deaminase Inhibitor
cDNA	Complementary DNA
CHA1	EGCG + DAC
ChIP-Seq	Chromatin Immunoprecipitation-Deep Sequencing
CI	Confidence Interval
CK	Cytokeratin
CLIP	Class II-Associated Ii Peptide
CMML	Chronic Myelomonocytic Leukemia
COX	Cyclooxygenase
CR	Complete Remission
CRi	Complete Remission with Incomplete Blood Count Recovery
CRS	Cytokine release syndrome
CSCs	Cancer stem cells
CSF	Cerebrospinal Fluid
CSF-1	Colony-Stimulating Factor -1
CTA	Cancer-Testis Antigen
CTCs	Circulating tumor cells
CTLs	Cytotoxic T Lymphocytes
CTLA-4	Cytotoxic T-Lymphocyte-Associated Protein 4

CXCL	CXC chemokine ligand
DAC	Decitabine
DAMPs	Danger-Associated Molecular Patterns
DCs	Dendritic Cells
DDX58	DExD/H-Box Helicase 58
DHX58	DExH-Box Helicase 58
DLAM	Division of Laboratory Animal Medicine
DLL1	Delta Like Canonical Notch Ligand 1
DLTs	Dose-Limiting Toxicities
DMEM	Dulbecco's Modified Eagle Medium
DNA	Deoxyribonucleic Acid
DNMT	DNA Methyltransferase
DNMTi	DNA Methyltransferase Inhibitor
DRs	Death Receptors
dsRNA	double-stranded RNA
EC	Epicatechin
ECG	epicatechin-3-gallate
EDTA	Ethylenediaminetetraacetic Acid.
EFS	Event Free Survival
EGC	Epigallocatechin
EGCG	Epigallocatechin-3-Gallate
EGFR	Epidermal Growth Factor Receptor
EMT	Epithelial-Mesenchymal Transition
EMT-TFs	EMT-inducing Transcription Factors
eNOS	Endothelial Nitric Oxide Synthase
EpCAM	Epithelial Cell Adhesion Molecule
ER	Estrogen Receptor
ER	Endoplasmic Reticulum
ERV3-1	Endogenous Retrovirus 3-1
ESCs	Embryonic stem cells
ESMO	European Society for Medical Oncology
FACS	Fluorescence-Activated Cell Sorting Analysis
FASLG	Fas Ligand
FBS	Fetal Bovine Serum
FDA	Food and Drug Administration
FOXP3	Forkhead Box P3
FZDs	Frizzled Receptors
GAS	Gamma Activated Sequence
GATA3	GATA Binding Protein 3
G-CSF	Granulocyte Colony Stimulating Factor
GM-CSF	Granulocyte/Macrophage Colony Stimulating Factor
GPCR	G protein-coupled receptor
GSEA	Gene Set Enrichment Analysis
GSK-3β	Glycogen Synthase Kinase 3β
GZMB	Granzyme B
H2Aa	Histocompatibility 2, Class II Antigen A, Alpha

H2Ab1	Histocompatibility 2, Class II Antigen A, Beta 1
H2d1	Histocompatibility 2, D Region
H2k1	Histocompatibility 2, K Region
HATS	Histone Acetyltransferases
HBP1	HMG-Box Transcription Factor 1
HDACs	Histone Deacetylases
HDMs	Histone Demethylases
HER2	Human Epidermal Growth Factor Receptor 2
HERVs	Human endogenous retroviruses
HIF-1	Hypoxia-Inducible Factors-1
HLA	Human Leukocyte Antigen
HMAs	Hypomethylating Agents
HMTs	Histone Methyltransferases
HSP90	Heat Shock Protein 90
IACUC	Institutional Laboratory Animal Care and Use Committee
ICAM-1	Intercellular Adhesion Molecule 1
ICIs	Immune Checkpoint Inhibitors
ICOS	Inducible T Cell Costimulator
ICOSLG	Inducible T Cell Costimulator Ligand
iDCs	Immature Dendritic Cells
IDO-1	Indoleamine 2,3-dioxygenase
IFI27	Interferon Alpha Inducible Protein 27
IFIH1	Interferon Induced with Helicase C Domain 1
IFIT	Interferon-Induced Protein with Tetratricopeptide Repeats
IFN	Interferon
IFNR	IFN receptor
IgG	Immunoglobulin G
IHC	Immunohistochemistry
Ii	Invariant Chain
IL	Interleukin
IM	Immunomodulatory
IPA	Ingenuity Pathway Analysis
irAEs	Immune-Related Adverse Events
IRF	IFN regulatory factor
ISGs	Interferon Stimulated Genes
ISG20	Interferon Stimulated Exonuclease Gene 20
ISGF3	Interferon Stimulated Genes Factor 3
ISRE	IFN-sensitive Response Element
ITT	Intent to Treat
JAG2	Jagged Canonical Notch Ligand 2
JAK	Janus kinase
LAG3	Lymphocyte-Activation Gene 3
LAR	Luminal Androgen Receptor
LAT	Linker For Activation of T Cells
LGP2	Laboratory of Genetics and Physiology 2
LGR5	Leucine-rich repeat-containing G protein-coupled receptor 5

LKB1	Liver Kinase B1
LSD1	Lysine-Specific Demethylase 1
LTRs	Long Terminal Repeats
JAK	Janus Kinase
M	Mesenchymal
MIIC	MHC class II compartment
MAF	Musculoaponeurotic Fibrosarcoma Oncogene Homolog
MAGE-A	Melanoma-Associated Antigen Family A
MAPK	Mitogen-Activated Protein Kinase
MAVS	Mitochondrial Antiviral-Signaling Protein
MDS	Myelodysplastic Syndrome
MDSCs	Myeloid-Derived Suppressor Cells
MES	Macrophage-Enriched Subtype
MHC-I	Major Histocompatibility Complex Class-I
MHC-II	Major Histocompatibility Complex Class-II
miRNAs	MicroRNAs
miRNA-sequencing	microRNA-sequencing
MRI	Magnetic Resonance Imaging
MTD	Maximum Tolerated Dose
mTOR	Mechanistic Target of Rapamycin
muERV-L	Murine Endogenous Retrovirus-Like
NES	Neutrophil-Enriched Subtype
NGS	Next-Generation Sequencing
MDA5	Melanoma Differentiation-Associated Gene 5
MDSCs	Myeloid-Derived Suppressor Cells
MSCs	Mesenchymal Stromal Cells
MSigDB	Molecular Signatures Database
MSL	Mesenchymal Stem Cell-Like
NFATC2	Nuclear Factor of Activated T Cells 2
NF-κB	Nuclear Factor-Kappa B
NK	Natural Killer Cells
NO	Nitric Oxide
NOD/SCID	Non-Obese Diabetic/Severe Combined Immunodeficiency
NOTCH3	Notch Receptor 3
NPs	Nanoparticles
NSCLC	Non-Small Cell Lung Cancer
NY-ESO-1	New York Esophageal Squamous Cell Carcinoma-1
OAS	2'-5'-Oligoadenylate Synthetase
OASL	2'-5'-Oligoadenylate Synthetase-Like Protein
ORR	Overall Response Rate
OS	Overall Survival
pAPC	Professional Antigen Presenting Cells
PBS	Phosphate-Buffered Saline
PBST	Phosphate-Buffered Saline Tween
pCR	Pathological Complete Response
pDCs	Plasmacytoid dendritic cells

PD-L1	Programmed Cell Death Ligand 1
PD-1	Programmed Cell Death Protein 1
PDVF	Polyvinylidene Difluoride
PFS	Progression-Free Survival
PI3Ks	Phosphoinositide 3-Kinases
PK	Pharmacokinetic
PKR	protein kinase R
PR	Progesterone Receptor
PRF1	Perforin-1
PRRs	Pattern Recognition Receptors
PSMB	Proteasome 20S Subunit Beta
pSTAT3	Phosphorylated Signal Transducers and Activators of Transcription 3
QD	Every day
QOD	Every Other day
qRT-PCR	Real-Time Quantitative Reverse Transcription Polymerase Chain Reaction
RANKL	Receptor Activator of Nuclear Factor Kappa-B Ligand
RCC	Renal Cell Carcinoma
RIG-1	Retinoic Acid-Inducible Gene I Protein
RIPA	Radioimmunoprecipitation Assay Buffer
RNA	Ribonucleic Acid
RNA-seq	RNA-Sequencing
ROS	Reactive Oxygen Species
RSPO	R-spondin
S1PR1	Sphingosine-1-Phosphate Receptor 1
scRNA-seq	Single-cell RNA sequencing
SDS-PAGE	Sodium Dodecyl Sulfate-Polyacrylamide Gel
sFRP1	Secreted Frizzled-Related Protein 1
shRNA	Short Hairpin RNA
SNAI	Snail Family Transcriptional Repressor
SOCS	Suppressor of Cytokine Signaling
SPI1	Spi-1 Proto-Oncogene
STAT	Signal Transducers and Activators of Transcription
Tem	Effector Memory T Cells
Th	Helper T Cells
Treg	Regulatory T cell
TAAs	Tumor-Associated Antigens
TAMs	Tumor-Associated Macrophages
TAP	Transporter Associated with Antigen Presentation
TCF/LEF	T Cell Factor/Lymphoid Enhancer-Binding Factor
TCGA	The Cancer Genome Atlas
TCR	T Cell Receptor
TE	Transposable Element
TGFB3	Transforming Growth Factor Beta-3
TIGIT	T Cell Immunoreceptor with Ig and ITIM Domains
TME	Tumor Microenvironment

TNBC	Triple Negative Breast Cancer
TNBC-BM	TNBC-Associated Brain Metastases
TNF	Tumor Necrosis Factor
TNFRSF1B	Tumor Necrosis Factor Receptor Superfamily, Member 1b
TNFRSF11B	Tumor Necrosis Factor Receptor Superfamily, Member 11b
TNM	Tumor Node Metastasis
TRAIL	TNF-Related Apoptosis-Inducing Ligand
TSAs	Tumor-Specific Antigens
tsMHC-II	Tumor-Specific MHC-II
TWIST	Twist Family BHLH Transcription Factor
VCAM	Vascular Cell Adhesion Molecule
VEGF	Vascular Endothelial Growth Factor
VEGFR	Vascular Endothelial Growth Factor Receptor
WBRT	Whole Brain Radiation Therapy
WGBS	Whole-Genome Bisulfite Sequencing
Wnt	Wnigless/Integrated
Wnt3a	Wnt Family Member 3A
Wnt4	Wnt Family Member 4
XAF1	XIAP-Associated Factor 1
ZEB	Zinc Binger E-Box Binding Homeobox 1

Chapter 1: Introduction

1.1. Breast Cancer

1.1.1. Classifications of Breast Cancer

Breast cancer is a pathological disease originated from breast tissue [1]. According to the global cancer project (GLOBOCAN 2020), breast cancer is the most commonly diagnosed cancer in the world exceeding lung cancer [2]. 2.3 million new breast cancer cases were estimated worldwide [2]. Thus, it is the most common cancer and the first leading cause of cancer death among women [2]. The risk factors associated with the incidence of breast cancer include alcohol intake, obesity, age at menarche, and age at menopause [3]. A common clinical presentation of breast cancer is a palpable breast mass detected upon on self-breast examination [3], but patients may suffer from other symptoms such as local pain or nipple discharge [3]. In addition, some symptoms associated with metastasis include fever, weight loss, night sweats, or bone pain [3]. Early and definitive diagnosis of breast cancer is important [1]. Radiological examination and imaging such as mammography, magnetic resonance imaging (MRI) and ultrasound in addition to clinical and immunohistopathological examinations play essential role in detecting breast cancer [1]. Furthermore, the tumor node metastasis (TNM) classification is used to identify the stage of the disease. Breast cancer can be classified according to some molecular biomarker, such as estrogen receptor-positive (ER^+), progesterone receptor-positive (PR^+), human epidermal growth factor receptor-2-positive ($HER2^+$), epidermal growth factor receptor-positive ($EGFR^+$), cytokeratin5/6-positive ($CK5/6^+$), vascular endothelial growth factor ($VEGF^+$), and $ki67^+$ [1, 4]. According to the 2013 St. Gallen International Breast Cancer Conference, breast cancers can be molecularly classified into the following subtypes: luminal A (ER/PR^+, $HER2^-$, Ki-67 low), HER2

negative luminal B (ER $^{+}$, HER2^{-}, and either Ki-67 high or PR low), HER2 positive luminal B-like (ER $^{+}$, HER2^{-}, any Ki-67, and any PR), HER2 enriched (ER^{-}, PR^{-}, HER2^{+}), basal-like TNBC (ER^{-}, PR^{-}, HER2^{-}), and other subtypes [5, 6]. Figure.1.1 represents the current molecular and histological characteristic of breast cancer subtypes [7].

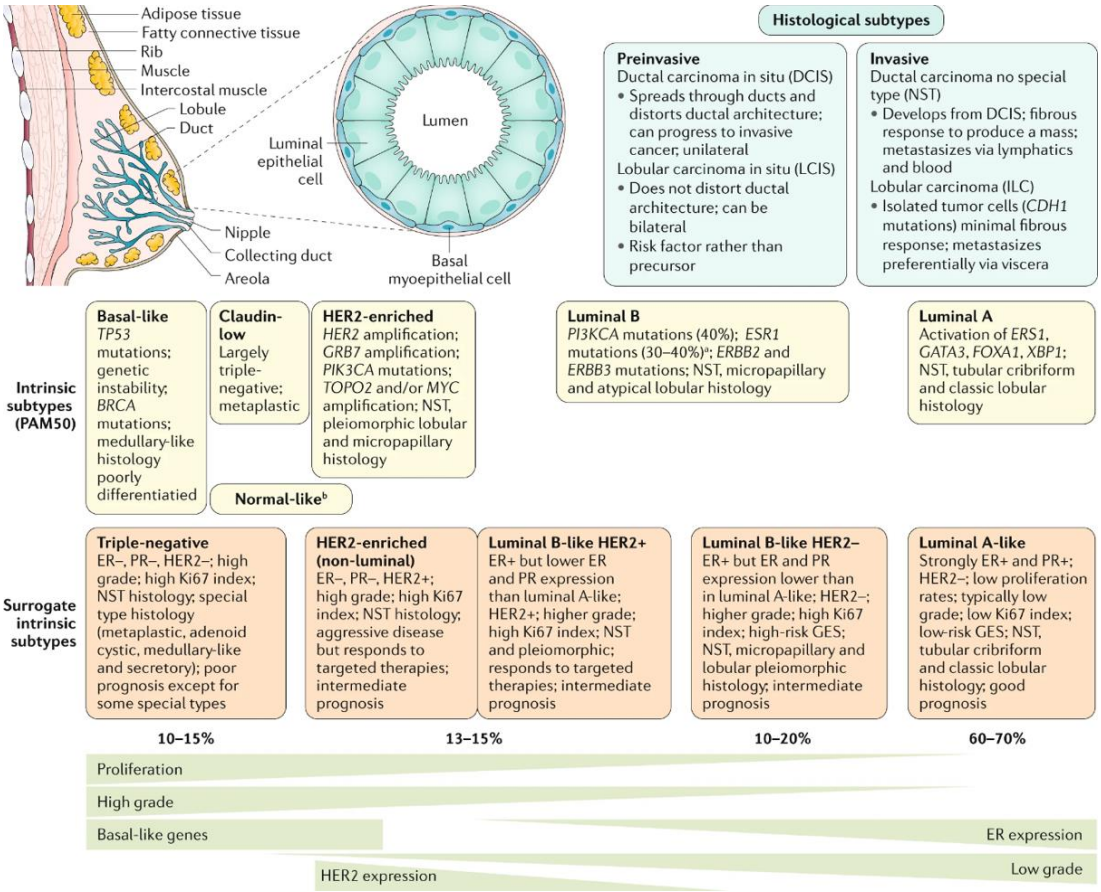

Figure 1.1. Molecular and Histological Characterization of Breast Cancer Subtypes. *Reprinted with permission from: Harbeck, N., et al., Breast cancer. Nature Reviews Disease Primers, 2019. 5(1): p. 66.*

1.1.2. Triple-Negative Breast Cancer (TNBC)

Triple negative breast cancer (TNBC) represents 15-20% of all breast cancer cases [3, 4, 8]. TNBC is often diagnosed in premenopausal young women under 40 years old, but can appear in older women [3, 4, 8]. The incidence of TNBC is higher in some

populations, for example, premenopausal African American and Hispanic patients [4, 8]. Several risk factors linked with TNBC such as the earlier age at menarche and the age at first pregnancy, and/or obesity, but there are no defined patterns for TNBC onset [4, 9]. TNBC is an aggressive type of breast cancer that is defined by what it is not [1, 7]. Specifically, TNBC does not express estrogen receptors, progesterone receptors, and does not have overexpressed HER2 receptors [1, 3, 7]. In 2011, Lehmann et al. classified TNBC based on genomic expression profile (GEP) assays into 7 molecular subtypes: basal cell-like type 1 (BL1), basal cell Like type 2 (BL2), immunomodulatory subtype (IM), mesenchymal subtype (M), mesenchymal stem cell-like subtype (MSL), luminal androgen receptor subtype (LAR), and unstable [10]. The gene expression profiles and the resident signal transduction pathways are differ amongst the TNBC subtypes [3] as shown in Figure.1.2.

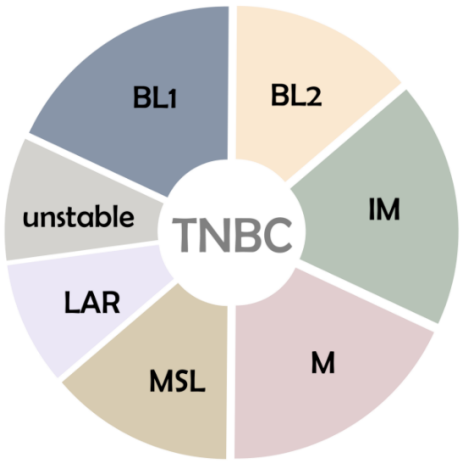

Types	Characteristics	Cell lines
BL1	Cellular proliferation, cell cycle, DNA repair	HCC2157, MDA-MB-468, HCC38, HCC1937
BL2	Growth factor, myoepithelial markers	HCC1806, SUM149PT, CAL851
IM	Immune mediated signaling	HCC1187, DU4475
M	EMT and differentiation	BT549, CAL51, CAL-120
MSL	MET, angiogenesis, differentiation and stemness	MDA-MB-157, MDA-MB-436, MDA-MB-231, SUM159
LAR	Hormone signaling, luminal gene up-regulation	MDA-MB-453, SUM185, CAL148, MFM223

Figure 1.2. Molecular Classification of Triple-Negative Breast Cancer subtypes. *Reprinted with permission from: Li, C.-J., et al., Pathogenesis and Potential Therapeutic Targets for Triple-Negative Breast Cancer. Cancers, 2021. 13(12): p. 2978.*

In 2016, Lehmann et al reclassified TNBC into four tumor-specific subtypes (BL1, BL2, M, and LAR) [11]. Furthermore, in 2019, Kim et al. added new TNBC subtypes for neutrophil-enriched subtype (NES) and macrophage-enriched subtype

(MES). This new classification also outlined differences in the efficacy and response to immune checkpoint inhibitors (ICIs) [12], providing a new useful information to guide the treatment of TNBC patients. Hence, the molecular subtypes and molecular classification of TNBC are important tools that can be used as prognostic and predictive measurements to determine the best treatment modality for TNBC patients with either conventional chemotherapy or targeted and immunotherapy therapies that currently in clinical trials [3].

Unfortunately, many TNBC patients suffer from poor prognosis and relapse [13]. Also, breast cancer metastasis is a common complication, with sites in the bone, lung, liver, and brain. Brain metastasis has increased dramatically with the improved management of non-brain metastases [13]. Fatal brain metastases account for up to 50% of metastases related death [14]. Breast cancer is commonly accompanied by brain metastases [15]. The frequency of developing brain metastases (BM) in TNBC patients is up to 46% with a median overall survival of 5 months when diagnosed [16]. Since most of cancer therapies do not cross the blood brain barrier, the treatment strategies for brain metastases include radiotherapy, neurosurgery, stereotactic radiosurgery, selected chemotherapy, and growth factor inhibitors [14, 17]. The successfulness of the treatments depends on many factors: patient's age, the present of extracranial disease, number of brain metastases, individual responsiveness to treatment, and intracranial relapse. Median overall survivals for patients who received these types of treatments range from weeks to months [14, 17]. The development of a new treatment of brain cancer and brain metastases is challenging since patients with brain metastases are often not included in clinical trials. In addition, there are few reliable and practical animal pre-clinical model

for human brain metastases [14, 17]. Hence, there is an urgent medical need for development of relevant pre-clinical models for TNBC-associated brain metastases (TNBC-BM) and understanding its molecular mechanisms and creating therapeutic strategies to improve patient outcome and quality of life.

1.2. Wnt/β-Catenin Pathway

1.2.1. Canonical Wnt/β-Catenin Pathway

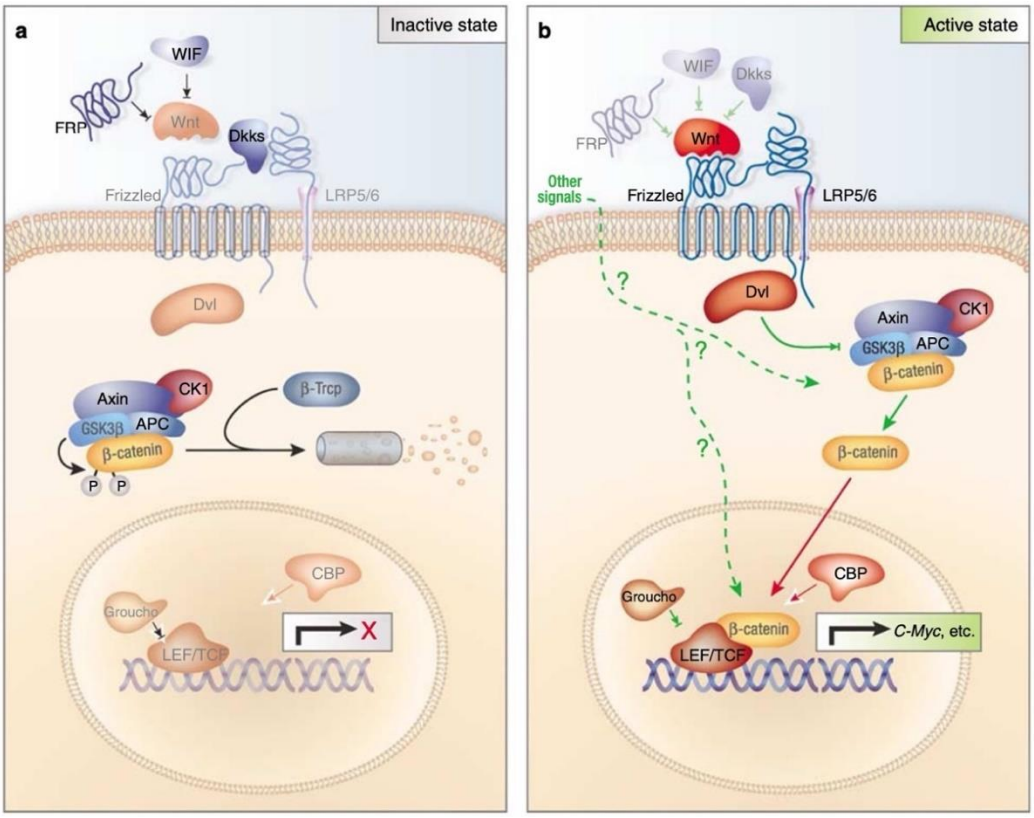

Figure 1.3. The Canonical Wnt/β-catenin Signaling Pathway. *Reprinted with permission from: Luo, J., et al., Wnt signaling and human diseases: what are the therapeutic implications? Laboratory Investigation, 2007. 87(2): p. 97-103.*

Aberrant activation of Wnt/β-catenin signaling plays an essential in regulation of cell proliferation, survival, and differentiation as well as embryonic development. Wnt/β-catenin signaling also plays a critical role in stem cell maintenance and thus the development of many cancers including colorectal, prostate, liver, and breast cancers [18,

19]. The Canonical Wnt/β-Catenin Pathway is represented in Figure 1.3. Cytosolic β-catenin serves as a downstream effector protein of the canonical Wnt signaling pathway in Wnt-stimulated cells. Regulation of Wnt pathway involves proteolysis of the β-catenin by the β-catenin destruction complex that consists of adenomatous polyposis coli (APC), AXIN and glycogen synthase kinase 3β (GSK-3β) [20]. Upon Wnt ligand binding, frizzled receptors (FZDs) trigger dissociation of the β-catenin destruction complex resulting in nuclear accumulation of β-catenin, which interacts with LEF/TCF transcription factors, resulting in activation of transcription of Wnt target genes such as Cyclin D1 and c-MYC [20].

Embryonic stem cells (ESCs) which are generated from the inner cell mass of a blastocyst possess the ability to differentiate into all cell types. The Wnt/β-catenin pathway plays essential role in the self-renewal of these ESCs through suppression of the repressor activity of endogenously expressed TCF-3. It has been reported that mutations in the components of canonical Wnt/β-catenin pathway such as APC or GSK3-β can lead to inability of ESCs to differentiate normally [21].

Wnt/β-catenin signaling has been attributed to the differentiation of adult stem cells [22]. Canonical Wnt/β-catenin signaling has important role in regulating the cell fate of mesenchymal stromal cells (MSCs) which are derived from the stroma of bone marrow, adipose tissue, or placental tissue, and they can differentiate into multiple cell types [21].

Wnt/β-catenin signaling plays essential roles in mammary gland stem cell maintenance at different stages of development [22]. It has been reported that the formation of mammary gland placodes during embryogenesis is accelerated by Wnt3a.

Furthermore, alveolar development during early pregnancy requires Wnt4 [22]. In addition, it has been shown that Wnt3a in transplantation assays has the ability to induce clonal expansion of mammary stem cells for several generations and maintains their ability to generate functional glands [22]. It has been reported that tumorigenic potential is greater in mammary stem cells that have high levels of Wnt/β-catenin signaling than stem cells with low Wnt/β-catenin signaling [23].

Cancer stem cells (CSCs) are defined as a population of cancer cells responsible for initiating and propagating neoplastic disease and have stem-like properties [24]. These cells have a roles in development of breast cancer and resulting metastases [25]. Since CSC possess self-renewal properties, these cells can differentiate into daughter cells that form the bulk of tumor cells, yet the cancer stem cells remain as a minority cell population with self-replicating potential [25].

The CSC theory states the tumor growth was fueled by small population of CSCs hidden in cancers. This could explain that inevitable recurrence of tumors after initially eradicated by chemotherapy and/or radiation therapy, the phenomenon of tumor dormancy, and metastasis. CSCs have been identified in many cancer types, including leukemia, breast cancer, colorectal cancer, and brain cancer [26].

The presence of CSCs in breast cancer can provide important explanation of the failure of current oncologic treatments in preventing tumor progression, metastasis, and recurrence [27]. CSCs are difficult to eliminate and are resistant to chemotherapy and they also plays a role in breast cancer recurrence [28]. In TNBC patient-derived xenograft (PDX) models, a resistant subpopulation of CD49f-positive cells that also known as

integrin α6, a marker of stem cells, was identified in tumors that were initially sensitive to docetaxel, leading to metastasis and progression [29].

A cross talk between several signaling pathways, including the Wnt signaling pathway, could be a possible mechanism for CSCs to evade chemotherapy [25]. Furthermore, it has been reported that CSCs have the ability to efficiently seed new tumors upon inoculation into a recipient host mouse, and are the responsible for effective colonization of distant tissues [24, 28]. Hyperstimulation of Wnt signaling is a possible mechanism of CSC self-renewal and metastases. Therefore, an essential aspect of cancer research is to target this pathway since it is linked to cancer fatalities [30].

Epithelial to Mesenchymal transition (EMT) plays a role in the transition of human epithelial mammary cells to breast CSCs [30]. The acquisition of EMT in the epithelium of an organ could be the first steps on the development of tumorigenesis [31]. Thus, the link between EMT and CSCs provides a correlation between CSCs and the metastatic potential of cancer [31]. It has been shown that there is an association between an increase in EMT markers and the aggressiveness of metastatic disease, which may be explained by increasing stemness of tumor-initiating CSCs and intrinsic resistance to standard therapies [31].

EMT activation plays a pivotal role in the development of malignant phenotype by epithelial cancer cells [32]. Epithelial cells that acquire mesenchymal phenotype enter subsequent steps of the invasion-metastasis cascade [32, 33]. Furthermore, there is a positive link between loss of E-cadherin and acquisition of EMT [34]. Also, there is an association between Wnt and E-cadherin [35]. β-catenin serves as a component of the cadherin complex [35]. Activation of Wnt signaling by translocation of β-catenin into the

nucleus is negatively correlated with E-cadherin expression [32, 36]. Therefore, cancer cells with hyperactive Wnt signaling passage through an EMT [32, 36].

Leucine-rich repeat-containing G protein-coupled receptor 5 (LGR5), an "orphan" receptor belonging to the G protein-coupled receptor (GPCR) family, is a stem cell marker in the small intestine, colon, stomach, hair follicle, kidney nephrons, and mammary gland [26, 37]. LGR5 expressing stem cells are major drivers of cancer progression in the intestine and colon, and LGR5 is overexpressed in other cancers, including breast cancer [27]. LGR5 plays important role in modulating canonical Wnt signaling pathway through binding to its ligand R-spondin (RSPO) [37]. LGR5 can potentiate the Wnt/β-catenin signaling pathway, resulting in activation of cancer stem cell proliferation and self-renewal [37]. Accumulating evidence reported that LGR5 can promote cancer cell mobility, tumor formation, and EMT in breast cancer cells via activation of Wnt/β-catenin signaling [27, 37]. The presence of LGR5 facilitates breast cancer cell tumorigenicity, promotes cell migration and tumor metastasis, and is required for the maintenance of breast CSCs [27].

Several strategies have been proposed to interfere with CSCs, some of which are currently in clinical trials. One of the strategies is targeting RSPO3 that encodes ligands for LGR5 receptor. Fusions affecting RSPO3 occurs in up to 10% of colorectal cancers, resulting in sustain high levels of Wnt signaling [38]. An anti-RSPO3 antibody demonstrated promising therapeutic responses in preclinical models of colorectal cancer by reduce stemness and induce differentiation [39]. Rosmantuzumab, an anti-RSPO3 antibody, has been evaluated in phase 1 clinical trial (NCT02482441). The study was

completed on August 11, 2020 (NCT02482441). Thus far, no results have been published [40].

1.2.2. Wnt/β-Catenin Pathway in TNBC

Development of a treatment for TNBC and its associated metastases requires identifying of functional molecular targets. Genomic and transcriptomic data for TNBC and metastases have identified the Wnt signaling pathway as potential therapeutic targets [41-43]. Mutations in APC, AXIN, or β-catenin, are rare in TNBC in contrast to other types of cancer such as colorectal cancer, however, overexpression of β-catenin is prevalent [44, 45]. Several studies suggested that loss of expression of negative Wnt pathway regulators such as secreted Frizzled-related protein 1 (sFRP1), which competes with FZD receptors for ligand binding may be the cause of deregulation of this pathway in TNBC [46-48]. Constitutive activation of Wnt signaling has been linked to breast cancer cells growth as well as to recurrence of the disease and an elevated level of β-catenin has been associated with poor prognosis [49, 50]. Furthermore, the risk of brain and lung metastases was significantly increased with activation of Wnt pathway in TNBC patients [51]. Various lines of evidences suggested that Wnt signaling is linked to angiogenesis, which plays important role in proliferation and metastatic spread of cancer cells [52, 53]. Two separate in vitro studies in TNBC cell lines MDA-MB-231 and BT-549 concluded that inhibition of Wnt pathway leads to inhibition of cell proliferation and migration, and induction of apoptosis [45, 54]. It has been found that blockade of Wnt signaling reduced tumor growth and metastasis in murine breast cancer xenograft model and TNBC cells MDA-MB-231 xenograft model [48, 55, 56]. Furthermore, one of the established models for breast cancer tumorigenesis study was transgenic mice that had

Wnt overexpression [57]. Hence, Wnt signaling pathway presents an attractive therapeutic target in TNBC**.**

1.3. Interferons (IFN)

1.3.1. Interferon Signaling Pathways

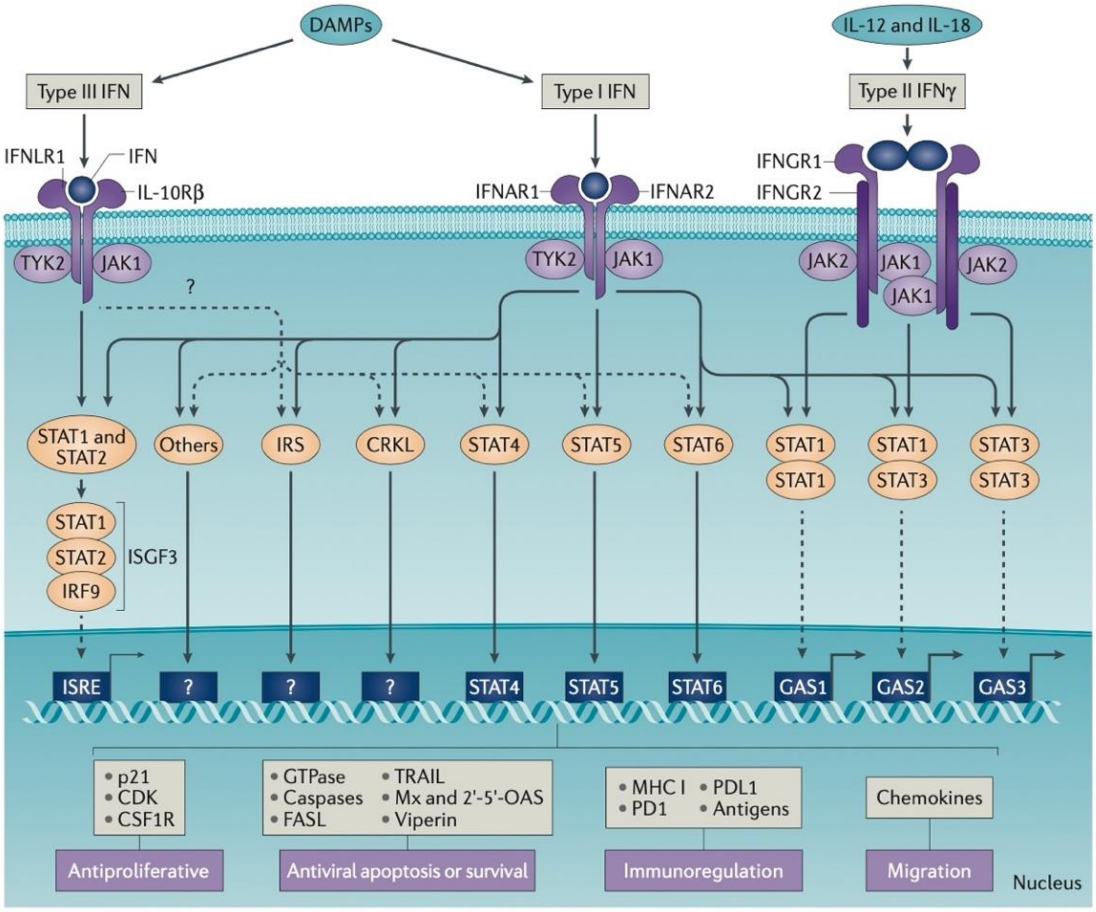

Figure 1.4. Interferon Signaling Pathways. *Reprinted with permission from: Parker, B.S., J. Rautela, and P.J. Hertzog, Antitumour actions of interferons: implications for cancer therapy. Nature Reviews Cancer, 2016. 16(3): p. 131-144.*

Interferons (IFNs) are pleiotropic cytokines that play essential roles in activating immune responses to protect against diseases [58]. In addition, IFNs are also involved in the development and treatment of cancer [58]. There are three major types of IFNs: Type I IFN, Type II IFN, and Type III IFNs. The type I IFNs are composed of a family of 17

proteins (13 sub-types of IFNα, IFNβ, IFNε, IFNκ, and IFNω) that bind to their receptors: the IFNα/β receptor 1 (IFNAR1) and IFNα/β receptor 2 (IFNAR2) subunits [58]. The type II IFN, IFNγ, binds to IFNγ receptor 1 (IFNGR1) and IFNγ receptor 2 (IFNGR2) subunits. The type III IFNs include IFNλ1, IFNλ2 and IFNλ3 (also known as interleukin-29 (IL-29), IL-28A and IL-28B, respectively) and IFNλ4, that bind the IFNλ receptor 1 (IFNLR1) and IL-10 receptor subunit-β (IL-10Rβ) heterodimeric receptor [58]. Type I and type III IFNs are induced through pattern recognition receptor (PRR) pathways; in contrast, type II IFN is mainly activated by mitogens or cytokines such as IL-12 and IL-18, which are expressed by immune cell types, particularly T cell and natural killer (NK) cell [58].

Figure 1.4. represents IFNs signaling pathways. IFNS bind to their receptors after they are released in response to danger-associated molecular patterns (DAMPs) in the case of type I IFNs and type III IFNs and to cytokines in case of type III IFNs [58]. IFN signaling pathways are mediated through Janus kinase (JAK). JAK phosphorylates signal transducers and activators of transcription (STATs) factors [58]. After phosphorylation, STATs can homodimerize and heterodimerize to form transcriptional activator complexes that translocate to the nucleus, where they bind to specific elements in the promoters of IFN-stimulated genes (ISGs) [58]. For example, the transcriptional activator complex for type I IFN is IFN gene stimulated 3 (ISGF3) complex, composed of STAT1, STAT2, and IRF9, that binds to IFN-sensitive response element (ISRE) and for type II IFNγ is STAT1 and STAT3 dimer that binds to gamma activated sequence (GAS) elements [58]. Type I IFNs have the ability to activate homodimerization and heterodimerization of all members of the STAT family, including STAT1, STAT3,

STAT4, STAT5, and STAT6- often cellular-context dependent, resulting in the induction of the transcription of a different set of genes in comparison with ISGF3 [58]. Type II IFNγ can activate homodimers and heterodimers of STAT1 and STAT3, considered the two major STATs induced by IFNγ [58]. In addition to induction of its distinct ISGs, IFNγ can induce some ISGs that are also activated by type I IFNs. Generally, the pathways induced by type III IFN are similar to the ones that are activated by type I IFN [58]. It has been reported that the unphosphorylated STATs proteins activated by IFN signaling possess the transcriptional ability to prolong the duration of IFN signaling and can induce the transcription of specific ISGs involved in the chemosensitivity and radiosensitivity of tumor cells [58, 59]. Furthermore, type I IFNs can activate non-STAT pathways such as MAPK activation, insulin receptor substrate (IRS), and CRK-like (CRKL) activation, resulting in the expression of additional ISGs [60].

IFNs signaling has been involved in regulating carcinogenesis via direct or indirect ways [58]. Type I IFNs can be secreted by most cell types in the body in response to an array of different stimuli. Plasmacytoid dendritic cells (pDCs) are considered the major IFNα-producing cells because of their high basal expression of IFN regulatory factor 7 (IRF7) [58]. The promoter of IFNB1 (which encodes IFNβ) consists of nuclear factor-κB (NF-κB) and activating protein 1 (AP1) as well as IRF binding sites, indicating it is important to understand the cellular sources and the different circumstances of IFNβ secretions. Physiological expression of IFNβ can be stimulated in myeloid cells via colony-stimulating factor-1 (CSF-1) and in osteoclasts via receptor activator of NF-κB ligand (RANKL) [58]. In addition, it has been reported that IFNβ can suppress the proliferation of the cells that produce it in an autocrine manner [58]. In the

context of tumors, type I IFN can be produced by infiltrating innate immune cells and lymphocytes, as well as the tumor cells themselves, indicating IFN-mediate antitumor immune responses via tumor-intrinsic or extrinsic mechanisms. Although the functions of IFNα and IFNβ have been well understood and characterized, the functions of other types I IFNs such as IFNε and IFNκ are less well studied and their expression seems to be tissue or disease specific [58]. The expression of type II IFNγ are primarily restricted to T cells and NK cells [58]. Regardless of their cellular sources of secretion, all IFNs have the potential ability to act directly on tumor cells and produce a direct antitumor effect or act on immune cells and exert indirect antitumor effects [58].

The ISGs often encode effector proteins that play important role in IFNs-related effects, including antiviral, antitumor, and immunoregulatory effects [58]. There are many overlaps between IFNs signaling pathways and thus explain their shared properties. IFN pathway is tightly regulated. The regulation of IFN signaling is through positive and negative feed-forward and feedback loops [58]. For example, IFN can suppress its own signaling by induction of several inhibitors such as the suppressor of cytokine signaling (SOCS) proteins, which function to ensure that the strength and duration of IFN response are effective yet limited and to prevent any toxic consequences of excessive signaling [61].

1.3.2. Anti-tumor Effects of IFNα/β and IFNγ

IFNα/β and IFNγ are involved in regulating the induction of the expression of several genes that can have direct effects on tumor cell growth, proliferation, differentiation, survival, migration [58]. It has been demonstrated that crude type I IFN preparations treatment of human breast cancer cell lines resulted in a direct anti-

proliferative effect that was contributed to the IFN-induced prolongation of all phases of the cell cycle [62]. Furthermore, treatment of prostate cancer cell lines with IFNα activated the expression of endogenous inhibitors of cyclin-dependent kinases, such as p21 [63]. In addition to the anti-proliferative effects, IFNs can induce apoptosis in cancer cell lines of various origins [58]. IFNs play an essential role in regulating the major apoptotic pathways: the extrinsic or death receptor-mediated pathway and the intrinsic or mitochondrial pathway [58]. The extrinsic pathway involves the ligation of cell-surface death receptors (DRs) to stimulate the initiator caspase 8, while the intrinsic pathway requires the release of apoptotic factors like cytochrome c from the mitochondria to stimulate other cytoplasmic caspases [58]. It has been demonstrated that type I IFN and the Toll-like receptor 3 (TLR3) agonist poly(I:C) induced apoptosis response in breast tumor cell lines by upregulation of the DR ligand, TNF-related apoptosis-inducing ligand (TRAIL) [64]. Furthermore, there are several ISGs such as FAS, FAS ligand (FASLG), protein kinase R (PKR), and 2′-5′-oligoadenylate synthetases (OASs) that are involved in the IFN-mediated apoptotic response [58].

IFNα/β and IFNγ play important role during cancer initiation and progression [58]. It has been reported that treatment with neutralizing IFNα- IFNβ polyclonal antiserum resulted in accelerated tumor growth and progression after transplantation of a series of mouse cancer cell lines, including multiple myeloma cell lines [65]. Furthermore, it has been demonstrated that *Ifnb1*- knockout mice developed more aggressive tumors in a Lewis lung carcinoma (LLC) allograft model [66]. In addition, it has been shown that *Ifngr1*-knockout mice have shorter survival compared to wild-type (WT) mice [67]. It has been reported that there was loss or reduced in the expression of

the IFNα/β and IFNγ pathways components in many cancers, including breast cancer (reduced IRF5 expression), melanoma (reduced expression of STAT1, STAT2, and IRF9), and chronic myeloid leukemia (reduced expression of STAT1) [58].

IFNα/β and IFNγ play important roles in the suppression of metastasis. It has been reported that one of the mechanisms of tumor escape during metastasis is through suppression of IFN signaling [58]. In the mouse model of mammary tumor metastasis, it has been shown that IRF7 and more than 200 predicted IRF7 target genes were expressed in tumor cells derived from primary tumors; however, this IRF7 signature was lost in bone-metastases [68]. In addition, restoration of IRF7 expression in highly metastatic tumor cells resulted in the suppression of their ability to develop bone metastasis. Furthermore, systemic IFNα therapy resulted in the suppression of the development of bone metastases and improved metastasis-free survival in the same animal model of breast cancer metastasis [68]. A similar finding was observed in humans [58]. It has been shown that loss of the IRF7-associated gene signature in primary tumors is associated with an increased risk of bone metastasis. It has been demonstrated that the levels of IFNα/β produced by leukocytes derived from patients with breast cancer were less than those from healthy patients [58]. In addition, normal levels of IFN production were restored after removing the primary tumor, indicating the ability of the tumor cells to suppress IFN production [58].

Taken together, these data support that IFNα/β and IFNγ signaling play a critical role in the antitumor immune response and defective in such signaling promotes an immunosuppressed environment, resulting in tumor development and metastatic dissemination.

1.3.3. The Immunomodulatory Effects of IFNα/β and IFNγ

In addition to the anti-tumor effects of IFNα/β and IFNγ, they also exert extrinsic effects on tumors by regulating different processes involved in tumorigeneses such as angiogenesis and immunity [58]. The immune system plays a critical role in restraining the process of cancer initiation and metastases development [58]. Both IFNα/β and IFNγ play important roles in promoting anti-tumor immunity, as shown in Figure 1.5. IFNα/β and IFNγ activation can promote the activity of immune effector cells such as cytotoxic T cells, T helper (Th) cells, natural killer (NK) cells, and dendritic cells (DCs), as well as suppressed the activity of immune-suppressive cells such as regulatory T (Treg) cells and myeloid-derived suppressor cells (MDSCs) and the conversion of tumor-associated macrophages (TAMs) [58]. IFNγ can suppress monocyte differentiation into M2-polarized macrophages, monocyte-derived TAMs, and can induce the switch of TAMs from M2 into M1-polarized macrophages, leading to the suppression of VEGF secretion in vitro and in vivo and thus inhibit angiogenesis [69].

One of the important mechanisms of IFNα/β and IFNγ mediated regulation of cancer immunity is the regulation of antigens presentation on tumor cells and antigen presentation by major histocompatibility complexes (MHCs) as well as ligands for receptors of immune checkpoints such as PD-L1 [58]. Another mechanism associated with the immunomodulatory effects of IFNα/β and IFNγ is their ability to induce the release of secondary mediators such as chemokines, cytokines, and interleukins such as IL-15, IFN-induced cytokine, that involved in the expansion and maintenance of the lymphocyte population after IFN exposure [58]. In addition, the optimal effector function of NK cells requires IFNα/β [58]. Moreover, IFNγ stimulation can induce several signals

in T cells that are required for effective T cell function. However, the loss of IFNγ signaling pathways in T cells can dampen T cell responses and promote tumor growth [69].

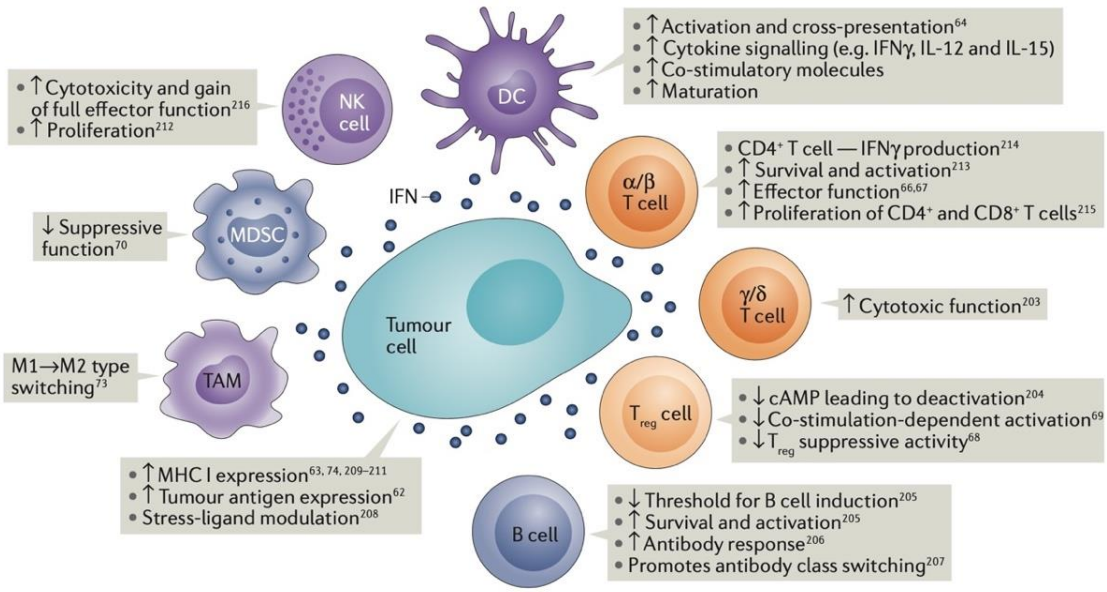

Figure 1.5. Immunomodulatory Effects of IFNα/β and IFNγ. *Reprinted with permission from: Parker, B.S., J. Rautela, and P.J. Hertzog, Antitumour actions of interferons: implications for cancer therapy. Nature Reviews Cancer, 2016. 16(3): p. 131-144.*

Several studies have demonstrated the clinical significance of IFNγ expression in human cancer. It has been found that treatment with anti-PD-L1 (durvalumab) in patients with metastasized NSCLC and urothelial cancer has been associated with upregulation of IFNγ gene signature (IFNγ, PD-L1, LAG3, and CXCL9) that is positively correlated with improved patient outcomes, increased overall response rates, and prolonged median progression-free survival [70]. This response was independent of PD-L1 expression, indicating that IFNγ gene signature may stratify patients with improved responses to anti-PD-L1. Furthermore, it has been demonstrated that treatment with an anti-PD-1 inhibitor in NSCLC patients and melanoma patients resulted in increased IFNγ protein expression

and significantly longer progression-free survival, suggesting that IFNγ could be used as a predictive biomarker for immune checkpoint blockade efficacy [71].

1.3.4. Viral Mimicry

Cancer has been considered a genetic disease, however, aberrant epigenetic modifications have also been implicated in tumorigenesis including tumor initiation and progression [72]. Recently, epigenetic therapies including DNA methyltransferases inhibitors (DNMTis), such as decitabine, have converged with cancer immunotherapy approaches due to a phenomenon known as viral mimicry [72]. Viral mimicry is a cellular state of active antiviral response that is mediated by reactivate the expression of endogenous retroviruses [72]. It has been reported that stimulation of viral mimicry by DNMTi can reactivate the transcription of human endogenous retroviruses (HERVs), resulting in IFN signaling activation [73, 74]. Human endogenous retroviruses (HERVs) are retrotransposons (a type of transposable element (TE)) that comprise 8.5% of the human genome [75, 76]. HERVs are inherited genetic germline elements derived from ancient germline infections by exogenous retroviruses throughout the evolution of the human genome. Both the intact HERVs and exogenous retroviruses shared some similarities [76]. For example, their lengths are approximately 7 kilobases, and they include 3-4 genes and 2 LTRs, which are putative promoters of HERVs [76]. The majority of HERVs are non-infectious due to evolutionarily acquired disruption or silencing mutations [75]. The main mechanism for silencing HERVs expression is by cytosine methylation via DNA methyltransferase (DNMT), particularly within the LTR regions [75, 76].

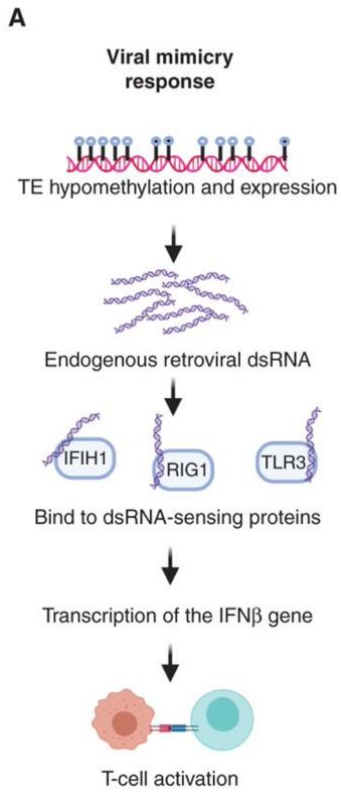

Figure 1.6. The Induction of Viral Mimicry Response after DNMTi. *Reprinted with permission from: Janin, M. and M. Esteller, Epigenetic Awakening of Viral Mimicry in Cancer. Cancer Discovery, 2020. 10(9): p. 1258-1260.*

Several studies have demonstrated that using DNMTi such as decitabine can reactivate the expression of HERVs in cancer cells and induce viral mimicry status that triggers an immune response via induction of viral defense genes [73, 74], as shown in Figure 1.6. Activation of HERVs can lead to the formation of a double-stranded RNA (dsRNA) [75, 77]. Once dsRNA is formed, it can be sensed by the dsRNA pattern recognition receptors (PRRs) such as RIG-1 (DDX58), LGP2 (DHX58), and MDA5 (IFIH1). This result in initiating the signaling cascades mediated through the aggregation of mitochondrial antiviral-signaling protein (MAVS) and the downstream activation of interferon regulatory factor 3 (IRF3) and IRF7, resulting in activation of IFN signaling [75]. Activated IFN signaling can stimulate anti-tumor immunity through intrinsic tumor

effects, including anti-proliferative and apoptotic effects and via the extrinsic effects on cytotoxic lymphocyte populations that lead to an increase in the infiltration of effector immune cells into the tumor microenvironment (TME) [75]. Consistent with stimulation of IFN signaling, it has been demonstrated that upregulation of HERVs in vivo was associated with increased infiltration of cytotoxic and helper T cells in the TME [78]. Furthermore, HERV expression may also promote an adaptive immune response by producing and presenting ERV-derived tumor-associated antigens [79]. Induction of HERVs can produce epitopes that can be detected by MHC-I at the surface of tumor cells, which can increase the recognition of tumor cells by the immune system, resulting in activation of cytotoxic T cell function [80]. Increased immunogenicity plays a critical role in overcoming resistance to immune checkpoint inhibitors in the treatment of solid tumors [75]. It has been reported that induction of HERVs viral mimicry after treatment with DNMTi can potentiate the anti-tumor effects of immune checkpoint inhibitors in melanoma mouse models [73, 74].

1.4. Antigen Presentation

1.4.1. Major Histocompatibility Complex Class-I (MHC-I) and Major Histocompatibility Complex Class-II (MHC-II)

Antigen presentation by major histocompatibility complex (MHC) class I and major histocompatibility complex class II play an essential in the adaptive immune system [81]. Both classes are involved in presenting antigenic peptides on the cell surface for recognition by T cells [81]. Effective anti-tumor T cells immune response could eradicate tumor cells [81]. MHC-class I (MHC-I) and MHC-class II (MHC-II) molecules are important for antigen presentation. The main function of MHC-I, which are

constitutively expressed by all nucleated cells including cancer cells, is to present endogenously derived peptide antigens to $CD8^+$ cytotoxic T cells [82]. On the other hand, the function of MHC-II, which are primarily expressed by professional antigen presenting cells (pAPC) such as dendritic cells (DC), B cells, and macrophages, is to present exogenously derived peptide antigens to $CD4^+$ helper T cells [82]. Cross-presentation can occur between the two pathways. MHC-I can present peptides of exogenous origin, while MHC-II molecules can present peptides of endogenous proteins that degraded in the endocytic pathway [82]. Both MHC-I and MHC-II expressions are induced by IFNγ [58].

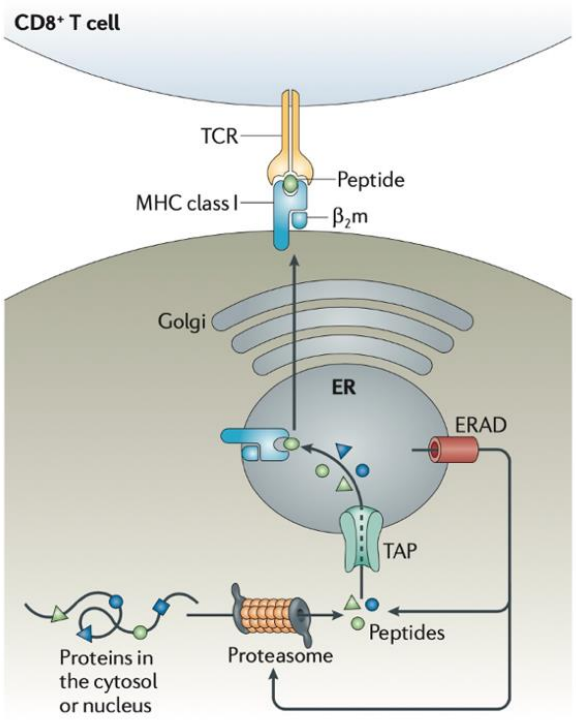

Figure 1.7. MHC-I Antigen Presentation Pathway. *Reprinted with permission from: Neefjes, J., et al., Towards a systems understanding of MHC class I and MHC class II antigen presentation. Nature Reviews Immunology, 2011. 11(12): p. 823-836.*

In humans, MHC class I heavy chains are encoded by three polymorphic genes (HLA-A, HLA-B, and HLA-C) [82]. MHC-I antigen presentation pathway is represented

in Figure 1.7. The first step of MHC-I intracellular antigenic peptides presentation involves proteasome-mediated degradation of endogenous proteins [82]. After generating the degraded peptides, the resulting peptides are transported via transporter associated with antigen presentation (TAP) into the endoplasmic reticulum (ER). In the ER, the peptides are loaded onto the fully assembled MHC-I heterodimer, consisting of a polymorphic heavy chain and a nonpolymorphic light chain known as β2-microglobulin (β_2M). When the peptides bind to MHC-I, the fully assembled peptide-MHC-I complexes are released from the ER and transported via the Golgi to the cell membrane for antigen presentation to cytotoxic $CD8^+$ T cells [82].

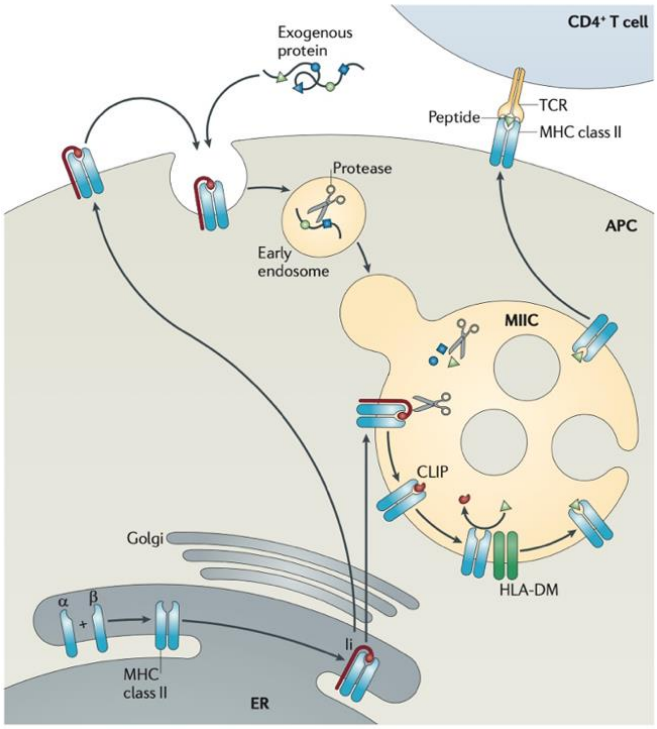

Figure 1.8. MHC-II Antigen Presentation Pathway. *Reprinted with permission from: Neefjes, J., et al., Towards a systems understanding of MHC class I and MHC class II antigen presentation. Nature Reviews Immunology, 2011. 11(12): p. 823-836.*

In humans, MHC-II molecules are encoded by three genes: HLA-DR, HLA-DQ, and HLA-DP, and all three are polymorphic [82]. Figure 1.8 represents the MHC-II

presentation pathway. The first step in MHC-II antigen presentation involves the assembly of MHC class II α- and β-chains in the endoplasmic reticulum (ER) that are associated with the invariant chain (CD74, Ii) [82]. The resulting complex consisting of Ii and MHC-II is translocated either directly and/or via the plasma membrane through the Golgi to a late endosomal compartment known as the MHC class II compartment (MIIC). In the MIIC, resident proteases digest endocytosed exogenous-proteins and Ii, leaving the class II-associated Ii peptide (CLIP) fragment of Ii in the peptide-binding groove of the MHC-II heterodimer. The CLIP exchange for an antigenic peptide derived from a protein degraded in the endosomal pathway is facilitated with the help of the chaperone HLA-DM. As a result, MHC-II molecules are transported to the cell membrane for antigenic peptides presentation to $CD4^+$ T helper cells [82].

1.4.2. Cancer-Testis Antigens (CTAs)

The development of successful immunotherapy for tumors requires identifying tumors antigen that can be used as targets for treatment, including cancer vaccines and T-cell therapy [83]. The expression of tumor antigen on the surface of tumor cells increases the immune recognition of tumor cells, resulting in T cell activation. Tumor antigens can be categorized into tumor-specific antigens (TSAs), expressed only in tumor cells, that can be derived from somatic mutations, internal deletions, and/or chromosomal translocations as well as tumor-associated antigens (TAAs), expressed in tumor tissues and some normal tissues, including cancer/testis antigens (CTAs) such as NY-ESO-1 and MAGE-A, and overexpressed antigens such as HER2 [83].

Cancer/testis antigens (CTAs) are TAAs that consist of approximately 250 genes, and their expressions are restricted to the tumor and immune-privileged sites such as the

testis, the placenta, and during fetal development [83, 84]. One of the important characteristics of CTAs is that they are not expressed in normal healthy tissues. Since the testis/placenta lacks the expression of MHC alleles, the immune system will not recognize CTAs as self-proteins [83, 84].

Certain types of cancers can express CTAs. Based on the frequency of CTAs expression, cancer can be classified into "CT-rich" tumors such as melanoma, ovarian cancer, and lung cancer; "CT-poor" tumors such as RCC, colorectal cancer, and lymphoma/leukemia; and "CT-intermediate" tumors such as breast cancer and prostate cancer [85, 86].

CTAs can be classified into two types: CT-X encoded on the X chromosome, such as MAGE-A and NY-ESO-1, and non-CT-X [83]. The first CT-X antigen identified in melanoma is MAGE-A [83]. In addition, NY-ESO-1 is another CT-X antigen identified in esophageal squamous carcinoma [83]. CT-X antigens are highly immunogenic and can elicit potent integrated natural humoral and cellular responses [83, 84]. In 2009, the National Cancer Institute conducted a pilot project to prioritize and score the potential for immunotherapy application of 75 tumor antigens. MAGE-A and NY-ESO-1 were among the promising potential target antigens for immunotherapy and ranked 8 and 10, respectively [87]. Therefore, CT-Xs are of potential interest as targets for immunotherapy. One of the advantages of targeting CTAs is activating a long-term response against CTA-expressing cancer cells with minimal side effects on normal tissue [83, 84].

CTAs are important source of antigens on the tumor cell surface, and they are targets for cancer vaccine and T-cell therapy, including CAR-T [83, 84]. However, the

expression of many CTAs such as MAGE-A and NY-ESO-1 is epigenetically silenced by DNA methylation [76]. Therefore, the use of DNMTi such as decitabine (DAC) reactivates their expression [76]. It has been It has been proposed that DAC can be used as a collaborative agent in tumor immunotherapy protocols [88]. Previous studies have found that DAC treatment results in the upregulation of CTAs on tumors cells including colorectal cancer and acute myeloid leukemia [89, 90]. It has been demonstrated that the upregulation of CTAs was specific to the tumors, which is important for clinical application [83].

1.4.3. The Significance of Antigen Presentation for Cancer Immunotherapy

Immunotherapy, including immune checkpoint inhibitors, has been associated with clinical benefits and improved survival of many cancer patients, including those with metastatic disease [91]. A proper antigen presentation of tumor antigens by MHC is essential for the ICI efficacy. A critical step of antigen presentation is mediated by MHC: T-cell receptor (TCR) interactions, resulting in activation of cytotoxic $CD8^+$ T-cells and/or $CD4^+$ T helper cells [91]. Thus, several strategies have been tried to enhance ICI efficacy through upregulation of tumor-specific antigen expression, enhance antigen presentation, and stimulate T cell functions. All these factors act together to promote immune recognition of cancer cells and enhance anti-tumor immunity against tumor antigens [91, 92]. It has been reported that there was a positive correlation between infiltration of $CD8^+$ and $CD4^+$ T cell, which is a good prognostic marker, and MHC expression [93, 94]. Furthermore, tumor regression in a patient with regressing melanoma lesions was correlated with the induction of MHC and interferon-stimulated genes, indicating an increase in antigen presentation of tumor cells [94]. Moreover, there were

similarities between the histological and molecular signature of tumor rejection mediated by $CD8^+$ cytotoxic T cells and the signature found in allograft rejection and graft versus host disease, indicating an activation of an immune system [94, 95].

Despite the success of ICIs, several patients do not respond to the treatment. In addition, many patients develop resistance to ICIs [91]. One of the resistance mechanisms to ICIs is mediated by alterations in the MHC-I antigen presentation pathway, such as downregulation of MHC-I molecules and loss of β_2M expression [92, 96]. It has been demonstrated that loss of β_2M expression can result in impaired antigen presentation to cytotoxic $CD8^+$ T cells due to the loss of MHC-I expression on the cell surface [92, 96]. Defective MHC-I antigen presentation can result in decreased immune recognition of tumor cells and, therefore, impair eradication of the tumor cells by cytotoxic $CD8^+$ T cells. It has been reported that infiltration of a high number of cytotoxic $CD8^+$ T cells is associated with MHC-I expression on tumor cells [92, 96]. Furthermore, it has been found that low expression of MHC-I in certain cancers, such as breast cancer, is correlated with infiltration of fewer cytotoxic $CD8^+$ T cells compared to MHC-I high cancers [92, 97]. In addition, loss of MHC-I is positively correlated with poor prognosis and worse clinical outcomes in many cancers, including melanoma, glioblastoma, colorectal, bladder, uterine, cervical, head/neck, and breast cancers [92]. One of the proposed strategies to restore MHC-I expressions is by using DNMTis such as DAC since their expression can be regulated by DNA methylation [92, 96].

Although cytotoxic $CD8^+$ T cells are considered the main effector immune cells for successful ICIs treatment, $CD4^+$ T helper cells also play essential roles for an effective response to ICI by supporting $CD8^+$ T-cell activation and production of memory

T cells [91, 98]. One important function of T helper 1 (Th1) $CD4^+$ cells is the secretion of IFNγ and other activating cytokines [91]. In contrast to $CD8^+$ T cells, $CD4^+$ T cells can recognize a wider range of antigens [91, 99]. One of the reasons for this difference might be the greater repertoire of MHC-II restricted antigens and thus could be important for tumors that express fewer numbers of neoantigens [91]. In addition, cytotoxic $CD8^+$ T cells requires $CD4^+$ T helper cells helps in order to generate an effective and long-lasting response [91, 98]. It has been demonstrated that co-stimulation of both $CD8^+$ cytotoxic T cells and $CD4^+$ T cells is required for anti-PD-1 therapy responsiveness in several murine models [98].

It has been reported that several human cancers can express MHC-II and related pathway components, such as melanoma, breast cancer, colorectal cancer, ovarian cancer, prostate cancer, classic Hodgkin lymphoma, glioma, and non-small cell lung cancer [91, 100-103]. Furthermore, it has been found that there is a strong association between tumor-specific MHC-II (tsMHC-II) expression and favorable patient outcomes in several studies in multiple cancer types [91, 100-103]. For example, there was a positive correlation between tsMHC-II expression and prolonged patient survival in melanoma and classic Hodgkin lymphoma patients who received anti-PD-1/anti-PD-L1 [91, 100, 101]. In addition, it has been shown that upregulation of tsMHC-II expression in TNBC patients with lymph node metastases following adjuvant radiotherapy and/or chemotherapy was positively associated with improved patient outcome [102]. Furthermore, there was a strong association between improved PFS and the mRNA levels of 13 genes of MHC-II pathway including CIITA, CD74, HLA-DPA1, HLA-DPB1, HLA-DPB2, HLA-DQA1, HLA-DRB1, HLA-DRB5, and HLA-DRB6 as well as CIITA

or CD74 alone in TNBC patients [103]. Furthermore, the expression of tsMHC-II has been shown to be linked to the presence of a higher number of both $CD4^+$ and $CD8^+$ tumor-infiltrating lymphocytes (TILs), loss of lymphovascular invasion, the presence of a higher number of tertiary lymphoid structures, increased expression of IFNγ-stimulated gene including PD-L1 and upregulation of IFNγ, IL2, and IL12 mRNA which are Th1 cytokines [91, 102]. Importantly, tsMHC-II could be a predictive clinical biomarker of a T cell-inflamed tumor since MHC-II expression is upregulated by IFNγ [91].

1.5. Tumor Microenvironment (TME)

1.5.1. Characteristics of Hot tumors and Cold Tumors

Several evidence indicated that cellular and acellular components in tumor microenvironment (TME) can reprogram the process of carcinogenesis including tumor initiation, growth, invasion, metastasis, and response to therapies, particularly immune check point inhibitors [104]. Cancer research and treatment have switched from a cancer-centric model to a TME-centric one [104]. Converting cold TME into hot one is one of the approaches to enhance the response to cancer immunotherapy including immune check points inhibitors [104]. The tumor microenvironment (TME), which is the environment surrounding the tumor cells, is the ecosystem that consists of immune cells, the extracellular matrix, blood vessels, and other cells, like fibroblasts [105]. Tumor cells can interact with their microenvironment through complex signaling networks and, therefore, can influence TME, positively or negatively [105, 106]. This interaction can affect tumor progression and determine whether the primary tumor is eradicated, metastasizes, or establishes dormant micro-metastases [105, 106]. Furthermore, TME plays a crucial role in shaping the therapeutic responses and resistance to immune

checkpoint inhibitors (ICIs) [106]. The presence of hot TME is essential to determining the responsiveness to ICIs [106]. Therefore, it is important to understand the mechanisms responsible for the existence of hot and cold tumors.

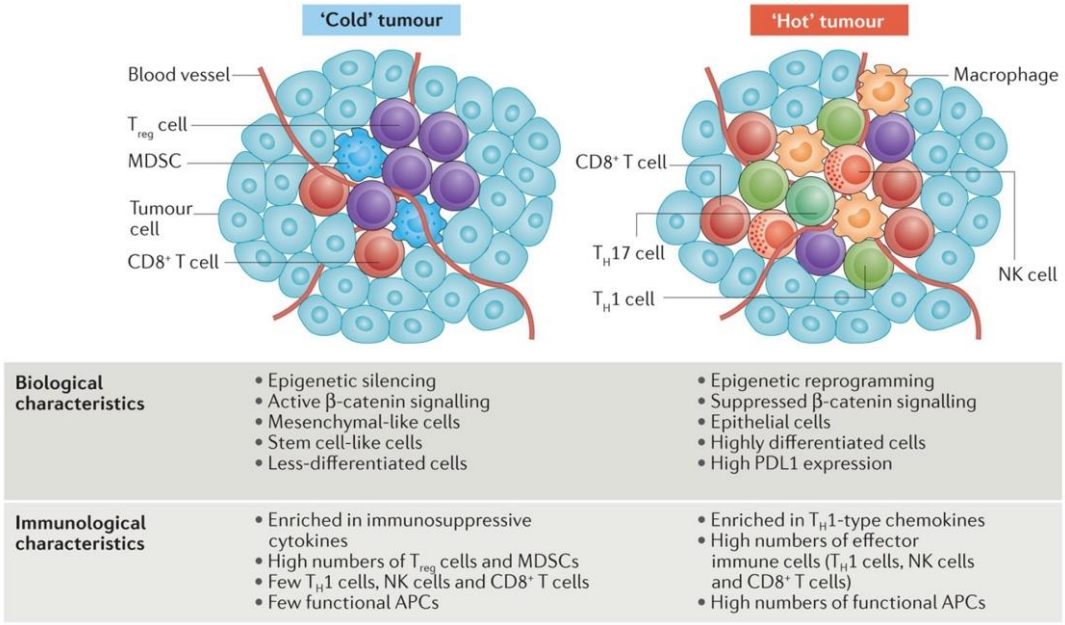

Figure 1.9. The Biological and Immunological Characteristics of Hot and Cold Tumors. *Reprinted with permission from: Nagarsheth, N., M.S. Wicha, and W. Zou, Chemokines in the cancer microenvironment and their relevance in cancer immunotherapy. Nat Rev Immunol, 2017. 17(9): p. 559-572.*

The biological and immunological characteristics of hot (inflamed) tumors and cold (non-inflamed) tumors are shown in Figure 1.9. In contrast to cold tumors, hot tumors have been associated with favorable responses to ICIs [106]. Hot tumors are characterized by increased infiltration of effector immune cells that exert antitumor effects such as cytotoxic $CD8^+$ T cells, $CD4^+$ T helper 1 (Th1) cells, polyfunctional Th17 cells, and natural killer (NK) cells [106, 107]. Cytotoxic $CD8^+$ T cells, Th1 cells, and NK cells can secrete IFNγ [58, 106]. IFNγ enhances antigen presentation via stimulation of MHC and immunoproteasome expression [58, 106]. Furthermore, IFNγ can suppress tumor cell growth by inducing the expression of several interferon-stimulated genes

(ISGs) that exert anti-proliferative and apoptotic effects. Moreover, IFNγ can induce the expression of PD-L1 [58, 106]. Furthermore, hot tumors infiltrate with high numbers of functional antigen-presenting cells (APCs) such as macrophages and dendritic cells that play an important role in activating the effector immune cells, thereby promoting tumor regression [107]. In addition, hot tumors exhibit several biomarkers include cytokines and chemokines release, high expression of T-cell associated factors such as perforin and granzyme B, and upregulation of PD-L1 [106, 107]. Also, hot tumors have low β-catenin levels and high numbers of epithelial cells [107].

In contrast to hot tumors, cold tumors are characterized by infiltration of immune suppressor cells such as myeloid-derived suppressor cells (MDSCs) and regulatory T (Treg) cells [107]. These cells exert pro-tumor effects and suppress antitumor immune responses and enhance and maintain cancer stemness and angiogenesis, resulting in cancer progression [107]. In addition, cold tumors are poorly infiltrated with cytotoxic $CD8^+$ T cells [106, 107]. One of the main characteristics of cold tumors is hyperactivation of the Wnt/β-catenin signaling pathway [106, 107]. Several studies have reported that high levels of β-catenin were negatively correlated with cytotoxic $CD8^+$ T cells infiltration and hot inflamed tumors [108-112]. For example, in melanoma, active tumor β-catenin signaling resulted in limiting the recruitment of $CD103^+$ dendritic cell (DC) and activation of cytotoxic $CD8^+$ T cell through downregulation of CCL4 expression [112]. In addition, high levels of tumor β-catenin can promote cancer stemness [107]. Furthermore, the expression of several genes associated with hot inflamed tumors including Th1-associated chemokines such as CXCL9 and CXCL10,

MHC molecules, and PD-L1 are repressed in cold tumors. The expression of these genes are epigenetically silenced by DNA methyltransferase (DNMT) [107].

One of the strategies to convert cold tumors into hot tumors and improve the responsiveness to ICIs is using DNMT inhibitors such as decitabine [106, 107]. In addition, Wnt/β-catenin inhibition could be another promising target [107]. Converting cold tumors into hot by epigenetic reprogramming and the suppression of Wnt/β-catenin signaling can result in promoting the infiltration of effector immune cells that exert antitumor effects such as cytotoxic $CD8^+$ T cells, Th1 cells, NK cells, and functional APCs, leading to tumor regression [107].

1.6. Cancer Immunotherapy

1.6.1. Immune Checkpoint Inhibitors (ICIs)

Cancer immunotherapy is a type of cancer treatment that can directly or indirectly target the immune system to trigger anti-tumor immune response [113]. Several approaches have been used to stimulate and enhance the immune system functions to fight the cancer cells. Examples of cancer immunotherapy include the use of specific drugs such as monoclonal antibodies (e.g. immune checkpoint inhibitors (ICIs)) that target specific proteins on the surface of cancer cells or immune cells, and other therapies like cytokines, oncolytic virus therapies, cancer vaccines or cell-based therapies (e.g. adoptive T cell transfer and chimeric antigen receptor T cell therapies) [113].

One of the fundamental pillars of cancer treatment is immune checkpoint inhibitors (ICIs) [113, 114]. ICIs can induce an anti-tumor immune response by inhibiting immune checkpoints. In normal physiological conditions, the main function of immune checkpoints, e.g. CTLA-4 and PD-1 pathways, is to downregulate T cell responses,

providing a protection of the body from damaging immune responses, such as autoimmune disease [113]. However, one of the mechanisms that tumors use to evade the immune system is through the stimulation of immune checkpoints and therefore, suppression the T cell response [113]. Thus, targeting these immune checkpoint pathways are one of the approaches to induce an anti-tumor immune response and convey potential therapeutic benefits in cancer patients [113, 114].

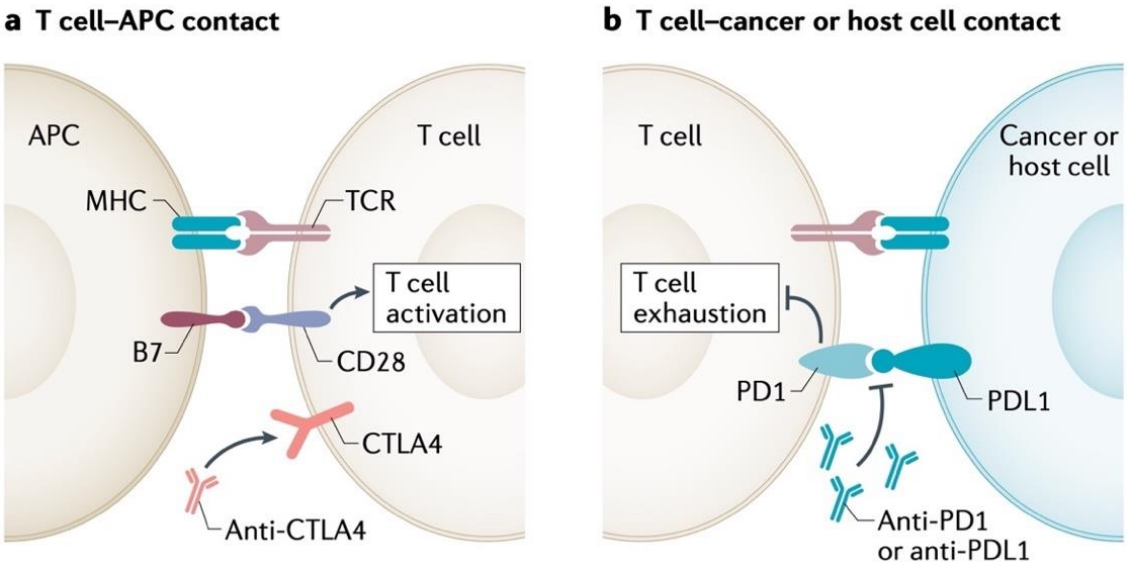

Figure 1.10. Mechanism of Actions of ICIs. *Reprinted with permission from: Wright, J.J., A.C. Powers, and D.B. Johnson, Endocrine toxicities of immune checkpoint inhibitors. Nature Reviews Endocrinology, 2021. 17(7): p. 389-399.*

The mechanism of actions of ICIs are represented in Figure 1.10. The two main pathways targeted by ICIs are CTLA-4 and PD-1/PD-L1 [113-115]. The activation of T-cells requires two distinct signals: first, the binding of a T cell receptor (TCR) on naïve T cells with the antigenic peptide presented on the surface of antigen-presenting cell (APCs) via MHC; and second, a co-stimulatory signal that is mediated through the binding of CD80 (B7-1) or CD86 (B7-2) on the APC with CD28 on the T cells [113-115]. During the early stages of T cell activation, the CTLA-4 is overexpressed on the T

cell surface. Both CTLA4 and CD28 share similar structure. However, CTLA-4 competes with CD28 and has higher affinity than CD28 for binding to CD80 and CD86, thereby blocking sustained T cell activation [113-115]. Pharmacological inhibition of CTLA-4 with ICIs can permit CD28-CD80 or CD28-CD86 and thereby facilitate T cell activation [113-115]. On the other hand, the checkpoint PD-1, which is a receptor on T cells, is upregulated during the late stages of T cell activation [113-115]. The interaction between PD-1 on T cells and its ligand PD-L1, that can be expressed on tumor cells and APCs, activated a cascade of T cell inhibitory processes known as T cell exhaustion [113-115]. This interaction is important to limit autoimmune reactions in physiological conditions. However, cancer cells utilize this process to evade from immune system by upregulating PD-L1 expression. Pharmacological targeting of either PD-1 or PD-L1 by ICIs can prevent PD-1-PD-L1 interaction, leading to impede T cell exhaustion, permit T cell activation and survival, and promote anti-tumor T cell activity [113-115].

ICIs that are approved by FDA: CTLA-4 inhibitor (Ipilimumab), PD-1 inhibitors (nivolumab, pembrolizumab and cemiplimab) and PD-L1 inhibitors (atezolizumab, avelumab and durvalumab) [113, 114]. ICIs have been approved by FDA either as monotherapy or in combination with other treatments such as targeted therapy or chemotherapy in 17 different types of cancer including cancers of the skin, kidney, lung, head and neck, bladder, breast, etc. [114]. The response rates are variable and ranged from 15–25% in most solid tumors including lung cancer to 40–60% in mismatch repair-deficient cancers and skin cancers, including melanoma to 80–90% in Hodgkin lymphoma [114]. Sometimes, the responses can be durable and can lead to a cure of the cancer [114]. Furthermore, ICIs show clinical benefits in metastatic patients and

approximately 50% of all patients with metastatic cancer can be eligible for ICIs treatment [114].

One of the key challenges of using ICIs is their uncontrolled effects on the immune system that can lead to development of immune-related adverse events (irAEs) [113, 114]. In 2018, there was nearly 13,000 cases reported of irAEs [113]. ICIs-related irAEs account for more than two-thirds of reported cases of cancer immunotherapy-related irAEs [113]. Furthermore, 60% of reported cases are associated with the use of anti-CTLA-4 (ipilimumab), and anti-PD-1 (nivolumab and pembrolizumab) [113].

IrAEs result from non-specific upregulation of the immune system and excessive activation of immunity against normal organs [113]. IrAEs are different than the adverse effects associated with standard chemotherapy. IrAEs can affect any organ system [113]. The median onset of irAEs has been reported within 2-16 weeks of ICI initiation, depending on the organ system involved [113]. However, irAEs can occur within a few days of ICI initiation, and up to one year after completion of treatment [113]. Dermatological toxicity is the most common early irAEs, occur between 1 and 12 weeks after treatment initiation, for anti-CTLA-4 and anti-PD-1 [113]. It has been reported that the most common irAEs associated with anti-CTLA-4, ipilimumab, are dermatological, gastrointestinal and renal toxicities, anti-PD-1, pembrolizumab, are arthralgia, pneumonitis and hepatic toxicities, anti-PD-1, nivolumab, are endocrine toxicities, and anti-PD-L1, atezolizumab, are hypothyroidism [113]. Consistent with the difference in the mechanism of action between anti-CTLA-4 and anti-PD-1/anti-PD-L1, irAEs related to anti-CTLA-4 or anti-PD-1/anti-PD-L1 can be distinguished. Generally,

irAEs associated with anti-PD-1/anti-PD-L1 are more tolerated than the ones associated with anti-CTLA-4 [113].

Management of irAEs is crucial to improve patients' quality of life and long-term outcomes [113]. The first-line treatment of irAEs for patients require a systemic therapy is glucocorticoids with an exception for the endocrine system toxicities [113]. In severe/refractory cases, other treatment options include immunosuppressants such as mycophenolate-containing immunosuppressants, cyclosporine and tacrolimus, intravenous immunoglobulin, plasma exchange, and monoclonal antibodies such as infliximab (TNF inhibitor) could be considered depending on the affected organ system [113]. These therapeutic suggestions are considered based on recommendations collected from different resources: official guidelines, data from some retrospective studies, and isolated published cases [113].

1.6.2. Immune Checkpoint Inhibitors in TNBC

The treatment landscape of TNBC has changed with the approval of ICIs, anti-PD-L1 and anti-PD-1. In March 2019, initial results from the phase III IMpassion130 (NCT02425891), a multicenter, international, double-blinded, placebo-controlled, and randomized trial, led to FDA granted accelerated approval of atezolizumab in combination with chemotherapy, nab-paclitaxel, for the treatment of metastatic TNBC or TNBC patients with unresectable locally advanced disease [116]. The approval was for subgroup of patients whose tumors were PD-L1 positive (PD-L1 positive patients were selected based on the FDA-approved test (VENTANA PD-L1 (SP142) Assay) and were defined as PD-L1 positive staining in tumor-infiltrating immune cells of any intensity covering ≥ 1% of the tumor area). 902 TNBC patients with unresectable locally advanced

or metastatic disease and who previously untreated with chemotherapy for metastatic cancer were enrolled into the IMpassion130 trial [116]. The patients were randomized in a 1:1 ratio (451 in each arm). The study group received atezolizumab at 840 mg IV on days 1 and 15 in combination with 100 mg/m^2 IV on days 1, 8, and 15 of a 28-day cycle. The control group received nab-paclitaxel with placebo [116]. The primary endpoints were progression-free survival (PFS) in the intent to treat (ITT) population and the PD-L1 positive subgroup as well as overall survival (OS) in the ITT population [116]. The OS was supposed to be tested in PD-L1 positive subgroup if it was significant in the ITT population. The trial was successful to meet its PFS primary endpoint in the ITT population and the PD-L1 positive subgroup. In the ITT population, the median PFS was 7.2 months and 5.5 months for the study group (atezolizumab + nab-paclitaxel) and for control group (placebo + nab-paclitaxel), respectively (hazard ratio (HR) for progression or death, 0.80; 95% confidence interval (CI), 0.69-0.92; *P*=0.002). In the PD-L1 positive subgroup, the median progression-free survival was 7.5 months for the study group and 5.0 months for the control group (HR, 0.62, 95% CI, 0.49-0.78; *P*<0.001) [116]. The study did not meet its OS primary endpoint. In the ITT population, the median OS was 21.3 months for the study group and 17.6 months for the control group (HR, 0.84; 95% CI, 0.69-1.02; *P*=0.08) [116]. In the PD-L1 positive subgroup, the median OS was 25.0 months and 15.5 months for the study group and for control group, respectively (HR, 0.62; 95% CI, 0.45-0.86) [116].

In September 2020, the final OS analysis was presented at the European Society for Medical Oncology (ESMO) Virtual Congress [117]. The data demonstrated that there were no statistical significance differences in OS between the two arms of the trial in the

ITT population. However, in the PD-L1 positive subgroup, patients who received atezolizumab + nab-paclitaxel had a prolonged OS of 7.5 months compared to the group who received placebo + nab-paclitaxel (25.4 months vs 17.9 months, respectively) [117]. According to the prespecified testing hierarchy of the trial, the statistical significance in OS between the study group and control group was not formally tested in the PD-L1 positive subgroup [116, 117].

In August 2021, Roche (the company who made atezolizumab) decided to voluntarily withdraw atezolizumab's accelerated approval with nab-paclitaxel for metastatic TNBC indication in the U.S. According to Roche's announcement, the decision was made after consultation with the FDA, build on the FDA's assessment of the current metastatic TNBC treatment landscape and in agreement with the requirements of the accelerated approval program [118].

In November 2020, anti-PD-1, pembrolizumab, in combination with chemotherapy (nab-paclitaxel, or paclitaxel, or gemcitabine plus carboplatin) was the second ICIs received FDA accelerated approval to be used in TNBC with locally recurrent unresectable or metastatic disease who had not been previously treated with chemotherapy in the metastatic setting [119]. The approval was for PD-L1 positive patients (combined positive score (CPS) ≥10). PD-L1 status was determined by an FDA approved test, the PD-L1 IHC 22C3 pharmDx (Dako North America, Inc.). The accelerated approval was based on the initial results of the phase III KEYNOTE-355 trial (NCT02819518), which was a multicenter, double-blind, randomized, placebo-controlled, that enrolled 847 patients [119]. The patients were randomized in a 2:1 ratio: 566 patients in the study group arm, pembrolizumab + chemotherapy, and 281 patients in the control

group arm, placebo + chemotherapy [119]. Importantly, this trial evaluated the efficacy of ICIs with non-taxane drugs and enrolled patients with more challenging refractory metastatic TNBC like those with short disease-free interval (6 months). The randomization was based on the type of chemotherapy partner (taxane or gemcitabine/carboplatin), PD-L1 status (CPS ≥1 vs <1), and prior neoadjuvant therapy with same-class chemotherapy [119]. The study group received 200 mg of pembrolizumab every 3 weeks in combination with one of three chemotherapy drugs: nab-paclitaxel 100 mg/m^2 on days 1, 8, and 15, every 28 days; paclitaxel 90 mg/m^2 on days 1, 8, and 15, every 28 days; or gemcitabine 1000 mg/m^2 plus carboplatin AUC 2 on days 1 and 8, every 21 days [119]. The co-primary endpoints were PFS and OS in the PD-L1 positive group with CPS ≥10, PD-L1-positive group with CPS ≥ 1, and ITT populations [119]. The study met its PFS endpoint in patients with PD-L1–positive tumors (CPS ≥10) [119]. In patients with CPS ≥10, median PFS in the study group was 9.7 months and 5.6 months in the control group (HR for progression or death, 0.65; 95% CI, 0.49-0.86; one-sided *P*=0.0012) [119]. In the group with CPS ≥ 1, median PFS was 7.6 months and 5.6 months for study group and control group, respectively (HR, 0.74; 95% CI, 0.61-0.90) [119]. The result in this group did not meet the boundary for statistical significance. In the ITT population, median PFS was 7.5 in the study group compared to 5.6 months in the control group (HR, 0.82; 95% CI, 0.69-0.97) [119].

In July 2021, pembrolizumab, in combination with chemotherapy (nab-paclitaxel, or paclitaxel, or gemcitabine plus carboplatin) received regular FDA approval to treat TNBC with locally recurrent unresectable or metastatic disease whose tumors are PD-L1 positive (CPS ≥10). The study met its OS primary endpoint in PD-L1 positive patients.

(CPS ≥10). The final result was presented at the European Society for Medical Oncology (ESMO) Annual Meeting 2021 [120]. In PD-L1 positive patients (CPS ≥10), the median OS was 23.0 months with the study group compared to 16.1 months for control group (HR, 0.73; 95% CI, 0.55-0.95; *P*=0.0093) [120].

In July 2021, the results of phase III KEYNOTE-522 trial (NCT03036488) led to FDA accelerated approval of anti-PD-1, pembrolizumab, in combination with chemotherapy as neoadjuvant treatment, followed by surgery and then continued as a single agent as adjuvant treatment for high-risk, early-stage TNBC [121]. 1174 newly diagnosed high-risk early-stage TNBC patients who did not previously treated were enrolled into KEYNOTE-522, a randomized, multicenter, double-blind, placebo-controlled trial [121]. The patients were randomized in a 2:1 ratio to either study group or control group regardless of PD-L1 status. The study group, pembrolizumab + chemotherapy, received neoadjuvant treatment of pembrolizumab (200 mg every 3 weeks) plus paclitaxel (weekly) and carboplatin (weekly or every 3 weeks) for four cycles, followed by pembrolizumab (200 mg every 3 weeks) plus cyclophosphamide and either doxorubicin or epirubicin (every 3 weeks) for four cycles before surgery [121]. Adjuvant treatment with nine cycles of pembrolizumab (every 3 weeks; n=784) was continued after surgery [121]. The control group received placebo with chemotherapy. The study met the dual primary endpoints: the pathological complete response (pCR) rate and event free survival (EFS) [121]. The pCR rate was 64.8% and 51.2% for the study group and control group, respectively [121]. There was 13.6% improvement in the study group (*P*=0.00055). After a median follow-up of 39 months, there was 37% reduction in EFS in the study group compared to control group (HR, 0.63; 95% CI, 0.48-0.82; *P*=

0.00031). The 3-year event-free survival rate was 84.5% and 76.8% for the study group and control group, respectively, reported during an ESMO Virtual Plenary presentation [122].

1.7. CHA1 Combinational Therapy

1.7.1. Epigallacatechin-3-gallate (EGCG)

Cancer chemoprevention approaches including the use of naturally occurring phytochemicals are aimed at preventing, delaying, or suppressing the process of carcinogenesis [123, 124]. Among natural compounds, green tea has been extensively studied worldwide in a variety of diseases and the resulting data demonstrated that green tea has beneficial effects on human health such as anti-cancer, anti-obesity, anti-diabetic, anti-cardiovascular, anti-infectious and anti-neurodegenerative effects [125]. Green tea leaves contain four main types of catechins: epigallocatechin-3-gallate (EGCG) that represents approximately 59% of the total catechins, epigallocatechin (EGC) (19%), epicatechin-3-gallate (ECG) (13.6%), and epicatechin (EC) (6.4%) [123, 124]. Figure 1.11 represented the chemical structures of green tea catechins.

EGCG is an active ingredient of green tea and is responsible for green tea's biological effects [125]. It has been shown that EGCG was effective in inhibition the growth of several types of cancer, including lung, skin, liver, and breast cancer [126, 127]. Antioxidant effect and the ability to scavenge reactive oxygen species (ROS), which facilitate oxidative DNA damage, mutagenesis, and tumor promotion, is one of the mechanisms by which EGCG exert its anti-cancer effects [125]. ROS can promote cancer cell growth, invasion, and metastases by activation of NF-κB which results in facilitating the expression of inflammatory genes such as cyclooxygenase (COX), nitric oxide (NO),

and tumor necrosis factor-α (TNF-α) [125]. Therefore, EGCG by scavenging ROS can inhibit NF-κB and suppress the expression of COX, NO and TNF-α, leading to anti-cancer effects [125].

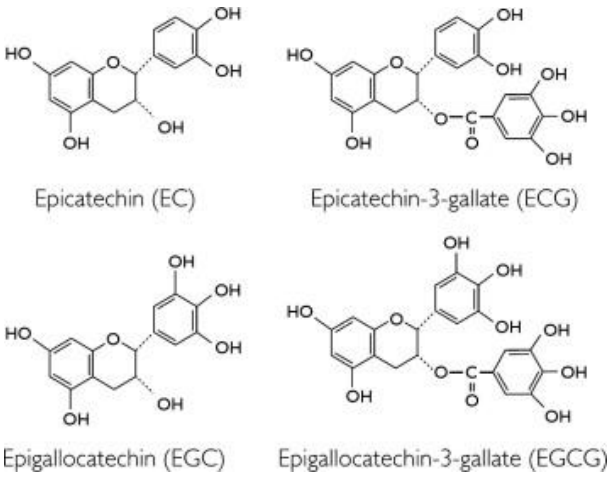

Figure 1.11. Chemical Structures of Green Tea Catechins. *Reprinted with permission from: Namal Senanayake, S.P.J., Green tea extract: Chemistry, antioxidant properties and food applications – A review. Journal of Functional Foods, 2013. 5(4): p. 1529-1541.*

In addition to antioxidant effect, EGCG can have pro-oxidant activity which is important for the induction of apoptosis and inhibition of cell growth of cancer cells [125]. Production of ROS by EGCG can activate AMPK, through induction of Ca^{2+}/calmodulin-dependent protein kinase (CaMKK) and/or liver kinase B1 (LKB1), which in turn resulted in suppression of mechanistic target of rapamycin kinase (mTOR), leading to anti-cancer effects [125]. It is not clear by which mechanism EGCG can act as an antioxidant or a pro-oxidant [125]. Several factors can contribute to EGCG's activity include cell types considered, cellular concentrations, and the co-presence of other antioxidants [125]. It has been reported that either the antioxidant or pro-oxidant activities of EGCG are involved in various mechanisms of EGCG's anti-cancer effects [125].

One important anti-cancer effect of EGCG is the induction of apoptosis [123, 125, 127]. Several studies have demonstrated EGCG's apoptotic effect and its mechanism of action [123, 125, 127]. ROS can activate gene expression of anti-apoptotic B-cell lymphoma-2 (Bcl-2) via activation of NF-κB [125]. Therefore, EGCG can downregulate Bcl-2 via quenching of ROS, resulting in apoptotic cell death of cancer cells [125]. Furthermore, EGCG can induce apoptosis via upregulation of apoptosis regulator Bcl-2 associated X (Bax) and activation of caspase-9, caspase-3, and caspase-8 [125]. It has been shown that treatment of breast cancer MCF-7 cells with EGCG induced apoptosis via stimulation of caspase-9, caspase-3, and poly (ADP-ribose) polymerase-1 cleavage [128].

Anti-angiogenesis effect of EGCG has been reported in several studies [123, 125, 127]. Treatment of gastric cancer SGC7901 cells under hypoxia induced by cobalt chloride with EGCG downregulated the protein expression of hypoxia-inducible factors-1 (HIF-1) and vascular endothelial growth factor (VEGF) proteins [129]. In E0771 syngeneic breast cancer model and in E0771 cultured cells, EGCG treatment resulted in decreased VEGF expression [130]. Furthermore, EGCG treatment of TNBC Hs578T cells resulted in inhibition of VEGF expression, suggesting the suppressive role of EGCG in TNBC cell migration [131].

The inhibitory effect of EGCG on Wnt/β-catenin has been reported [132]. Treatment of MDA-MB-231 TNBC human cell lines with EGCG resulted in suppressing the growth of MDA-MB-231 cells by downregulating the protein expression of β-catenin, cyclin D1, and phosphorylated Akt (p-AKT) [132]. In addition, the suppressive effect of EGCG on β-catenin expression was potentiated when MDA-MB-231 cells were pre-

treated with inhibitors of phosphoinositide 3-kinases (PI3Ks) (LY294002 or wortmannin) [132]. Taken together, these data suggest that EGCG could retard the growth of MDA-MB-231 TNBC human cell lines by inactivating the β-catenin signaling pathway.

One important mechanism linked to EGCG's anti-cancer effects is epigenetic modification [125]. The ability of such compounds to inhibit DNA methyltransferase (DNMT) and histone deacetylase (HDAC) makes them potential anti-cancer drugs [125]. It has been reported that EGCG treatment of human cervical carcinoma HeLa cells resulted in reduced the proliferation of HeLa cells and expression of DNMT1 [133]. Furthermore, it has been demonstrated that treatment of HeLa cells with EGCG caused inhibition of the expression of DNMT3B and HDAC1 in a time-dependent manner [134].

Notwithstanding encouraging pre-clinical outcomes of EGCG, its applicability to humans was with limited success [123, 127]. The data obtained from in vivo studies and human epidemiological studies on different types of cancers were inconsistent and in some cases were contradictory [127]. Moreover, EGCG showed poor bioavailability and poor stability which highlights the differences between in vitro and in vivo conditions, indicating a limitation for the use of EGCG in human populations [123, 127]. One of the strategies to overcome this issue and to improve EGCG's stability and bioavailability was based on the use of nanoparticles (NPs) in which EGCG is encapsulated [123, 127].

1.7.2. Decitabine (DAC)

Abnormal epigenetic modifications play critical role in tumorigenesis development [135]. DNA methylation of the cytosine-phosphate-guanine (CpG) dinucleotide islands in the promoter regions of tumor suppressors genes is a major driver of tumorigenesis in many cancers including TNBC [135, 136]. DNA methylation

involves the transfer of a methyl group from *S*-adenosyl-l-methionine to C-5 position of cytosine, mostly within CpG dinucleotide [135, 137]. DNA methyltransferases (DNMTs) include DNMT1, DNMT3A, and DNMT3B catalyze this reaction [135, 137]. DNMT1 is responsible to maintain the methylation pattern from the parental DNA that is copied onto the newly synthesized DNA strand during DNA replication. DNMT3A and DNMT3B catalyze *de novo* DNA methylation of previously unmethylated DNA [135, 137].

Decitabine (DAC), which acts as DNMTi, is an FDA-approved drug for treatment of myelodysplastic syndromes (MDS) [138]. In addition, it has an off-label use in acute myeloid leukemia (AML) [138]. Despite the successful use of DAC in hematological tumors, it does not work as monotherapy in solid tumor [139]. It has been suggested that DAC can be used to sensitize the tumors to ICIs response in solid tumors [139].

The mechanism of action of DAC is shown in Figure 1.11. DAC has different mechanism of action at low dose compared to high dose [135, 140]. At low dose, DAC inhibits DNMT and reactivates the expression of methylated-silence genes that are associated with induction of cell differentiation, apoptosis, and senescence, and anti-proliferation. In contrast, at high dose, DAC causes cytotoxicity [135, 140].

After cellular uptake of DAC by the nucleoside transport system, it is converted by deoxycytidine kinase and by other kinases to its active triphosphate form which is then incorporated into DNA by DNA polymerase [137]. Incorporation of low dose of DAC triphosphate causes formation of a covalent complex between DAC-DNA and DNMT at CpG methylation sites and traps the enzymes on DNA, leading to depletion of the DNMT pool and inhibition of DNMT function [135, 140]. On the other hand, incorporation of a

high dose of DAC triphosphate can induce DNA damage, and inhibit DNA synthesis, resulting in cell cycle arrest and cell death [135, 140].

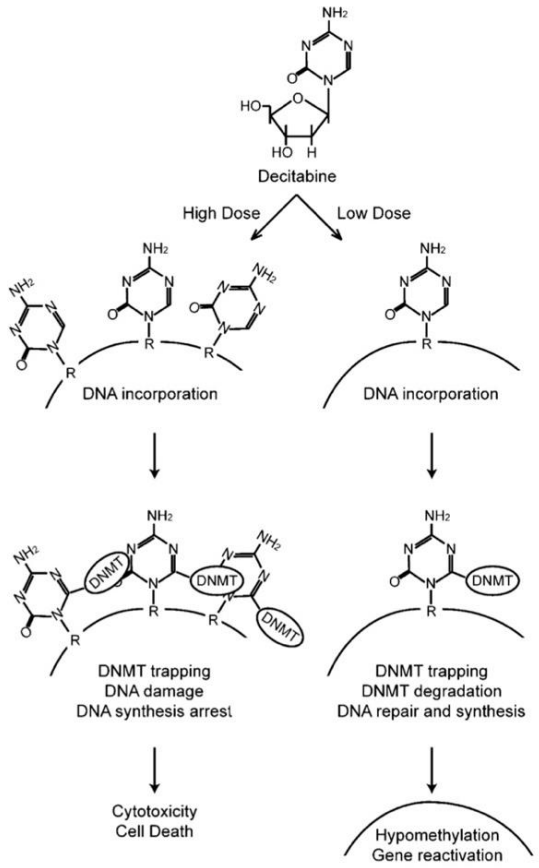

Figure 1.12. Mechanism of Actions of Decitabine. *Reprinted with permission from: Oki, Y., E. Aoki, and J.-P.J. Issa, Decitabine-Bedside to bench. Critical Reviews in Oncology/Hematology, 2007. 61(2): p. 140-152.*

One of the important effects of DAC is reactivation of the expression of tumor suppressor genes such as P53, P15, P16 and BRCA1 [135, 137]. Furthermore, DAC can reinduce the expression of genes involved in apoptotic pathway such as XAF1, and TRAIL receptor-1, which are involved in interferon-induced apoptosis, and APAF1, a downstream element of the p53 apoptotic pathway [135].

It has been reported that DAC can induce the expression of several genes that play central role in immune system regulation such as MHC, IFNγ, and PD-L1 [135, 141]. In

addition, DAC can upregulate the expression of CTAs that can trigger cellular and humoral immune responses and increase the immune system recognition of tumor cells [76, 135]. Taken together, these DAC's expression-restoring properties suggest that DAC could sensitize the tumor to ICIs.

1.7.3. CHA1 Treatment

The Yee lab has identified HMG-box transcription factor 1 (HBP1) as a Wnt repressor and has shown that the expression of HBP1 was deleted, mutated or decreased in TNBC [142]. HBP1 inhibits Wnt/β-catenin signaling by binding to the LEF/TCF complex and prevents its function as a transcriptional activator [143]. In addition, the Yee lab has found that there was a reduction or loss of HBP1 in clinical invasive breast cancer samples [142]. It also has been found that HBP1, by suppressing Wnt/β-catenin signaling, inhibits tumorigenesis of mammary gland cells [56]. The survival rate for patients with invasive breast cancer was reduced by 30% when the disease is accompanied by reduction or loss of HBP1 [56]. Hence, targeting HBP1 to inhibit Wnt/β-catenin signaling could be one potential candidate for anti-TNBC therapy.

The Yee lab has been exploring CHA1 which is a combinatorial drug approach to suppress Wnt signaling, using epigallocatechin-3-gallate (EGCG), the active ingredient of green tea, and Decitabine (DAC). Several epidemiological studies have reported that green tea consumption is associated with reduced breast cancer incidence and relapse [144-146]. Furthermore, EGCG has been studied in a large number of clinical trials for various types of cancers but has yielded controversial results [146, 147]. Mechanistically, the Yee's lab demonstrated that EGCG inhibits Wnt signaling *in vitro* through post-transcriptional stabilization of HBP1 mRNA [56]. In addition, EGCG can suppress DNA

methyltransferase (DNMT) activity and reactivate the expression of methylation-silenced genes in cancer cells [148]. From a mechanistic perspective, our work subsequently demonstrated that DNMT1 is a transcriptional target of HBP1 repression [149].

DAC is approved by FDA for the treatment of myelodysplastic syndromes and it is used in the treatment of acute myeloid leukemia [138]. It acts epigenetically to restore silenced genes through inhibition of DNMT [140]. Among the methylated genes that are regulated by DNMT and DNA methylation is the Wnt inhibitor sFRP1 [150, 151]. Impairing DNA methylation would be predicted to increase the expression of the sFRP1.

Taken together, these studies suggested that the combination of the DNMT inhibitor DAC and EGCG that induces HBP1 mRNA stabilization resulting in transcriptional downregulation of DNMT1 could have a more significant effect on DNMT1 function and thus DNA methylation. Thus, CHA1 combinational treatment could potentially restore the expression of Wnt inhibitors, HBP1 and sFRP1, indicating augmenting Wnt signaling inhibition could be achieved. The overall rationale for the combinatorial therapy is outlined in Figure 3.1.

One of special characteristic of EGCG is its ability to cross the blood brain barrier (BBB) [152]. Furthermore, it is distributed almost equally between brain and mammary gland [153]. Like EGCG, DAC can cross the BBB [154]. Thus, a combination therapy of CHA1 could be beneficial for TNBC patients with brain metastases since both drugs cross the BBB.

1.8. Hypothesis and Study Objectives

Triple-negative breast cancer (TNBC) is the most aggressive type of breast cancer, which is ER negative, PR negative, and does not have overexpressed HER-2 [1,

3, 7]. Since TNBC lack expression of common target markers, its treatment is challenging and is limited to chemotherapy, radiation, and surgery [155]. Therefore, finding a therapeutic target to manage TNBC becomes of great interest. Hyperactivation of the Wnt signaling pathway, which contributes to poor prognosis and metastasis, is a common feature of TNBC [34-36]. So, Wnt signaling is a potential therapeutic target to manage TNBC.

Preliminary data from the Yee lab indicated that CHA1 in combination inhibited tumor growth in TNBC human xenograft mouse model, while individually they had almost no effect. The mechanism relies on increasing HBP1 and sFRP1 expression levels as the Yee lab showed that tumors with knockdown of HBP1 and sFRP1 did not respond to CHA1. In addition, CHA1 treatment resulted in reduction of brain metastasis. Mechanistically, the Yee lab had shown that CHA1 biochemically suppressed the Wnt signaling pathway. Furthermore, transcriptomic and bioinformatic analysis using RNA-seq data from CHA1-treated tumors suggested a broad activation of cell-cycle inhibition, activation of apoptosis and other tumor-inhibitory pathways.

Treatment of TNBC with immune checkpoint inhibitors has recently gained significant attention after FDA approval of ICI, anti-PD-1 in combination with chemotherapy (nab-paclitaxel, or paclitaxel, or gemcitabine plus carboplatin) for PD-L1 positive patients (combined positive score (CPS) ≥10) [119]. Unfortunately, not all TNBC patients can be treated with anti-PD-1. In addition, the indication of anti-PD-L1, atezolizumab, in combination with nab-paclitaxel in TNBC was withdrawn after it failed to meet OS endpoint between the two arms of the trial in the ITT population [116, 118]. Therefore, there is only one option available for TNBC patients. One of the strategies that

used to enhance ICIs responsiveness is combining ICIs with a collaborative agents [139]. There is unmet need to identify and investigate the ideal collaborative agents.

The hypothesis of the study was that CHA1 increased the susceptibility of immune system to recognize the tumors and converted cold tumors into hot tumors. In addition, CHA1 could be a collaborative agent to improve the response to ICIs.

The first aim of the study was to investigate the immune therapeutic effects of CHA1. Upregulation of Wnt/β-catenin pathway and downregulation of IFN pathway have been associated with the development of resistance to ICIs [108]. Unbiased analysis of RNA-seq data from CHA1 treated tumors using Ingenuity Pathway Analysis (IPA) was used to identify the potential target molecular pathways. Activation of antigen presenting pathways was one of the most upregulated in the IPA analysis. Thus, I both proposed and completed multiple molecular tests to investigate how CHA1 changed the tumor microenvironment in TNBC human xenograft and TNBC syngeneic models. I showed that CHA1 treatment resulted in suppressing Wnt/β-catenin pathway and in increasing tumor immunogenicity via upregulation of cancer testis antigen, re-activation of antigen presentation, and induction of IFN signaling activity. I also found that CHA1 upregulated PD-L1 expression and induced T-cell inflamed gene signature beyond PD-L1. All this support that CHA1 could turn cold tumors into hot tumors, suggesting CHA1 could be a potential collaborative agent with ICIs.

The second aim of the study was to evaluate the efficacy of CHA1 in combination with immune check point inhibitors (ICIs). I investigated whether CHA1 sensitized the tumor to the ICIs. I showed that combination of CHA1 with anti-PD-L1 significantly suppressed TNBC tumor growth in a syngeneic mouse model.

Chapter 2: Materials and Methods

2.1. Cell Lines

Human cell lines: The IS13 cell lines, a derivative of MDA-MB-231 cell lines that express both luciferase and GFP, a gift from Dr. Gail Sonenshein, were used for the TNBC human xenograft experiment.

Mouse Cell Lines: 4-T1 cell lines, purchased from ATCC, were used for the TNBC syngeneic model.

2.2. Mutant Cell Construction in Human Cell Lines

Lentivirus knockdowns: LM1 cells, derivative of MDA-MB-231 cell lines, were transfected with lentiviral particles. Three shRNA constructs targeting HBP1, sFRP1 and pLKO control were used. The lentiviral transduction protocol from Sigma-Aldrich was used for viral transfection. 8 μg/ml of hexadimethrine bromide was added for enhancing transduction. Cells were selected with 1 to 2 μg/ml of puromycin. Knockdown of HBP1 and sFRP1 were confirmed with real time PCR by comparing the gene knockdown constructs to control.

2.3. Treatment Regimen for *in vitro* Study

DAC and EGCG were dissolved in PBS and ethanol with PBS, respectively. Cells were treated with 1μM of DAC + 10μM of EGCG (combination treatment), 1μM of DAC, 10μM of EGCG, and no treatment. Treatment was conducted for 96 hours All cells were maintained in the normal the media that contained Dulbecco's Modified Eagle Medium (DMEM) supplemented with 10% fetal bovine serum (FBS), antibiotics, and anti-trypsin during treatment. Media and drugs were replaced every 24 hours (four times during the 96-hour treatment period).

2.4. Animals

Six- to eight-week-old female NOD/SCID mice and Balb/c mice were purchased from Jackson Laboratory. Mice were housed in a sterile environment and maintained by DLAM (Division of Laboratory Animal Medicine) personnel in accordance with guidelines established by the Institutional Laboratory Animal Care and Use Committee (IACUC) at Tufts University-Tufts Medical Center.

2.5. Cells Preparation for Animal Surgery

Cells were cultured in the normal growth media (DMEM supplemented with 10% FBS, penicillin (100 units/ml), streptomycin (0.1 mg/ml), and 10 mM L-glutamine) and allowed to grow to no more than 85% confluence. To harvest cells, cells were initially trypsinized with 0.05% trypsin and subsequently washed with PBS. The cells were then re-suspended in serum-free, antibiotic-free Dulbecco's Modified Eagle Medium. To determine cell concentration for accurate inoculation into xenograft models, cells were stained with 0.4% trypan blue solution (Sigma) and counted using a hemocytometer. A 1:1 volume ratio of Matrigel (BD Biosciences) was used to set the cells for implantation/inoculation into the mammary fat pad of each individual mouse.

2.6. Animal Surgery

All animal surgeries were carried out in a procedure room under a sterile environment following guidelines for animal surgery establishment by Tufts Medical Center's Division of Laboratory Animal Medicine. Animals were initially anesthetized in an isoflurane chamber. During surgery, mice were administrated a steady flow of isoflurane through a nose conical. *Surgery:* area around the 4^{th} mammary fat pad was prepared by shaving hair and sterilizing with iodine and alcohol. Care was taken to locate

the 4^{th} mammary fat pad and an incision was made according to expose the area for implantation of cancer cells. Connective tissues were released to fully access the area for the inoculation of cells. A total volume of 30 µl or 35 µl containing $3 \times 10^5 – 5 \times 10^5$ cells suspended in a 1:1 ratio of serum-free, antibiotic-free media and Matrigel was injected into the mammary fat pad using a Hamilton Syringe. Following inoculation of cells, the incision was repaired using wound clips. The animals were allowed to recover from anesthesia under close monitoring. Buprenorphine was used as an analgesic (0.06 mg/kg). Animals were monitored for three days post-surgery for proper healing and any post-operative complication.

2.7. Treatment Plan for *in-vivo* Study

When tumors reached approximately 0.125 cc, treatments were initiated. Both EGCG (Sigma) and DAC (Sigma) were dissolved in sterile PBS. A 28-gauge insulin syringe was used for intraperitoneal injection (i.p). All treatments continued for the indicated time unless tumor size exceeded that allowed by IACUC guidelines or if the animal's health appeared to be deteriorating. Treatment plan was carried out in human xenograft model with MDA-MB-231 tumors, HBP1 knockdown MBA-MB-231 tumors and sFRP1 knockdown MBA-MB-231 tumors as well as in syngeneic model with 4-T1 tumors.

CHA1 QOD treatment protocol in TNBC human xenograft and TNBC syngeneic models: mice were randomly assigned to either control or experimental groups with at least five mice in each group. Mice in the CHA1 experimental group were injected i.p. on alternating days with either 16.5 mg/kg EGCG or 0.5 mg/kg DAC. Control mice were injected i.p. with 100 µL of saline each day.

EGCG QOD monotherapy in TNBC human xenograft: mice were injected i.p. on alternating days with 16.5 mg/kg of EGCG.

DAC QOD monotherapy in TNBC human xenograft: mice were injected i.p. on alternating days with 0.5 mg/kg of DAC.

CHA1 QD treatment in TNBC syngeneic models: mice were randomly assigned to either control or experimental groups with at least five mice in each group. 16.5 mg/kg of EGCG and 0.5 mg/kg of DAC were administrated concomitantly via i.p. injections during cycle 1 and cycle 2. The duration of each cycle was 5 days. There was 5 days recovery period between the cycles.

CHA1 + ICIs treatment in TNBC syngeneic models: mice were randomly assigned to either control or experimental groups with at least eight mice in each group. CHA1 QD treatment protocol was followed. Mice in ICIs treatment group and CHA1+ ICIs group received two doses of either anti-PD-L1 antibody (clone 10F.9G2, Bio X cell), anti-PD-1 antibody (clone RMP1-14, Bio X Cell), or anti-CTLA-4 antibody (clone 9H10, Bio X Cell). The doses were two days apart and administrated during the recovery period between the cycles of CHA1 treatment. The first dose of ICIs (100 μg/mouse) was administrated via i.p. injections on the first day of the recovery period and the second dose was administrated via i.p. injections on the fourth day of the recovery period.

2.8. Monitoring of Tumor Growth: Caliper Measurements

After cells implantation, animals were palpated for evidence of tumor. Once a measurable tumor was noted, caliper measurements were taken every other day. The two longest dimensions of the tumor were used to calculate tumor volume (the formula width^2 x length was used to determine tumor volume).

2.9. Bioluminescence Imaging for Quantitative *in vivo* Luminescence

Bioluminescence imaging quantitative in vivo luminescence was accomplished using the IVIS Imaging System (Xenogen). MDA-MB-231 cells used contain a luciferase gene construct that enabled visualization of live cells upon administration of luciferin (0.1mg/mouse). Animals were anesthetized in an isoflurane chamber after i.p. injection of luciferin and remained so through a nose conical during the entire imaging procedure. Acquisition time was 60 seconds when tumors were small and signal strengths were low. As tumor size increased, acquisition time was reduced to 30 seconds to avoid saturation. Analysis was performed using Living Image software (Xenogen). Measurements were collected as photon flux (measured in photons/s/cm^2/steradian) within a defined region of interest. Background flux was also measured in order to normalize data.

2.10. Termination of *in-vivo* Study

All animals were carefully monitored to ensure that tumor size is within limits established by IACUC and the animals were in good health. There were two instances where animals were sacrificed before the entirety of the experiment: tumor sizes exceeded 1 cm^3 limit and evidence that animal's health was deteriorating. After termination of animal, an autopsy was performed to look for any evidence of metastases and abnormalities. Suspected tissues were harvested for analysis. The primary tumor was harvested from each mouse and fixed with formalin. Fixed tissues were preserved in 70% ethanol. A small, unfixed sample from each mouse was stored at -80˚C for further analysis.

2.11. Immunohistochemistry and Immunofluorescence

Immunostainings of MHC-I and MHC-II of human xenograft tumor samples were performed by Tufts University Core Facility (Boston, MA). Immunostainings of Ki67, β-catenin, PD-L1, CD8, F4/80, FOXP3 of syngeneic tumor samples were performed by iHisto (Salem, MA). Cell membrane immunostaining for control and treated tumors was assessed by three investigators in a blinded fashion. The Allred scoring method was used as previously described for assessing the membrane proportion and staining intensity in scale between 0 to 8 [156]. The score was calculated from the sum of a proportion score (0-5 scale reflecting the percentage of cells with any stain) and a staining intensity score (0-3 scale reflecting the intensity of staining among the positive cells) [156]. A score between 0 and 2 indicates negative staining and a score between 3 and 8 indicates positive result [156]. Immunofluorescence staining of Ki67 and CD8 of syngeneic tumor samples was performed by iHisto (Salem, MA).

2.12. Total RNA Extraction and cDNA Synthesis

For in vitro experiment: cells were harvested for total RNA extraction after completion of treatments. For in vivo experiment: a small sample of tumor tissue was used for total RNA isolation. RNA extraction was performed using RNeasy Plus Mini Kit (Qiagen) and was eluted with RNase-free water. Nanodrop spectrophotometer (Thermo Scientific) was used to measure RNA concentration by measuring absorbance at 260nm. After determining RNA concentration, 500 μg of RNA was used to synthesize cDNA using iScript cDNA Synthesis Kit (Bio-Rad).

2.13. SYBR Green Real-time RT-PCR

cDNA synthesized from cells and animal tumors tissues was used for real-time PCR performed on iCycler (Bio-Rad) using a 2x SYBR Green master mixture (Bio-Rad) in a 20 μl reaction. All quantizations were normalized to endogenous 18 S RNA control. The relative quantitative value for each target gene compared with the calibrator for the target was expressed as comparative Ct ($2^{-(\Delta Ct-Cc)}$) method (Ct and Cc are the mean threshold cycle differences after normalizing to 18 S). Real-time RT-PCR experiments were performed in triplicates. Primer sequences were presented in Table 2.1 and Table 2.2. Human primers for HLA-DRB1 and VCAM1 were purchased from Bio-Rad.

Table 2.1. Human Primer Sequences

	Forward	Reverse
18s	GCCCGAAGCGTTTACTTTG	CTTAATCATGGCCTCAGTTCC
AXIN2	GTGTGAGGTCCACGGAAACT	GAATCATCCGTCAGCGCATC
CD74	CAGCGCGACCTTATCTCCAA	GGTACAGGAAGTAGGCGGTG
CTLA-4	TAATTGATCCAGAACCGTGCC	CTCTGTTGGGGGCATTTTCAC
DDX58	CTGGACCCTACCTACATCCTG	GGCATCCAAAAAGCCACGG
DHX58	GGGCCTCCAAACTCGATGG	TTCTGGGGTGACATGATGCAC
ERV3-1	AGCCGGAGCTTCTGGTGTAG	AGTGGGTCCTGGCGTCTTA
FASL	TGGAAATAAACTGCACCCGGAC	CTCTTTGCACTTGGTGTTGCTGG
HBP1	GGCGACGGGTTTGTC AGAG	TGCCAGATTGGGTAGGATCAC
HLA-B	CTAGCAGTTGTGGTCATCGGAG	GGAGGCGTGAAGAAATCCTG
HLA-DRB5	AGCATGGTGTGTCTGAAGC	CCCGTTGAAGAAATGACACTCA
ICAM1	CTATAAAGGATCACGCGCCC	GGCAGGATGACTTTTGAGGG
IFI27	TTCTTTGGGTCTGGCTCAAGT	GCCACAACTCCTCCAATCACA
IFIH1 (MDA-5)	GGAGTCAAAGCCCACCATCT	GGTGACGAGACCATAACGGA

IFIT1	AAGCAGGACCCACAAGAATGT	GGCATTTCATCGTCATCAATGG
IFIT3	GAACATGCTCAAGCAGA	CAGTTGTGTCCACCCTTCCT
IFTI2	AACAAAAAGGAACCAGAGGCCA	TAGTTGCCGTAGGCTGCTCTC
ISG20	GAAGCACGACTTCCAGGCAC	TCTTCCACCGAGCTGTGTCC
MAGE-A3	CCCTGAGCAACGAGCGAC	GACTCTGGTCAGGGCAACAG
MAGE-A6	CCCTGAGCAACGAGCGA	ACTCTGGTCAGGGCAACAG
NY-ESO-1	TGTCCGGCAACATACTGACT	AAAAACACGGGCAGAAAGCAC
OAS1	TCCGTGAAGTTTGAGGTCCAG	AGGTTTATAGCCGCCAGTCA
OAS2	GCTCAGAAGCTGGGTTGGTTT	GGATGTCACGTTGGCTTCTCT
OAS3	CGTCAAACCCAAGCCACAAG	TTCCACAACCCCTGTAGGCA
OASL	GAAGGAAGAGGTGCTAGACGC	GAAACAGCTCAGAAACGCCAC
PD-L1	TATGCCTTGGTGTAGCACTGA	CCGATGAACCCCTAAACCACA
PD-L2	GAACCCAGGACCCATCCAAC	CCCAAGACCACAGGTTCAGA
PSMB9	GGGGCGTTGTGATGGGTTC	GCAGCCAAAACAAGTGGAGGT
sFRP1	CTGATAACTGGTTGCTGTGTC	CATCCATGTCCTGTGTATCTGC

Table 2.2. Mouse Primer Sequences

	Forward	Reverse
Axin2	GACAGTAGCGTAGATGGAGTCC	CGGCTTTCCAGCTCCAGTTT
β2m	TCGCTTCAGTCGTCAGCAT	GCAGTTCAGTATGTTCGGCT
Ccl4	TCTCTCCTCTTGCTCGTGGC	ATCTGTCTGCCTCTTTTGGTCA
Ccl5	TGCTGCTTTGCCTACCTCTC	TTGAACCCACTTCTTCTCTGGG
Cd4	TGGGGAAGGAAGGGGAATCA	AACCATCAAACTGCGAAGGC
Cd8a	CGGATTGGACTTCGCCTGT	TGCAAACACGCTTTCGGCT
Ctla-4	TCCAAGGACTGAGAGCTGTT	GGGCATTTTCACATAGACCCC
Cxcl10	TGAGAGACATCCCGAGCCAA	CCCTATGGCCCTCATTCTCAC
Cxcl9	CTCGGACTTCACTCCAACACA	GTAGTGGATCGTGCCTCGG
Fasl	TGAGTTCACCAACCAAAGCCT	TCACTCCAGAGATCAGAGCGG
Gzmb	TGTGTGCTATGTGGCTGGTT	CCCGAAAGGAAGCACGTTTG

H2Aa	TGGAGGTGAAGACGACATTGA	AGCTATGTTTTGCAGTCCACC
H2Ab1	CCTGTGCCTTAGAGATGGCT	GTTGGTGAAGTAGCACTCGC
H2d1	AAGTGGGAGCAGAGTGGTG	ATGTCAGCAGGGTAGAAGCC
H2k1	ATCGCCCTGAACGAAGACC	CACATGGGCCTTTGGGGAA
Hbp1	GGAAGACTTTGCTAGAGCCG	CAGTGAGCAAGCCATCTTCT
Ido1	GCTTTGCTCTACCACATCCAC	TGTCCTCTCAGTCCGTCCG
Ifi27	TGGAGAGAGCTGGGGAAATCG	AAAACGCCATGAGGACCAGT
Ifit1	GCTACCACCTTTACAGCAACC	CCTTTCAGGTGCCTCACGTA
Ifit3	CTCAGCCCACACCCAGCTTTT	GTTGCACACCCTGTCTTCCATA
Ifng	ATGAACGCTACACACTGCATC	CCATCCTTTTGCCAGTTCCTC
Lag3	CTGTCACGTTGGCGGTCATC	GGACAGATTGTTCAGGGGACG
Mage-a3	AAGAGAGTGCTCAGGCCCAA	TGCCACACAGGGAGAGTAGG
MuERV-L	TGGTGGTCGAGATGGAGGTTA	CCGTGAATGGTGGTTTTAGCA
Oas1a	TGTACGAGGTTCAGCATGAGAG	GGCTTGCTGGAAGTATTAACATGA
Oas1b	TCTGCTTTATGGGGCTTCGG	TCGACTCCCATACTCCCAGG
Oas1g	TTGAGGTCCAGAGTTCATGGTG	CAGATGAGGATGGTGTAGATTAAGG
Oas3	TGGGTCACAAGTCTGCCTTC	ACTTGAGTCAGGAAGTGGCG
Oasl1	AGACCTGGGAGACCATCACT	TTTGACCAACCGAAGGAGGC
Oasl2	GAAGAACCTCCTCCGGTTGG	CACGGCTACGAACCCTTCAT
Pd-1	GGAGACTGCTACTGAAGGCG	GTGAAGGTGGCATTTGCTCC
Pd-l1	GGACTACAAGCGAATCACGC	TTCTCTTCCCACTCACGGGT
Pd-l2	TCGGTGTGATTGGCTTCCAG	TCTTTAGGGGCTGTCACGGT
Prf1	CCCACTCCAAGGTAGCCAAT	GAGCTGTTAAAGTTGCGGGG
Psmb10	GAATGCGTCCTTGGAACACG	GGGGCGATGAAGTGGATCTT
Sfrp1	ACTGGCCCGAGATGCTCAAA	CATCCTCAGTGCAAACTCGCT

Stat1	CTGTCATCCCGCAGAGAGAA	CTGCTGAAGCTCGAACCACT
Tigit	TGAGCCAGTTTCAGTTGGAGG	TATCTATCGTGCCTGCTGTGG

2.14. Protein Extraction

Cell and tumor lysates were lysed for 30 minutes at 4°C with RIPA buffer (Thermo Scientific) that mixed with protease and phosphatase inhibitor cocktail (100X) (Thermo Scientific Halt^{TM} kit) and 0.5 M EDTA (Thermo Scientific) (1:100 dilution). The lysate was centrifuged for 10 minutes at 14,000 rpm at 4°C. The supernatant was kept and frozen at -80°C. Protein concentration measurement was done following Thermo Scientific Quant-iT^{TM} Assay. Protein concentration was measured with Qubit^{TM} fluorometer (Thermo Scientific).

2.15. Western Blotting

Table 2.3. Primary Antibodies used for western blotting

Reagent	Source
β-actin	Sigma-Aldrich
β-catenin	Millipore
E-cadherin	Cell signaling
pSTAT-3^{Y705}	Cell signaling
STAT-3	Cell signaling

30 μg protein extracts were separated on 7.5% gradient polyacrylamide gel (Mini-PROTEAN TGX gel, Bio-Rad) by electrophoresis (SDS-PAGE). Then, proteins were transferred to PVDF membrane (Bio-Rad), washed with PBST (1xPBS, 0.1% Tween) and blocked with 5% BSA solution for at least one hour at 4°C. Once the membrane is done blocking, primary antibodies were incubated overnight at 4°C. The list of primary antibodies used was presented in Table 2.3. The western blot results were developed with

SuperSignal West Femto Chemiluminescent substrate (Thermo Scientific) and quantitated by the Chemidoc MP Imaging System (Bio-Rad).

2.16. RNA Sequencing

RNA from treated and control tumors was sequenced at the Tufts University Medical Campus core facilities (Boston, MA). RNA from three CHA1 treated tumors and three saline treated tumors were submitted and 25-28 million reads were analyzed for each sample. The data were analyzed using IPA (QIAGEN Inc., https://www.qiagenbioinformatics.com/products/ingenuity-pathway-analysis). GSEA analysis was done using Molecular Signatures Database (MSigDB) [157]. REACTOME gene set was used for the analysis.

2.17. The Cancer Genome Atlas (TCGA) Analysis

The data were generated using the cBioPortal for Cancer Genomics (http://www.cbioportal.org) [158, 159]. Data were obtained from the following breast cancer dataset: "METABRIC, Nature 2012 & Nat Commun 2016 (n=2509)" [160-162], "TCGA, PanCancer Atlas (n=1084)" and "TCGA, Cell 2015 (n=818)" [163]. mRNA expression relative to all samples with z-score threshold of 1.3 was used to extract the data.

2.18. Statistical analysis

All experiments were performed in triplicate. Student's unpaired *t*-test was used for comparison between two groups. One-way ANOVA with Tukey's post-hoc test was used for multiple comparison. The Manne-Whitney U-test was used to compare between tumor volumes and tumor weights. Kaplan-Meier survival curve with the hazard ratio (HR), 95% confidence intervals (CIs) and log-rank *p*-value was used for survival

analysis. A *p*-value less than 0.05 was considered statistically significant. All analyses were performed by GraphPad Prism 9. Linear regression analysis was performed using Pearson r values.

Chapter 3: Results

3.1. EGCG and DAC combination (CHA1) Suppressed Wnt signaling *in-vitro*

As outlined, we hypothesized that potent Wnt signaling inhibition could be achieved by combining EGCG induction of HBP1, a transcriptional inhibitor of DNMT1 [149], with inhibition of DNMT1 using decitabine (DAC). Further, the gene for sFRP1 is silenced by DNA methylation, which is coordinated by the DNMT1 and other family members [150, 151]. Thus, the combination may potentially increase at least two Wnt inhibitors, HBP1 and sFRP1. The hypothetical model for the combination function is shown in Figure 3.1. We treated cultured human TNBC cells (MDA-MB-231) using concentrations we or others have used previously (up to 1µM DAC, up to 10 µM EGCG) individually or in combination [164, 165]. These concentrations can be achievable in mice and at attainable clinical range in humans blood levels as previously reported [164-178]. As shown in Figures 3.2A and 3.2B, EGCG treatment increased HBP1 mRNA as we had previously shown [56] as well as sFRP1 mRNA as hypothesized, while the combination was best at increasing both inhibitors. Further, nuclear β-catenin was ablated by EGCG and DAC in combination, demonstrating repression of Wnt signaling (Fig. 3.2C). Additional in vitro tests all supported the proposed mechanism, including analysis of HBP1 or sFRP1 knockdown cells, which demonstrated lack of combinatorial treatment function (Figures 3.2D, 3.2E). Knockdown of HBP1 lowered both basal and induced sFRP1 response to the combination, demonstrating HBP1 dependence to treatment. Unsurprisingly, sFRP1 knockdown completely blunted activation of sFRP1 by the drug combination. These initial tests of the combination treatment, which we now refer to as CHA1, provided sufficient confirmation of Wnt signaling inhibition that we proceeded with in vivo testing using drug doses attainable in clinical practice.

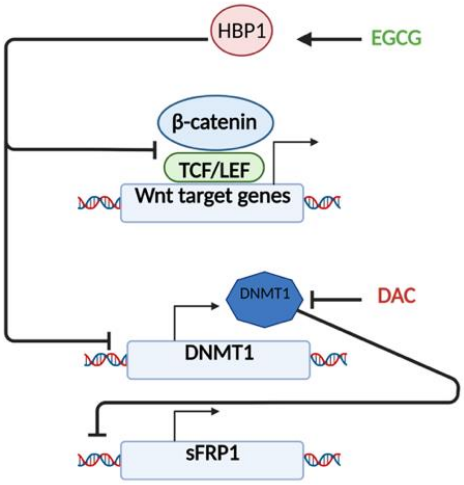

Figure 3.1. The Proposed Mechanism of Action of CHA1 Treatment. CHA1 (EGCG and DAC) is a combinatorial drug approach to inhibit Wnt signaling. EGCG exert its action to inhibit Wnt by post-transcriptional stabilization of mRNA of a Wnt inhibitor HBP1. DNMT1 is a transcriptional target of HBP1 repression. DAC is a DNMT inhibitor that acts epigenetically to reactivate Wnt inhibitors HBP1 and sFRP1, therefore, downregulation of Wnt signaling.

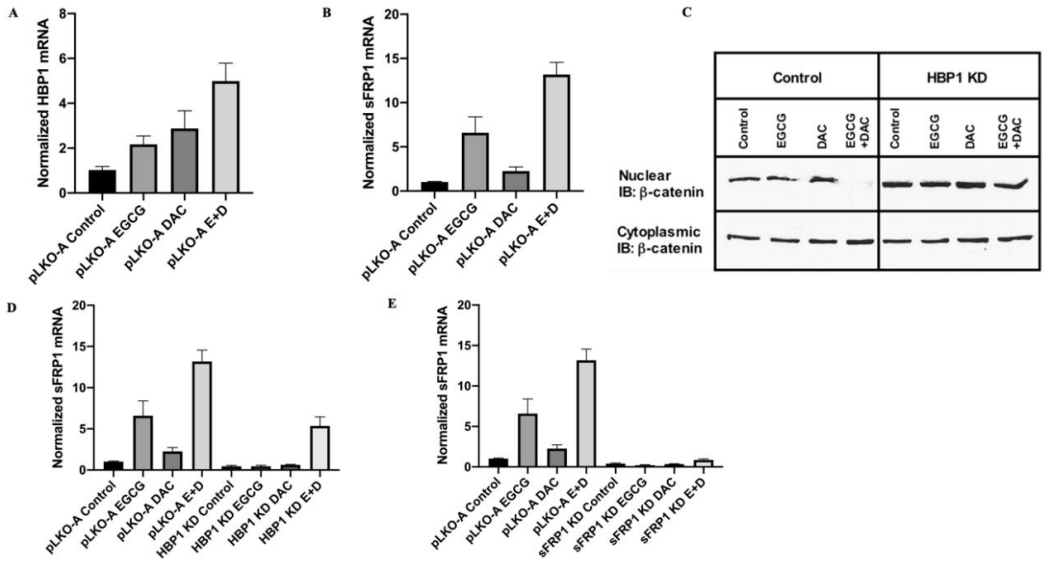

Figure 3.2. The Mechanistic Rationale of CHA1 Treatment (EGCG+DAC) to Suppress Wnt Signaling. A-C) CHA1 suppressed Wnt signaling in TNBC cells MDA-MB-231 cells. CHA1 upregulated the expression of Wnt inhibitors **A)** HBP1 and **B)** sFRP1 at higher levels compared to monotherapy. The gene expression of Wnt inhibitors HBP1 and sFRP1 was measured by qRT-PCR in MDA-MB-231 treated with 10 μM EGCG or 1 μM DAC or both. **C-E)** CHA1 treatment requires HBP1 for complete efficacy. **C)** CHA1 was able to decrease the protein expression of nuclear β-catenin in control MDA-MB-231 cells but not in HBP1 KD MDA-MB-231 cells. EGCG or DAC monotherapy had no effect. The protein expression of cytoplasmic and nuclear β-catenin was measured by western blot in control TNBC cells MDA-MB-231 and in HBP1 KD TNBC cells MDA-MB-231 treated with 10 μM EGCG or 1 μM DAC or both. **D-E)** CHA1 was not able to upregulate sFRP1 gene in HBP1 KD and in sFRP1 KD MDA-MB-231. **D)** The basal and induced sFRP1 mRNA expressions were decreased in HBP1 KD

MDA-MB-231 after CHA1 treatment compared to control cell lines. **E)** The sFRP1 gene expression was completely abolished after CHA1 treatment in sFRP1 KD MDA-MB-231 compared to the expression in the control cells. Gene expression of Wnt inhibitors sFRP1 was measured by qRT-PCR in control TNBC cells MDA-MB-231 (PLKO-A), in HBP1 KD, and in sFRP1 KD TNBC cells MDA-MB-231 treated with 10 μM EGCG or 1 μM DAC or both. All experiments were done in triplicate in three independent experiments. Data were represented as mean ± SEM.

3.2. CHA1 Treatment Suppressed Tumor Growth, Metastases, and Wnt Signaling in TNBC Human Xenograft and TNBC Syngeneic Models

We first assessed the efficacy of CHA1 in an immune compromised human TNBC xenograft model, which lacks an adaptive immune system. Treatment groups received saline, EGCG (16.5 mg/kg), DAC (0.5 mg/kg) or both compounds (CHA1) at achievable blood levels of either compound three times per week on alternating days (QOD) (Figure 3.3A) [166-178]. As shown in Figure 3.3B, CHA1 inhibited tumor growth in the human TNBC xenograft model, while the individual compounds had much less effect. Other dose combinations of EGCG and DAC in this delivery schedule were less effective (data not shown). Expression of either HBP1 or sFRP1 was required for CHA1 efficacy as tumors with knockdown of sFRP1 and HBP1 did not respond or had reduced response to CHA1 (Figure 3.3D, 3.3E). Because EGCG and DAC cross the blood brain barrier, we found that CHA1 treatment resulted in reduction of brain metastases (Figure 3.3F).

CHA1 in the same alternating day modality also inhibited tumor growth in an immune competent syngeneic model using mouse 4T1 TNBC cell lines (Figure 3.4B). In addition, CHA1 QOD treatment decreased cell proliferation in syngeneic model (Figure 3.4C, 3.4D). Lastly, we altered the delivery modality to better reflect clinical use of DAC, treating tumors in the immunocompetent 4T1 model with both DAC and EGCG together

for five-day straight (QD), followed by a five-day recovery period before another CHA1 cycle (Figure 3.4E). This multi-cycle treatment modality was also effective at suppressing tumor growth (Figure 3.4 F, 3.4G).

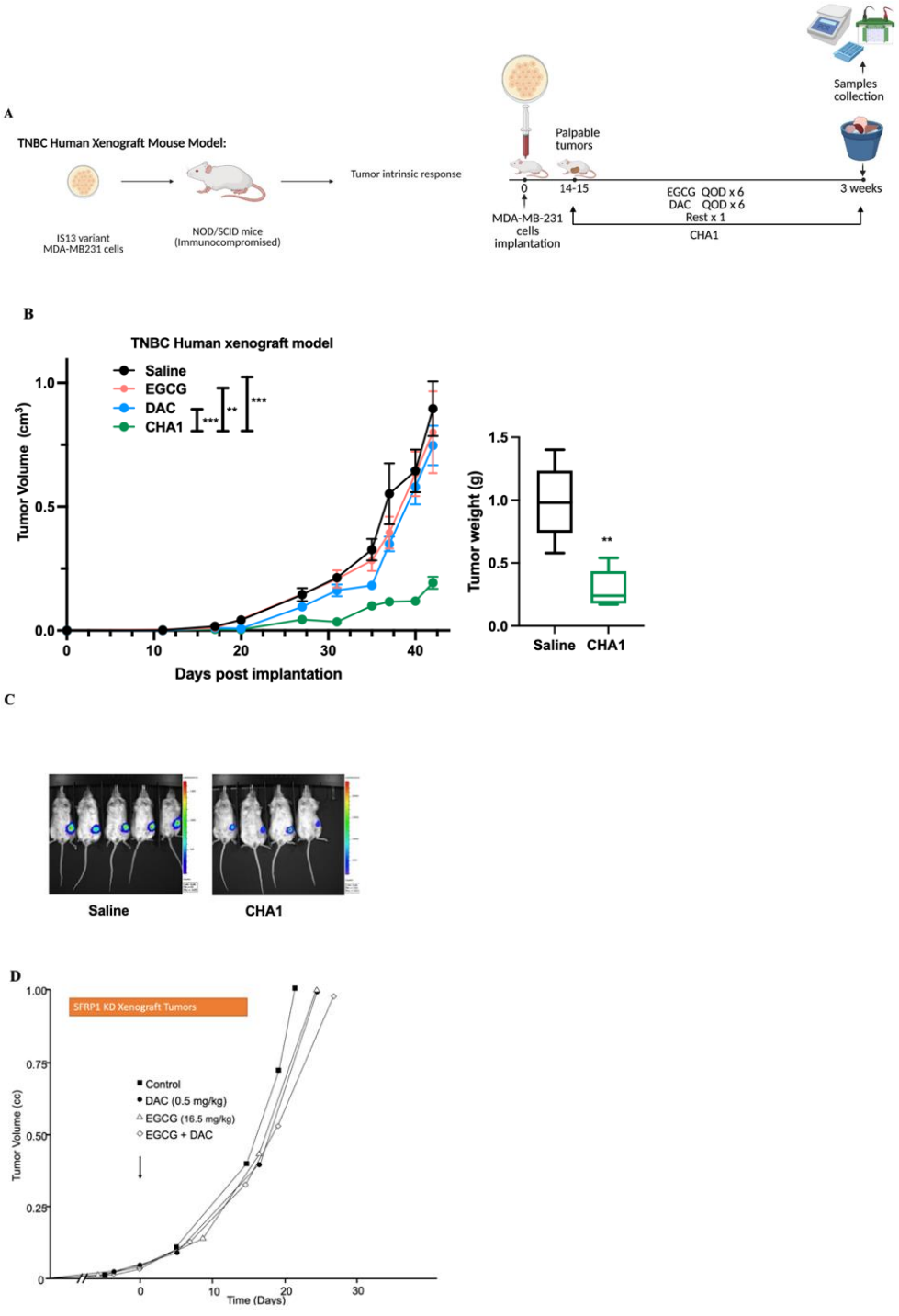

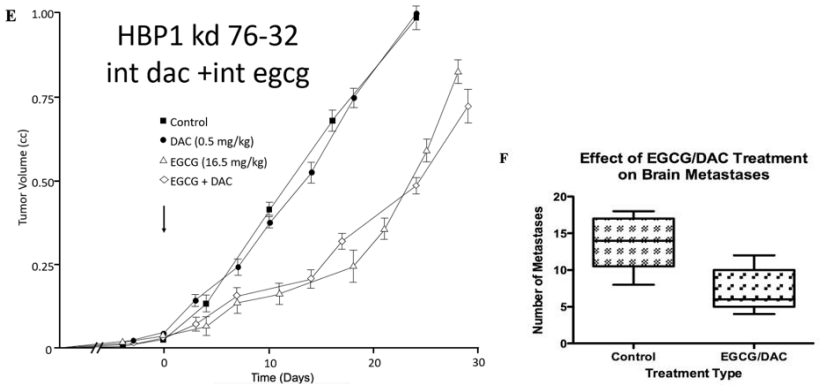

Figure 3.3. CHA1 Reduced Tumor Growth and Brain Metastases in TNBC Human Xenograft. A) Human xenograft model: MDA-MB-231 human TNBC cells were implanted orthotopically into NOD/SCID mice to study tumor intrinsic response. **B)** CHA1 QOD treatment suppressed tumor growth in TNBC Human xenograft while monotherapy had no effect on tumor growth (n=5-6). The study was a combination of two different studies. **C)** Bioluminescence imaging of CHA1 QOD treated TNBC human xenograft mice demonstrated reduction in the primary tumor size prone to metastasis compared to the untreated group. Implanted MDA-MB-231 cell tumors were grown for approximately 3 weeks. At the end of the experiment, mice were anesthetized with isofluorane and injected i.p. with 90 µl of luciferin. **D-E)** CHA1 treatment required HBP1 and sFRP1 in TNBC xenograft model. The growth inhibitory effect of CHA1 was abolished in HBP1 and sFRP1 KD TNBC xenograft model. Control (plko), sFRP1 KD MDA-MB231 cells, and HBP1 KD MDA-MB231 cells were implanted orthotopically into NOD-SCID mice. At least 5 mice were treated with CHA1, EGCG or DAC for the indicated time. Tumors were measured with calipers**. F)** CHA1 decreased brain metastases in TNBC xenograft model**.** The brain metastases were assessed in control and CHA1 treatment mice. The IS13 brain-metastasizing variant of MDA-MB-231 cells that orthotopically implanted and tagged with GFP were treated with CHA1 or saline for 2 weeks. GFP-labeled metastatic foci were counted on dissected brain. **B, D&E)** Tumor volume was measured with calipers. Tumors were weighted at the end of the experiment. Box and whiskers plot was used to represent tumor weight and brain metastases data. The median represented the mid-point of the data and was shown by the horizontal line that divided the box into two quartiles. 75% of the data were below the upper quartile value. 25% of the data were below the lower quartile value. The error bars represented the upper and lower whiskers which showed the values outside the middle 50% (i.e. the lower 25% of values and the upper 25% of values). Mann-Whitney U-test was used for tumor volume and tumor weight comparison. * $P < 0.05$, ** $P < 0.05$, *** $P < 0.005$, **** $P < 0.001$.

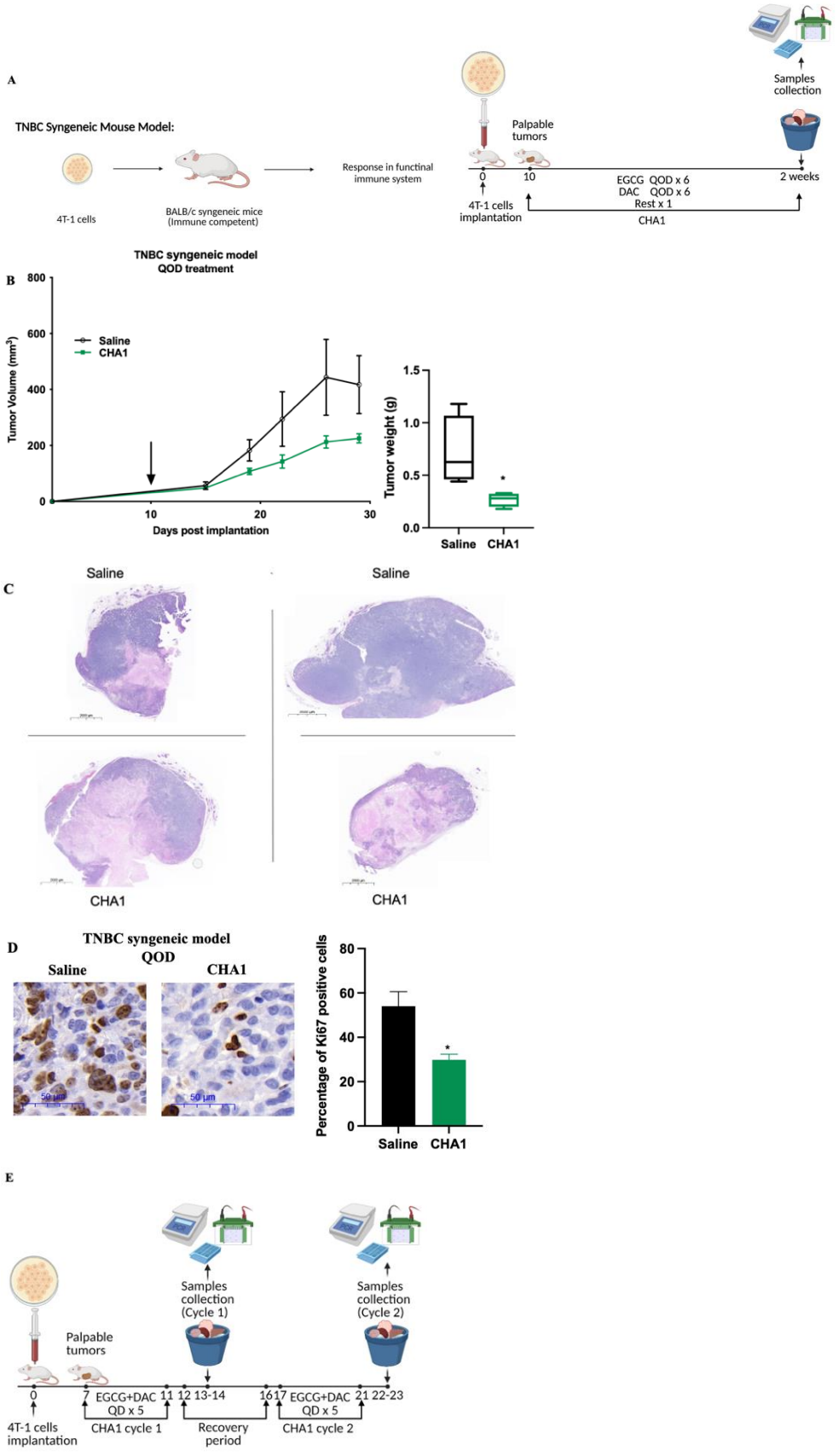
A
TNBC Syngeneic Mouse Model:
4T-1 cells
BALB/c syngeneic mice
(Immune competent)
Response in functinal
immune system
Palpable
tumors
Samples
collection
0
10
2 weeks
EGCG QOD x 6
DAC QOD x 6
Rest x 1
4T-1 cells
implantation
CHA1
B
TNBC syngeneic model
QOD treatment
Tumor Volume (mm³)
Saline
CHA1
Days post implantation
Tumor weight (g)
Saline
CHA1
C
Saline
Saline
CHA1
CHA1
D
TNBC syngeneic model
QOD
Saline
CHA1
50 µm
50 µm
Percentage of Ki67 positive cells
Saline
CHA1
E
Samples
collection
(Cycle 1)
Samples
collection
(Cycle 2)
Palpable
tumors
0
7
EGCG+DAC
QD x 5
11
12
13-14
16
17
EGCG+DAC
QD x 5
21
22-23
4T-1 cells
implantation
CHA1 cycle 1
Recovery
period
CHA1 cycle 2

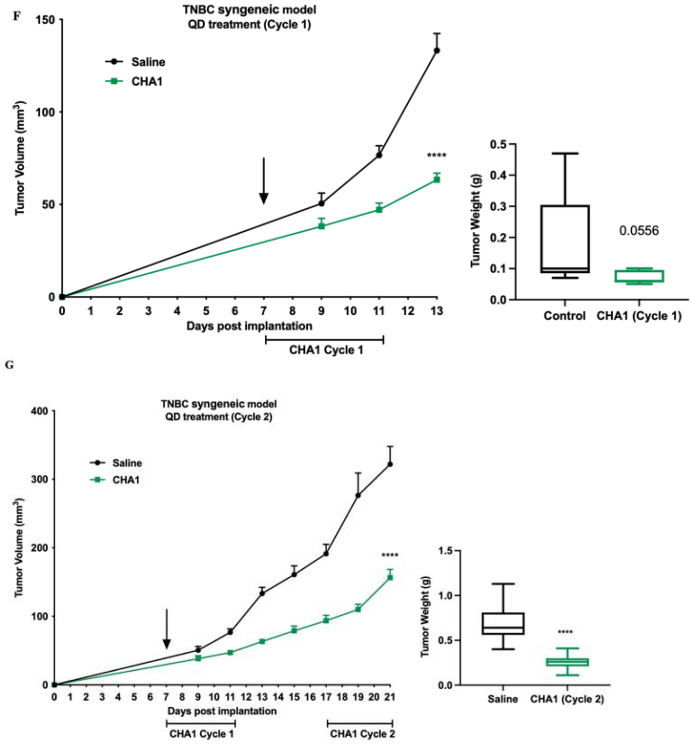

Figure 3.4. CHA1 Suppressed Tumor Growth in TNBC Syngeneic Mouse Model. A) Syngeneic mouse model: 4-T1 TNBC cells were implanted into Balb/c mice to study CHA1 response in immunocompetent mice. The CHA1 QOD treatment regimen: EGCG (16.5 mg/kg) or DAC (0.5 mg/kg) was administrated 3 times per week on alternating days for up to up to 2 weeks in syngeneic model. **B)** CHA1 QOD treatment suppressed tumor growth in syngeneic mouse model (n=4). **C-D)** CHA1 QOD treatment reduced cell proliferation in 4-T1 Syngeneic mouse model. **C)** H&E staining showed decreased the tumor density after CHA1 QOD treatment. **D)** IHC of Ki67 after saline and CHA1 QOD treatment demonstrated decreased in cell proliferation in CHA1 group. Sections of saline and CHA1 treated tumors were stained with anti-ki67 antibody. Representative immunostaining section with quantification of the percentage of Ki67 positive cells in untreated and CHA1 treated tumors (n= 3 mice/ group). **E)** CHA1 QD treatment timeline in 4-T1 syngeneic model: EGCG (16.5 mg/kg) and DAC (0.5 mg/kg) was co-administrated for two cycles. Each cycle was 5 days with 5 days recovery period. **F-G)** CHA1 QD treatment decreased tumor volume and tumor weight after cycle 1(n=15-23) and cycle 2 (n=15-23). The results were the combinations of 3 different studies. **(B, F&G)** Tumor volume was measured with calipers. Tumors were weighted at the end of the experiment. Box and whiskers plot was used to represent tumor weight and brain metastases data. The median represented the mid-point of the data and was shown by the horizontal line that divided the box into two quartiles. 75% of the data were below the upper quartile value. 25% of the data were below the lower quartile value. The error bars represented the upper and lower whiskers which showed the values outside the middle 50% (i.e. the lower 25% of values and the upper 25% of values). Mann-Whitney U-test was used for tumor volume and tumor weight comparison. * $P < 0.05$, ** $P < 0.05$, *** $P < 0.005$, **** $P < 0.001$.

CHA1 effectively suppressed Wnt signaling in tumors, recapitulating results in cultured cells. mRNA levels of both sFRP1 and HBP1 in each tumor model with different CHA1 treatment modality was significantly increased (Figure 3.5A-3.5D). Similarly, there was a decrease in β-catenin protein level in each TNBC mouse model treated with CHA1 compared to untreated group (Figure 3.5E-3.5G). The western blot result was confirmed by immune-histochemical (IHC) staining of tumors, which showed a significant reduction in β-catenin-expressing cells after CHA1 treatment in human and mouse TNBC tumors (Figure 3.5H, 3.5I). We confirmed the requirement for both components of CHA1 to maximally inhibit Wnt signaling by analyzing mRNA levels of Wnt target gene AXIN2. CHA1 treatment significantly decreased AXIN2 gene expression compared to saline in TNBC tumors in both the immune compromised and immune competent xenograft models (Figure 3.5J, 3.5K). In the human xenograft model, EGCG had no effect on AXIN2 mRNA levels, while DAC treatment resulted in a surprising increased in AXIN2 mRNA levels (Figure 3.5L). These results demonstrated that the CHA1 combination treatment in vivo could inhibit both growth and Wnt signaling in TNBC tumors.

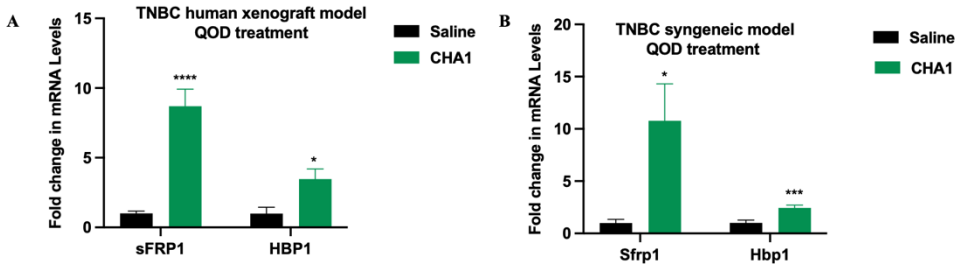

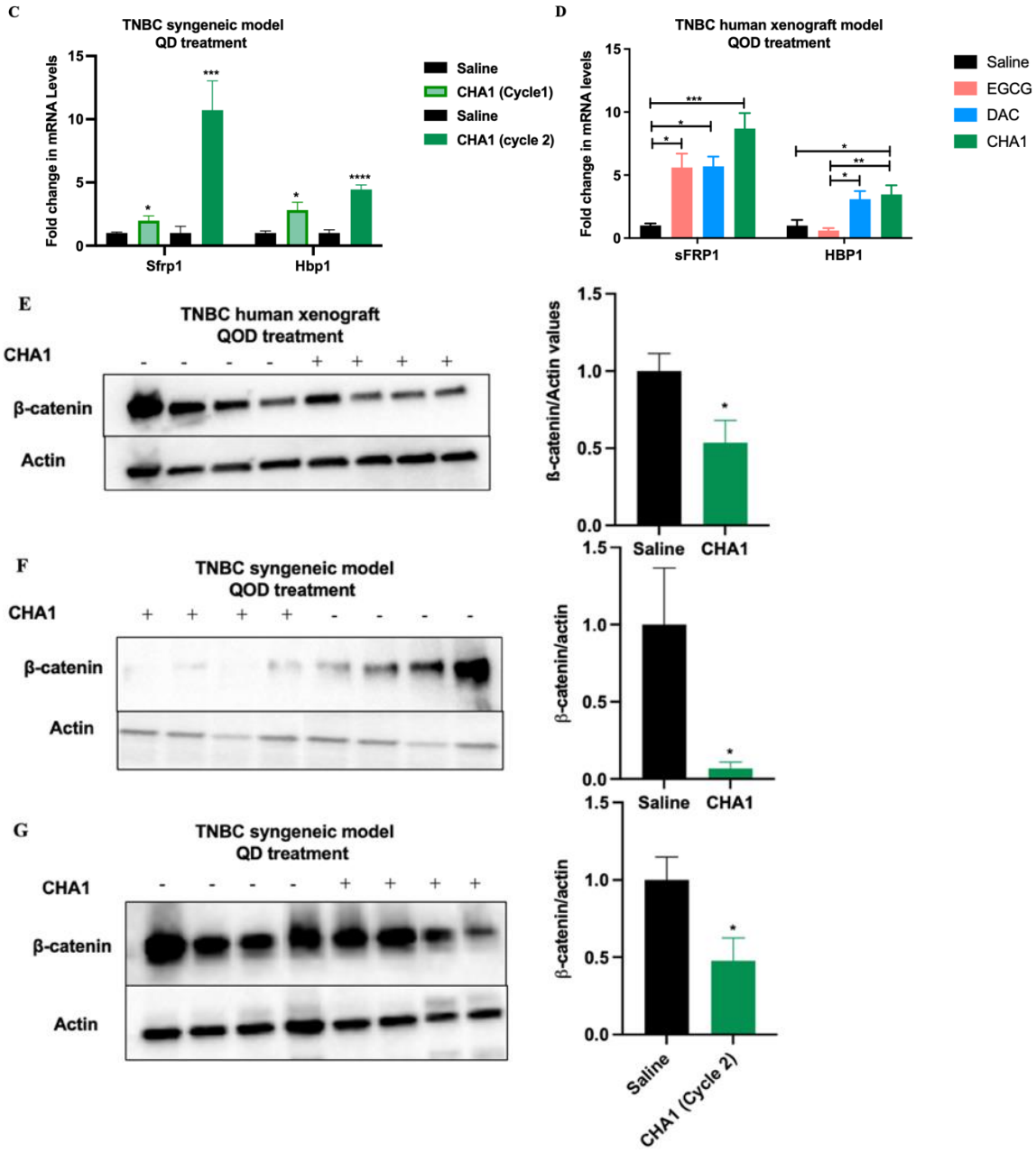
C
TNBC syngeneic model
QD treatment
Fold change in mRNA Levels
Sfrp1
Hbp1
Saline
CHA1 (Cycle1)
Saline
CHA1 (cycle 2)
D
TNBC human xenograft model
QOD treatment
Fold change in mRNA levels
sFRP1
HBP1
Saline
EGCG
DAC
CHA1
E
TNBC human xenograft
QOD treatment
CHA1
β-catenin
Actin
β-catenin/Actin values
Saline
CHA1
F
TNBC syngeneic model
QOD treatment
CHA1
β-catenin
Actin
β-catenin/actin
Saline
CHA1
G
TNBC syngeneic model
QD treatment
CHA1
β-catenin
Actin
β-catenin/actin
Saline
CHA1 (Cycle 2)
H
TNBC human xenograft
QOD treatment
Saline
CHA1

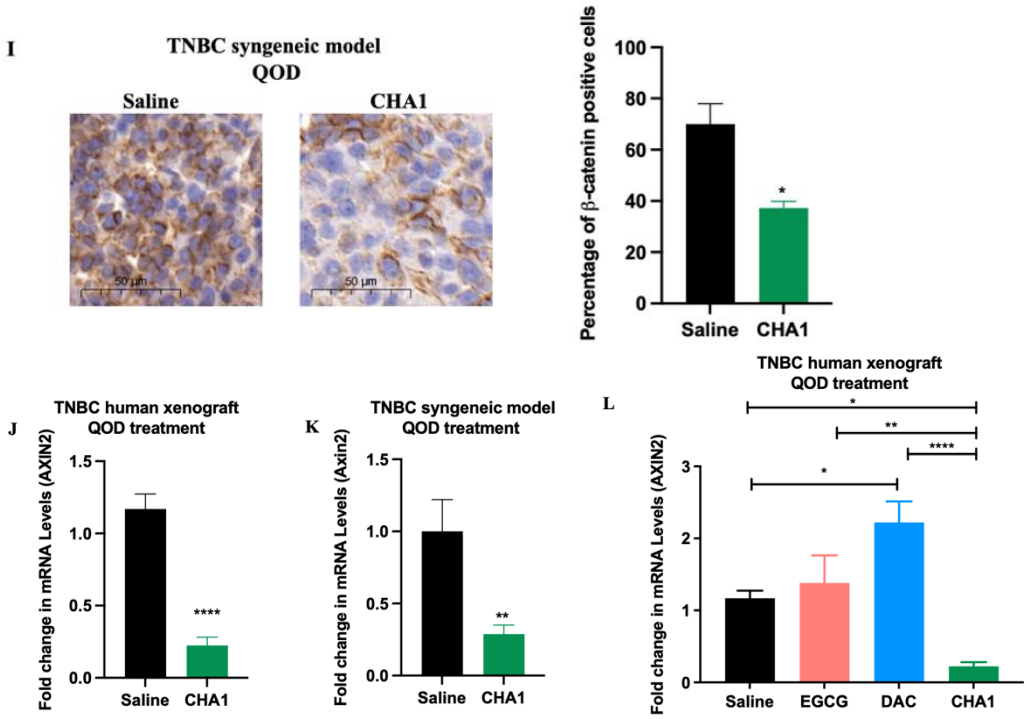

Figure 3.5. CHA1 Treatment Inhibited Wnt Signaling in TNBC Human Xenograft and TNBC Syngeneic Mouse Model. A-C) mRNA levels of Wnt inhibitors HBP1 and sFRP1 were upregulated after CHA1 QOD treatment in TNBC human xenograft and TNBC syngeneic mouse model and CHA1 QD treatment in TNBC syngeneic mouse model. The gene expression of HBP1 and sFRP1 was measured by qRT-PCR in untreated and CHA1 treated tumors (human xenograft QOD, n=5-6 mice, syngeneic QOD, n=5-6, syngeneic QD cycle 1, n= 4, syngeneic QD cycle 2, n=6-7). **D)** The expression of sFRP1 was induced after CHA1, EGCG, and DAC QOD treatment in TNBC human xenograft (n= 5-6 mice/group). The gene expression of HBP1 was upregulated after CHA1 and DAC QOD treatment in TNBC human xenograft (n= 5-6 mice/group). **E-G)** The protein levels of β-catenin were decreased after CHA1 QOD treatment in TNBC human xenograft and TNBC syngeneic mouse model and CHA1 QD treatment in TNBC syngeneic mouse model. Representative western blot (left) with quantification (right) of saline and CHA1 treatment tumors (n=4 mice/ group). **H)** IHC of β-catenin after saline and CHA1 QOD treatment in TNBC human xenograft. **I)** IHC of β-catenin after saline and CHA1 QOD treatment in TNBC syngeneic model demonstrated strong membrane staining of β-catenin and increased number of β-catenin positive cells (Average Allred score = 8) in untreated tumors compared to CHA1 treated tumors (Average Allred score = 5). Sections of tumors were stained with anti-β-catenin antibody. Representative immunostaining section with quantification of the percentage of β-catenin positive cells after saline tumors and CHA1 treatment (n= 3 mice/ group). **J-K)** The gene expression of Wnt target genes AXIN2 was downregulated after CHA1 QOD treatment in TNBC human xenograft and TNBC syngeneic mouse model. AXIN2 gene expression was tested by qRT-PCR after saline and CHA1 treatment (human xenograft QOD, n=6 mice, syngeneic QOD, n=5). **L)** CHA1 decreased mRNA levels of Wnt target genes AXIN2 while EGCG or DAC QOD treatment had no effect (n= 5-6 mice/group). Unpaired two-

tailed t-test was used for the comparison between two groups. Adjusted one-way ANOVA was used for multiple comparison. * $P < 0.05$, ** $P < 0.05$, *** $P < 0.005$, **** $P < 0.001$. qRT-PCR experiments were done in triplicates in three independent experiments. Western blots quantifications were the combination of two different experiments (n=4/experiment). Data were represented as mean ± SEM.

3.3. Unbiased Bioinformatic Analysis Revealed CHA1 Treatment Re-programed Multiple Pathways Including Tumor Evasion and Epithelial-Mesenchymal Transition (EMT)

We sought mechanistic insight into the tumor-intrinsic consequences of CHA1-inhibition of Wnt signaling, hypothesizing that CHA1 may in effect re-program tumor cell functions to reduce immune evasion. Therefore, we probed the human tumor-mouse xenograft, which is uncomplicated by the mouse adaptive immune system, using an unbiased RNA-seq and bioinformatics approach. Figure 3.6A displayed the top 20 canonical pathways significantly affected by CHA1 treatment using Ingenuity Pathway Analysis (IPA). As predicted from the results of Figures 3.1-3.5, Wnt signaling was downregulated. Expression of multiple Wnt targets identified in the RNA-seq was significantly inhibited (Figure 3.6B), supporting our prior analysis of Wnt inhibition in Figure 3.5.

Intriguingly, the tumor-intrinsic analysis revealed that multiple pathways involved in immune surveillance were activated. Overlapping gene sets included antigen presentation, autoimmune thyroid disease signaling, graft-vs-host disease signaling, Th1 and Th2 activation and allograft rejection signaling. As shown in Table 3.1-3.6, the core set consisted of MHC class I and class II antigen presentation genes. MHC-I and MHC-II are also IFN-stimulated genes. Because evidence supports crosstalk between Wnt and IFN signaling [179-181], we used a second unbiased analysis of the RNA-seq dataset

(Gene Set Enrichment Analysis, GSEA) to refine the molecular pathways that are altered upon CHA1 treatment. As shown in Figure 3.6C, the top-ranked pathways include, cytokine signaling in immune system, interferon signaling, interferonα/β signaling, interferonγ signaling, and adaptive immune system. Other tumor-altering mechanisms potentially regulated by CHA1 treatment include broad inhibition of cell-cycle, inhibition of cellular movement, activation of apoptosis and other tumor-inhibitory pathways (Figure 3.6D). In addition, IPA analysis demonstrated that there was inhibition of Epithelial-Mesenchymal Transition (EMT) after CHA1 treatment. This was confirmed by increased E-cadherin protein levels after CHA1 QOD treatment in TNBC human xenograft and syngeneic models (Figure 3.6E, 3.6F).

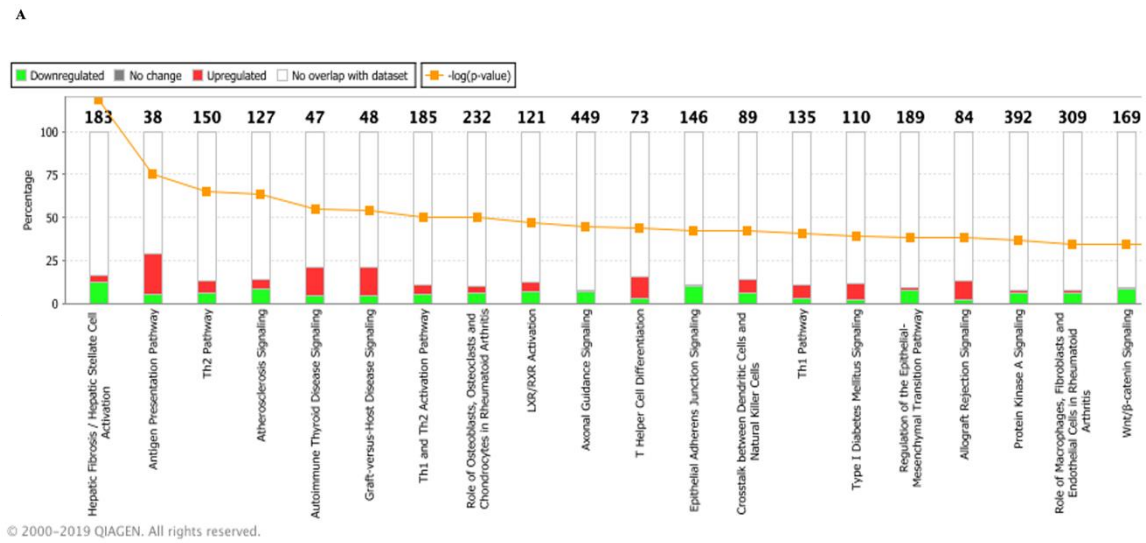

B

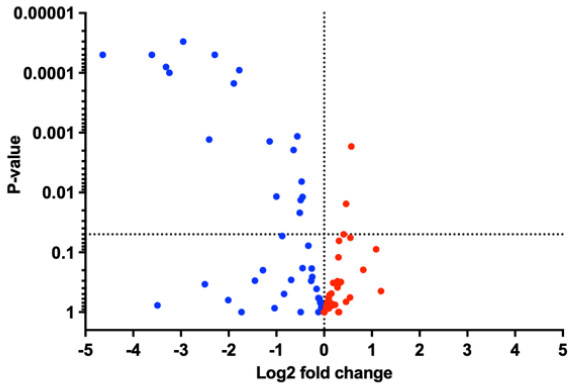

Symbol	log2 Fold Change	p value
MMP2	-2.95	0.00003
NTRK2	-4.64	0.00005
SMO	-3.61	0.00005
TWIST1	-3.24	0.0001
TCF4	-2.29	0.00005
IGF1	-3.31	0.00008
ID2	-1.78	0.00009
CEBPD	-1.89	0.00015
CTGF	-0.56	0.00115
SFRP2	-2.41	0.0013
TGFB3	-1.14	0.0014
VEGFA	-0.64	0.00195
DKK1	-0.47	0.00655
TCF7L1	-1.00	0.01165
TLE1	-0.45	0.0119
EGR1	-0.49	0.0134
EFNB1	-0.51	0.02185

C

CHA1 GSEA Analysis

Gene Set Name [# Genes (K)]	# Genes in Overlap (k)	Hypergeometric p-value	FDR q-value
REACTOME CYTOKINE SIGNALING IN IMMUNE SYSTEM [719]	64	$2.83 e^{-22}$	$4.54 e^{-19}$
REACTOME DEVELOPMENTAL BIOLOGY [1143]	79	$2.11 e^{-20}$	$1.7 e^{-17}$
REACTOME INTERFERON SIGNALING [203]	32	$7.05 e^{-19}$	$3.77 e^{-16}$
REACTOME EXTRACELLULAR MATRIX ORGANIZATION [301]	37	$6.87 e^{-18}$	$2.76 e^{-15}$
REACTOME SIGNALING BY RECEPTOR TYROSINE KINASES [504]	45	$4.63 e^{-16}$	$1.48 e^{-13}$
REACTOME INTERFERON ALPHA/BETA SIGNALING [73]	18	$9.35 e^{-15}$	$2.5 e^{-12}$
REACTOME INTERFERON GAMMA SIGNING [93]	19	$6.89 e^{-14}$	$1.58 e^{-11}$
REACTOME ADAPTIVE IMMUNE SYSTEM [825]	53	$8.49 e^{-13}$	$1.7 e^{-10}$
REACTOME INTEGRIN CELL SURFACE INTERACTIONS [85]	17	$2.06 e^{-12}$	$3.67 e^{-10}$
REACTOME HEMOSTASIS [678]	46	$4.46 e^{-12}$	$7.15 e^{-10}$

D

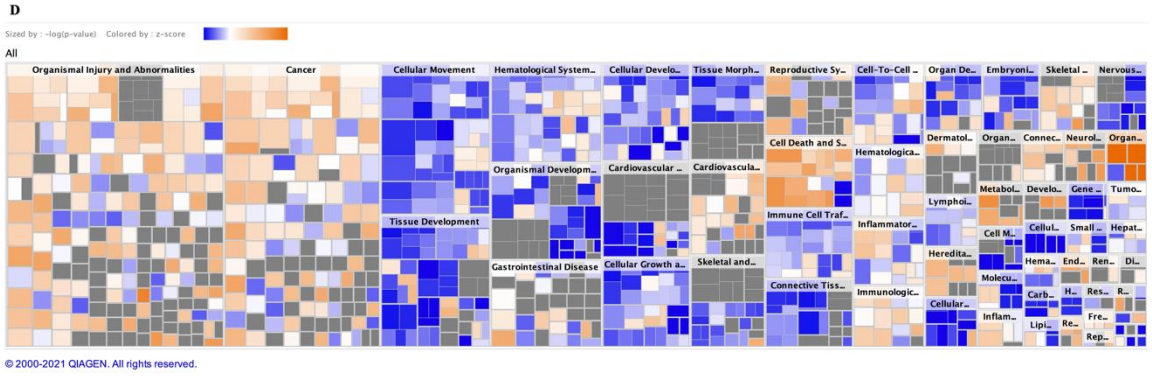

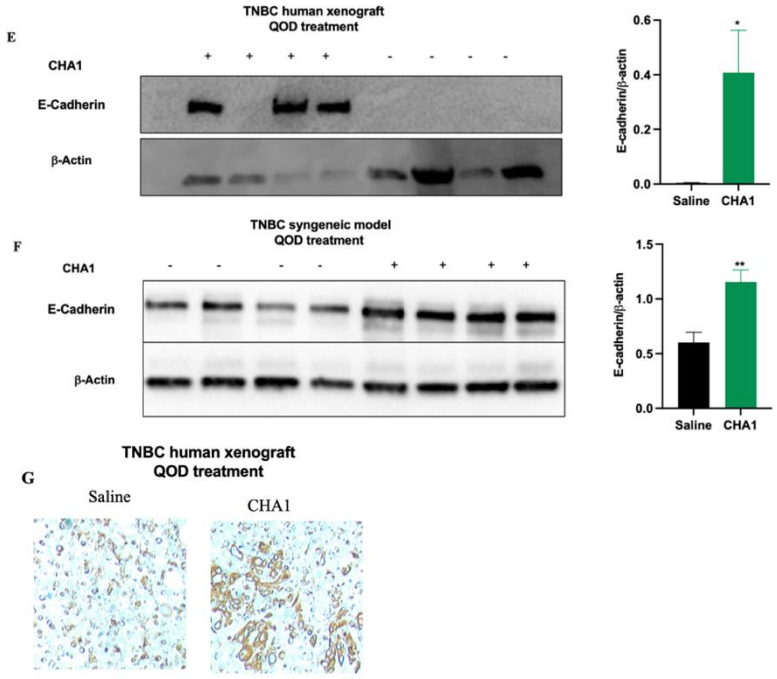

Figure 3.6. Bioinformatic Analysis Indicated a Broad Activation of Immune-related Pathways and Downregulation of Wnt Pathway after CHA1 Treatment in TNBC Human Xenograft Model. Saline and CHA1 treated tumors were subjected to RNA Seq. **A)** The data was analyzed by IPA. The top 20 canonical pathways significantly altered after CHA1 treatment were depicted. There was a broad activation of immune system related signaling pathway e.g., antigen presentation, autoimmune thyroid disease signaling, graft-vs-host disease signaling, Th1 and Th2 activation and allograft rejection signaling. Antigen presentation pathway was activated that indicated upregulation of the genes involved in anti-tumor immune response. Also, Wnt signaling was downregulated. **B)** Volcano plot indicated inhibition of Wnt/β-catenin signaling pathway after CHA1 treatment. The Wnt target gene set was extracted from IPA after analysis of CHA1 RNA-seq (n=83). 48 out of 83 genes were downregulated after CHA1 treatment. 17 out of 48 genes were downregulated with $p < 0.05$ after CHA1.The cut-off for significant values for downregulation of gene expression was log2 fold change < 1 and p-value < 0.05. **C)** GSEA analysis identifying the REACTOME gene sets of CHA1 treated tumors indicated activation of IFNγ and IFNα/β. **D)** Changes in biological function after CHA1 treatment. CHA1 reduced cell growth and proliferation and cellular movement (blue), as well as increased of cell death (orange). **E-F)** Reverse EMT after CHA1. E-cadherin protein expression was elevated after CHA1 QOD treatment in TNBC human xenograft and TNBC syngeneic mouse model. Representative western blot (left) with quantification (right) of saline and CHA1 treatment tumors (n=4 mice/ group). **G)** IHC of E-cadherin demonstrated induced E-cadherin protein after CHA1 QOD treatment in TNBC human xenograft. Representative immunostaining section of E-cadherin after saline and CHA1 QOD treatment in human xenograft. Unpaired two-tailed t-test was used for the comparison between two groups. * $P < 0.05$, ** $P < 0.05$, *** $P < 0.005$, **** $P < 0.001$. Western blots quantifications were the combination of two different experiments (n=4/experiment). Data were represented as mean ± SEM.

3.3.1. Table 3.1-3.7: Immune Related Pathways Altered after CHA1 Treatment in TNBC Human Xenograft Model

The tables were retrieved from IPA. The cut-off for significant values for downregulation of gene expression was log2 fold change ≤1 and p-value < 0.05. The cut-off for significant values for upregulation of gene expression was log2 fold change ≥1 and p-value < 0.05 [182, 183].

Table 3.1. Antigen Presentation Pathway

Gene ID	Log2 Fold Change	P-value
CD74	1.646	5.00E-05
HLA-B	0.72	5.00E-05
HLA-DMA	0.894	0.0161
HLA-DMB	1.616	0.01965
HLA-DPA1	1.527	0.00875
HLA-DRA	1.204	0.00865
HLA-DRB1	1.31	0.01205
HLA-DRB5	1.699	0.0725
HLA-F	-2.036	0.0036
HLA-G	-3.024	5.00E-05
PSMB9	1.457	5.00E-05

Table 3.2. Autoimmune Thyroid Disease Signaling

Gene ID	Log2 Fold Change	P-value
HLA-B	0.72	5.00E-05
HLA-DMA	0.894	0.0161
HLA-DMB	1.616	0.0197
HLA-DPA1	1.527	0.00875
HLA-DRA	1.204	0.00865
HLA-DRB1	1.31	0.012
HLA-DRB5	1.699	0.0725
HLA-F	-2.036	0.0036
HLA-G	-3.024	5.00E-05
LAT	1.362	0.0011
TGFB3	-1.143	0.0014
TNFRSF11B	0.892	0.0179
TNFRSF1B	0.964	0.0261

Table 3.3. Graft-versus-Host Disease Signaling

Gene ID	Log2 Fold Change	P-value
FASLG	3.6177	0.01905
HLA-B	0.72	5.00E-05
HLA-DMA	0.894	0.0161
HLA-DMB	1.616	0.01965
HLA-DRA	1.204	0.00865
HLA-DRB1	1.31	0.01205
HLA-DRB5	1.699	0.0725
HLA-F	-2.036	0.0036
HLA-G	-3.024	5.00E-05
PRF1	3.68202	0.0038

Table 3.4. Allograft Rejection Signaling

Gene ID	Log2 Fold Change	P-value
FASLG	3.6177	0.01905
HLA-B	0.72	5.00E-05
HLA-DMA	0.894	0.0161
HLA-DMB	1.616	0.01965
HLA-DPA1	1.527	0.00875
HLA-DRA	1.204	0.00865
HLA-DRB1	1.31	0.01205
HLA-DRB5	1.699	0.0725
HLA-F	-2.036	0.0036
HLA-G	-3.024	5.00E-05
PRF1	3.68202	0.0038

Table 3.5. Th1 Pathway

Gene ID	Log2 Fold Change	P-value
APH1B	0.728	0.0049
DLL1	-5.148	0.00355
GATA3	-1.767	5.00E-05
HLA-B	0.72	5.00E-05
HLA-DMA	0.894	0.0161
HLA-DMB	1.616	0.0197
HLA-DPA1	1.527	0.00875
HLA-DRA	1.204	0.00865
HLA-DRB1	1.31	0.012
HLA-DRB5	1.699	0.0725
ICAM1	1.331	0.0013
ICOSLG	1.551	0.00745

NFATC2	-1.1	0.0394
NOTCH3	1.329	0.00105

Table 3.6. Th2 Pathway.

Gene ID	Log2 Fold Change	P-value
APH1B	0.728	0.0049
BHLHE41	-0.905	0.0007
DLL1	-5.148	0.00355
GATA3	-1.767	5.00E-05
HLA-B	0.72	5.00E-05
HLA-DMA	0.894	0.0161
HLA-DMB	1.616	0.0197
HLA-DPA1	1.527	0.00875
HLA-DRA	1.204	0.00865
HLA-DRB1	1.31	0.012
HLA-DRB5	1.699	0.0725
ICAM1	1.331	0.0013
ICOSLG	1.551	0.00745
JAG2	-1.323	0.00545
MAF	-0.923	0.021
NFATC2	-1.1	0.0394
NOTCH3	1.329	0.00105
S1PR1	-2.063	0.00045
SPI1	-0.89	0.0336

Table 3.7. Th1 and Th2 Activation Pathway

Gene ID	Log2 Fold Change	P-value
APH1B	0.728	0.0049
BHLHE41	-0.905	0.0007
DLL1	-5.148	0.00355
FGFR2	-4.486	5.00E-05
GATA3	-1.767	5.00E-05
HLA-B	0.72	5.00E-05
HLA-DMA	0.894	0.0161
HLA-DMB	1.616	0.0197
HLA-DPA1	1.527	0.00875
HLA-DRA	1.204	0.00865
HLA-DRB1	1.31	0.012
HLA-DRB5	1.699	0.0725
ICAM1	1.331	0.0013
ICOSLG	1.551	0.00745
JAG2	-1.323	0.00545

MAF	-0.923	0.021
NFATC2	-1.1	0.0394
NOTCH3	1.329	0.00105
S1PR1	-2.063	0.00045
SPI1	-0.89	0.0336

3.4. CHA1 Treatment Activated Antigen Presentation

The bioinformatic analysis highlighted the induction of antigen presentation in CHA1-treated tumors, in particular the HLA genes comprising the major histocompatibility complexes (MHC) (IPA data, Figure 3.6A). MHC-I and MHC-II components are required for proper antigen presentation. Confirming the bioinformatic results, IHC staining revealed that CHA1 treatment increased MHC-I and MHC-II proteins in human xenograft (Figure 3.7A, 3.7B). Similarly, MHC-I and MHC-II genes expression were upregulated after CHA1 treatment in both TNBC human xenograft and TNBC syngeneic models (Figure 3.7C-3.7E). The effect of CHA1 or the individual CHA components on the induction of the expression of MHC-I and MHC-II genes was tested in TNBC human xenograft (Figure 3.7F). The data demonstrated that CHA1 significantly upregulated the expression of MHC-II genes. However, DAC or EGCG monotherapy had no effect on MHC-II gene expression (Figure 3.7F). The finding that CHA1-induced MHC-I and MHC-II expression as well as the number of cells with MHC expression suggested that CHA1 treatment re-activated antigen presentation. Also, the induction of MHC-II after CHA1 in human xenograft indicated that CHA1 induced tumor-specific MHC-II (tsMHC-II) and enhanced tumor recognition by the immune system [184]. It has been reported that tsMHC-II correlated with favorable response to ICIs in humans and with tumor rejection in murine models [100, 185-188]. Our data also showed upregulation of the expression of CD74, MHC class II invariant chain (li), after CHA1 in

human xenograft model. CD74 has an important role in proper folding and trafficking of MHC class II complex, leading to $CD4^+$ Th cells activation [189]. Furthermore, our data showed that the expression of PSMB9 and Psmb10 was significantly elevated after CHA1 in human xenograft and syngeneic models, respectively. Both PSMB9 and Psmb10 are subunits of immunoproteasome that plays important role in processing internal antigen and loading it into to MHC-I complex, and, therefore, activation of $CD8^+$ cytotoxic T-cells [190].

In addition to reinduction of the expression of antigen presentation machinery, we observed induction of the expression of cancer testis antigens (CTAs). CTAs such as NY-ESO-1 and MAGE-A family are tumor-associated antigens that represent a class of antigens that may increase immune recognition of cancers as a result of their restricted expression in normal adult tissue [191, 192]. CHA1 upregulated the expression of CTAs NY-ESO-1, MAGE-A3 and MAGE-A6 in human xenograft and Mage-a3 in syngeneic model (Figure 3.7G-3.7I). A more detailed analysis of CTAs MAGE-A3, MAGE-A6 and NY-ESO-1 with each component (EGCG or DAC monotherapy) compared to CHA1 in human xenograft (Figure 3.7J) was performed. The data showed that EGCG had a negligible effect on CTAs expression, while DAC treatment induced CTAs expression, consistent with previous work [191]. However, the CHA1 treatment resulted in what appeared to be a synergistic response, even compared to the substantial DAC response. These data are consistent with the bioinformatic analysis and supported the hypothesis that CHA1 treatment may result in an increase in tumor immunogenicity.

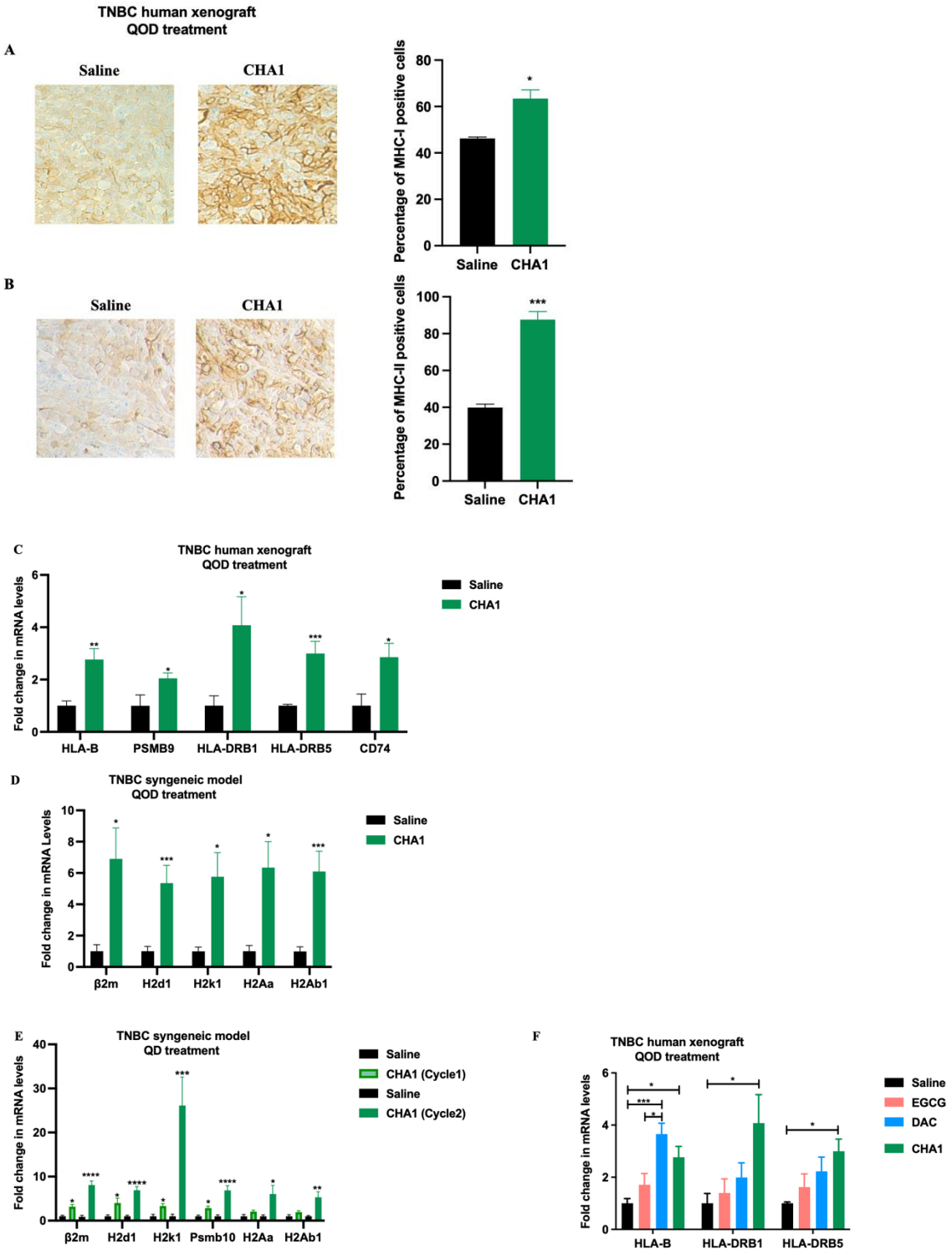
TNBC human xenograft
QOD treatment
A
Saline
CHA1
Percentage of MHC-I positive cells
Saline
CHA1
B
Saline
CHA1
Percentage of MHC-II positive cells
Saline
CHA1
C
TNBC human xenograft
QOD treatment
Fold change in mRNA levels
HLA-B
PSMB9
HLA-DRB1
HLA-DRB5
CD74
Saline
CHA1
D
TNBC syngeneic model
QOD treatment
Fold change in mRNA Levels
β2m
H2d1
H2k1
H2Aa
H2Ab1
Saline
CHA1
E
TNBC syngeneic model
QD treatment
Fold change in mRNA levels
β2m
H2d1
H2k1
Psmb10
H2Aa
H2Ab1
Saline
CHA1 (Cycle1)
Saline
CHA1 (Cycle2)
F
TNBC human xenograft
QOD treatment
Fold change in mRNA levels
HLA-B
HLA-DRB1
HLA-DRB5
Saline
EGCG
DAC
CHA1

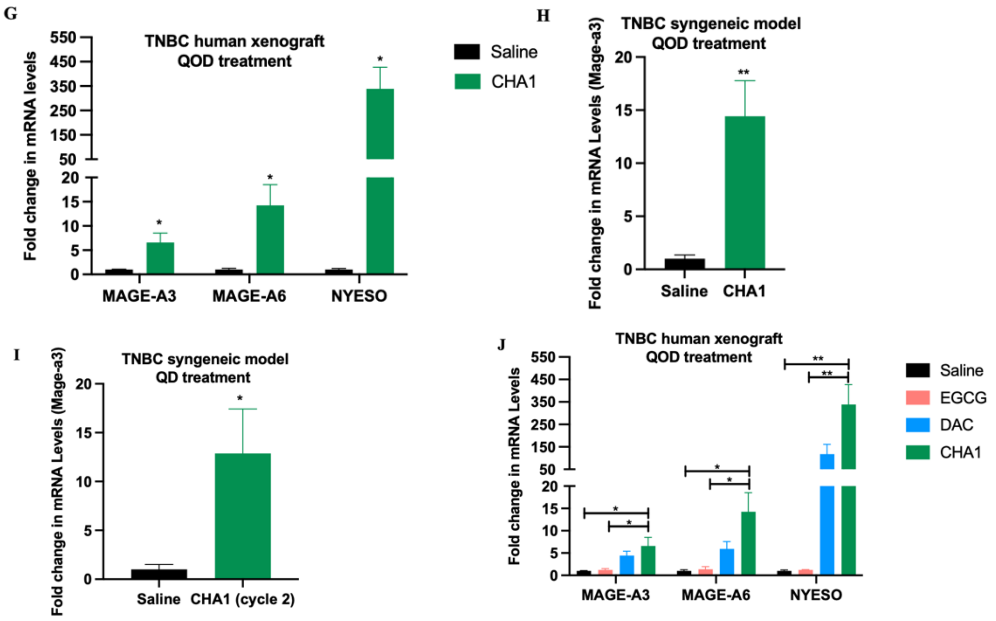

Figure 3.7. CHA1 Treatment Induced Antigen Presentations in TNBC Human Xenograft and TNBC Syngeneic Mouse Model. A-B) IHC of MHC-I and MHC-II after CHA1 QOD treatment in TNBC human xenograft. There was a weak staining of MHC-I and MHC-II in saline group (Average Allred score =4-5) and strong MHC-I and MHC-II staining in CHA1 treated group (Average Allred score = 8). Sections of tumors were stained with pan anti-MHC-I antibody and with anti-MHC-II antibody. Representative immunostaining section of MHC-I and MHC-II with quantification of the percentage of MHC-I and MHC-II positive cells in saline tumors and CHA1 treated tumors (n= 3 mice/ group). **C)** CHA1 QOD treatment in TNBC human xenograft upregulated the gene expression of MHC-I (HLA-B), MHC-II (HLA-DRB1 and HLA-DRB5), immunoproteasome subunit PSMB9, and the invariant chain (Ii) CD74. **D-E)** CHA1 QOD treatment and CHA1 QD treatment in TNBC syngeneic model elevated the gene expression of MHC-I (β2m, H2d1 and H2k1) and MHC-II (H2Aa and H2Ab). CHA1 QD treatment increased the expression of immunoproteasome subunit Psmb10. **F)** In TNBC human xenograft model, CHA1 QOD and DAC QOD treatment induced the gene expression of HLA-B (MHC-I) while EGCG QOD treatment had no effect. CHA1 QOD treatment induced the gene expression of HLA-DRB5 and HLA-DRB1 (MHC-II) while DAC or EGCG QOD treatment had no effect. **G-I)** CHA1 QOD treatment in TNBC human xenograft and TNBC syngeneic model and CHA1 QD treatment in TNBC syngeneic model upregulated the gene expression of CTAs. **J)** In TNBC human xenograft model, CHA1 QOD and DAC QOD treatment elevated CTAs gene expression while EGCG QOD treatment had no effect. **C-J)** The gene expression was measured by qRT-PCR in saline, EGCG, DAC and CHA1 treated tumors (human xenograft QOD, n=4-6 mice, syngeneic QOD, n=6, syngeneic QD cycle 1, n=3-4, syngeneic QD cycle 2, n=4-6). Unpaired two-tailed t-test was used for the comparison between two groups. Adjusted one-way ANOVA was used for multiple comparison. * $P < 0.05$, ** $P < 0.05$, *** $P < 0.005$, **** $P < 0.001$. qRT-PCR experiments were done in triplicates in three independent experiments. Data were represented as mean ± SEM.

3.5. CHA1 Treatment Stimulated IFN Signaling Pathway

CHA1 stimulation of IFN signaling was initially confirmed by pSTAT3^{Y705} western blot in untreated and CHA1-treated tumors in TNBC human xenograft and TNBC syngeneic models (Figure 3.8A, 3.8B). The requirement for both components of CHA1 for maximal pSTAT3^{Y705} was demonstrated in tumors treated with CHA1, or DAC or EGCG monotherapy (Figure 3.8C). Next, we examined the expression of selected IFN-stimulated genes (ISGs) derived from the overlap between our RNA-seq of CHA1-treated human xenograft mice and the IFNα/β and IFNγ GSEA REACTOME dataset. There were 18 genes overlap between our RNA-seq and IFNα/β GSEA REACTOME dataset and 19 genes overlap between our RNA-seq and IFNγ GSEA REACTOME dataset (Figure 3.8D). In order to verify the stimulation of each pathway after CHA1 treatment, hypergeometric probability test was conducted, indicating we required to confirm the induction of at least 8 genes in such pathway after CHA1 treatment. Our data showed a significant induction in the transcription of ISGs after CHA1 in TNBC human xenograft and TNBC syngeneic models (Figure 3.8E-3.8G). According to GSEA REACTOME dataset, the HLA-B, OAS1, OAS2, OAS3, and OASL were genes that overlap between the IFNα/β and IFNγ pathways. IFIT1, IFIT2, IFIT3, ISG20, and IFI27 were IFNα/β-specific target genes while HLA-DRB1, HLA-DRB5, ICAM-1, VCAM1 were IFNγ-specific target genes. Analysis in TNBC human xenograft model indicated that CHA1 treatment was required for upregulation of IFNα/β and IFNγ stimulated genes. DAC monotherapy induced the expression of some IFNα/β and IFNγ stimulated genes, however, the gene expression stimulated by CHA1 treatment was higher. EGCG monotherapy had no effect on ISGs except OAS1 (Figure 3.8H). The strength of

interferon signaling was highly correlated with ISG expression as shown by plotting pSTAT3^{Y703} levels against OAS1, OAS2, OAS3, OASL, IFIT1, IFIT2 and IFIT3 mRNA level, with r^2 values between 0.6 and 0.8 (Figure 3.8I). One possible mechanism of interferon induction is through viral mimicry. Previous work has shown that DNMT inhibition can induce the expression of endogenous retroviruses (ERVs), elevating the level of dsRNA and activating dsRNA pattern recognition receptors such as RIG-1 (DDX58), LGP2 (DHX58), and MDA5 (IFIH1) [193]. Indeed, CHA1 upregulated the expression of endogenous retrovirus (ERV3-1) in TNBC human xenograft and induced murine endogenous retrovirus like-1 (muERVL-1) in TNBC syngeneic model (Figure 3.8J-3.8L). In addition, CHA1 treatment activated gene expression of dsRNA pattern recognition receptors in TNBC human xenograft model (Figure 3.8J).

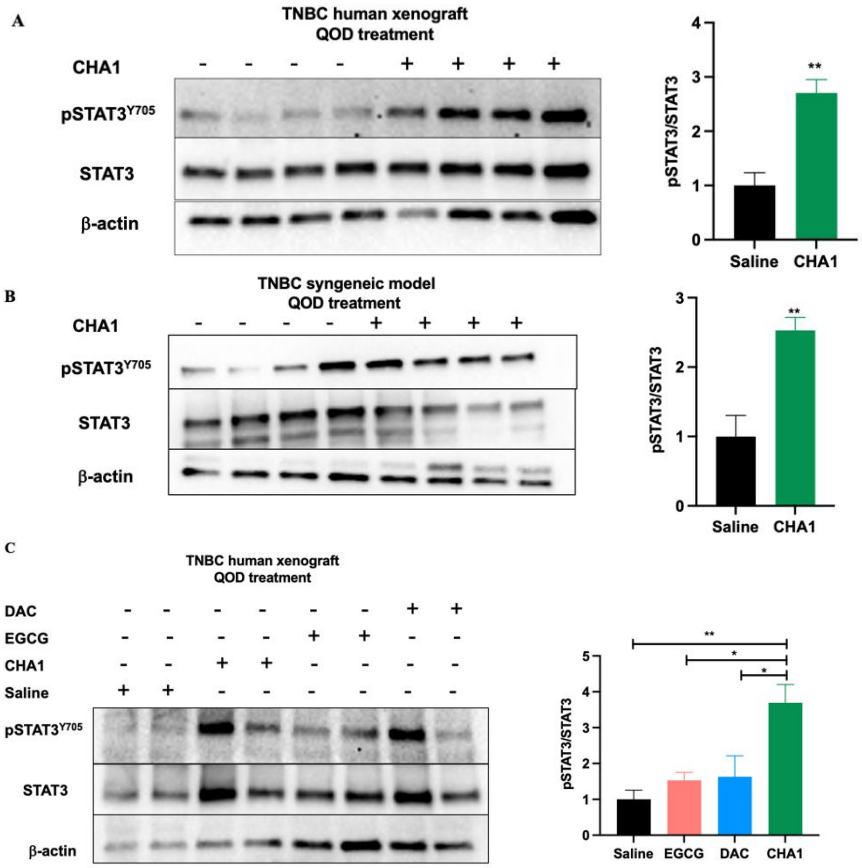

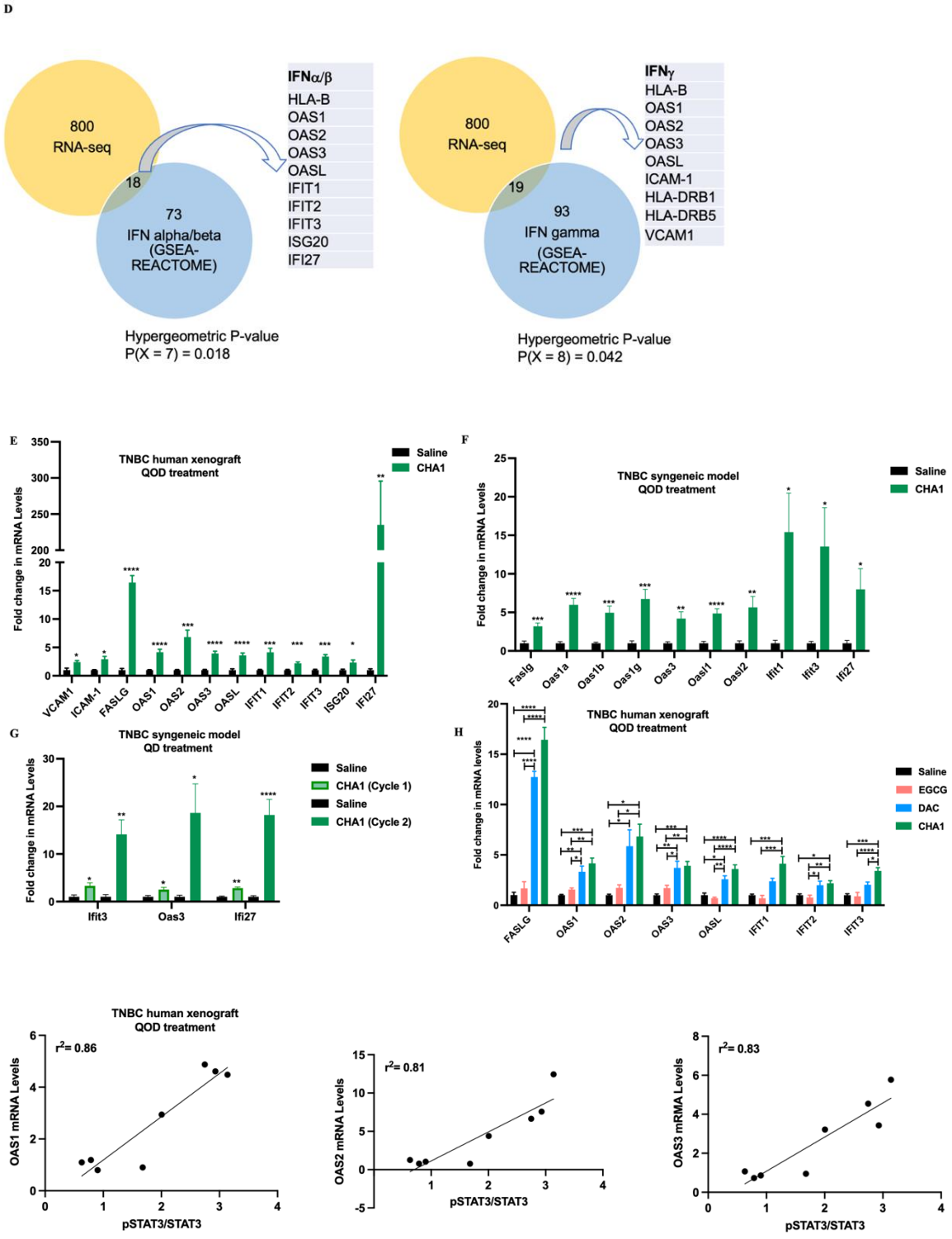
D
800
RNA-seq
18
73
IFN alpha/beta
(GSEA-
REACTOME)
IFNα/β
HLA-B
OAS1
OAS2
OAS3
OASL
IFIT1
IFIT2
IFIT3
ISG20
IFI27
Hypergeometric P-value
P(X = 7) = 0.018
800
RNA-seq
19
93
IFN gamma
(GSEA-
REACTOME)
IFNγ
HLA-B
OAS1
OAS2
OAS3
OASL
ICAM-1
HLA-DRB1
HLA-DRB5
VCAM1
Hypergeometric P-value
P(X = 8) = 0.042
E
TNBC human xenograft
QOD treatment
Fold change in mRNA Levels
Saline
CHA1
VCAM1
ICAM-1
FASLG
OAS1
OAS2
OAS3
OASL
IFIT1
IFIT2
IFIT3
ISG20
IFI27
F
TNBC syngeneic model
QOD treatment
Fold change in mRNA Levels
Saline
CHA1
Fasl g
Oas1a
Oas1b
Oas1g
Oas3
Oasl1
Oasl2
Ifit1
Ifit3
Ifi27
G
TNBC syngeneic model
QD treatment
Fold change in mRNA Levels
Saline
CHA1 (Cycle 1)
Saline
CHA1 (Cycle 2)
Ifit3
Oas3
Ifi27
H
TNBC human xenograft
QOD treatment
Fold change in mRNA levels
Saline
EGCG
DAC
CHA1
FASLG
OAS1
OAS2
OAS3
OASL
IFIT1
IFIT2
IFIT3
TNBC human xenograft
QOD treatment
r2= 0.86
OAS1 mRNA Levels
pSTAT3/STAT3
r2= 0.81
OAS2 mRNA Levels
pSTAT3/STAT3
r2= 0.83
OAS3 mRNA Levels
pSTAT3/STAT3

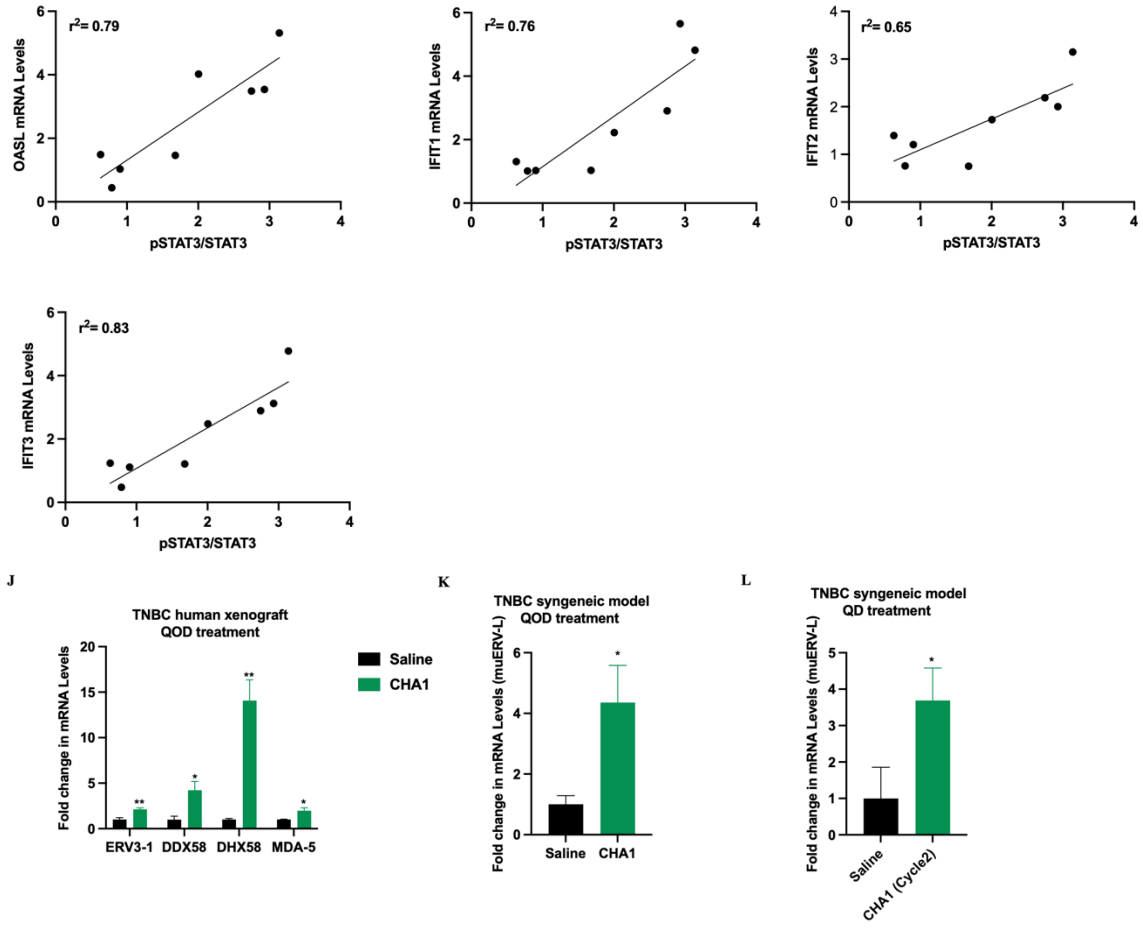

Figure 3.8. CHA1 Treatment Activated IFNα/β and IFNγ Pathways in TNBC Human Xenograft and TNBC Syngeneic Mouse Model. A-B) CHA1 QOD treatment tumors in TNBC human xenograft and TNBC syngeneic model increased the protein expression of pSTAT3^{Y705}. Representative western blot (left) with quantification (right) of saline and CHA1 treatment tumors (n=4 mice/ group). **C)** In TNBC human xenograft, CHA1 QOD treatment upregulated pSTAT3^{Y705} protein levels while EGCG or DAC QOD treatment had no induction effect. Representative western blot (left) with quantification (right) of saline, EGCG, DAC and CHA1 treatment tumors (n=4 mice/ group). **D)** The overlapping genes between CHA1-RNAseq and REACTOME IFNα/β and FNγ gene sets. A hypergeometric probability test indicated that at least 8 genes in each interferon pathway was required to validate activation of such pathway. **E-G)** CHA1 QOD treatment in TNBC human xenograft and TNBC syngeneic model and CHA1 QD treatment in TNBC syngeneic model upregulated the gene expression of ISGs. The gene expression was measured by qRT-PCR in saline and CHA1 treated tumors (human xenograft QOD, n=4-6 mice, syngeneic QOD, n=5-6, syngeneic QD cycle 1, n=3-4, syngeneic QD cycle 2, n=4-6). **H)** In TNBC human xenograft, CHA1 QOD treatment induced ISGs. DAC QOD also increased the expression of ISGs except IFIT1 and IFIT3, however, the fold change in the gene expression was higher after CHA1 treatment. EGCG QOD had no effect on ISGs. The gene expression was tested after saline, EGCG, DAC and CHA1 treatment (n= 4-6 mice/group). **I)** In TNBC human xenograft, STAT3

phosphorylation status (Figure 3.8A) was positively correlated with mRNA levels of IFIT1, IFIT2, IFIT3, OAS1, OAS2, OAS3, and OASL (Figure 3.8E) after CHA1 QOD treatment. r^2 value was calculated using GraphPad Prism. **J-L)** CHA1 QOD treatment tumors in TNBC human xenograft and TNBC syngeneic model and CHA1 QD treatment in TNBC syngeneic model induced viral mimicry status. The gene expression of ERV3-1 and dsRNA PRRs was tested in saline and CHA1 QOD treatment in human xenograft (n=4-6). The gene expression of muERVL-1 was tested after CHA1 QOD (n=5) and CHA1 QD cycle 2 (n=4-6) treatment in TNBC syngeneic model. Unpaired two-tailed t-test was used for the comparison between two groups. Adjusted one-way ANOVA was used for multiple comparison. * $P < 0.05$, ** $P < 0.05$, *** $P < 0.005$, **** $P < 0.001$. qRT-PCR experiments were done in triplicates in three independent experiments. Western blots quantifications were the combination of two different experiments (n=4/experiment). Data were represented as mean ± SEM.

3.6. CHA1 Treatment of TNBC in an Immune Competent Environment: A Heightened Immune Response

For the most successful ICIs treatments, the tumor often has a combination of conditions that promote treatment success and include the changes we observe in Figures 3.2-3.8 [107, 194, 195]. Tumors infiltrated with high numbers of $CD8^+$ T-cells, NK cells and macrophages, termed “hot” tumors, are the most responsive to ICIs treatment. In contrast, tumors infiltrated with immune-suppressive cells such as Treg cells, absent the “hot” components, are often less responsive. As demonstrated in Figures 3.2-3.8, in mice both with and without an adaptive immune system, CHA1 treatment resulted in significant changes that may promote the “hot” tumor state, including suppression of Wnt signaling, activation of antigen presentation machinery, induction of CTAs, stimulation of IFN signaling. Together, this was, sufficient to dramatically reduce tumor growth. Therefore, we sought to test if CHA1-treated tumors in mice with a full immune system acquired some or all of the “hot” state characteristics.

Extending the mechanism of CHA1 function to the tumor immune environment (TME), we first examined infiltration of T-cells by staining for $CD8^+$ T-cells in CHA1-

treated and untreated tumors. As shown in Figure 3.9A, the number of $CD8^+$ T-cells infiltrated into TME was significantly higher after CHA1 treatment. Moreover, CHA1 treatment increased the percentage of $Ki67^+$ $CD8^+$ T-cells in TME, indicating that CHA1 treatment increased recruitment of active IFNγ-secreting cytotoxic T cells into TME (Figure 3.9B) [196]. To assess the immune cells in the tumor microenvironment, macrophages were stained using F480 as a marker. As shown in Figure 3.9C, CHA1 treatment increased infiltration of $F480^+$ cells. Finally, we examined the effect of CHA1 treatment in Treg cells infiltration. As shown in Figure 3.9F, Foxp3 staining declined dramatically after CHA1 treatment. Furthermore, CHA1 upregulated the gene expression of mouse Prf-1 and Gzmb in human xenograft that lacks T-cells, indicating NK cell functionality [197] (Figure 3.9G). These results were consistent with the activation of antigen presentation, and IFN signaling, suggesting that the TME was dramatically altered following CHA1 treatment.

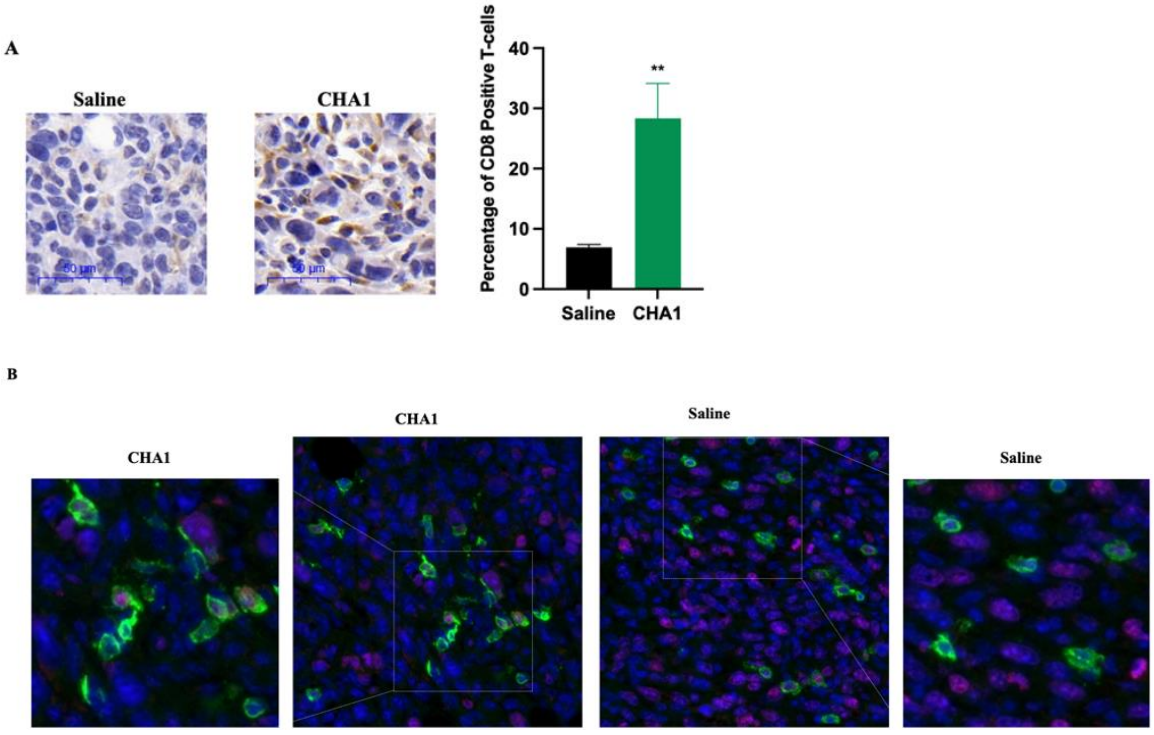

Green=CD8$^+$ T-cells
Pink= Ki67$^+$ cells

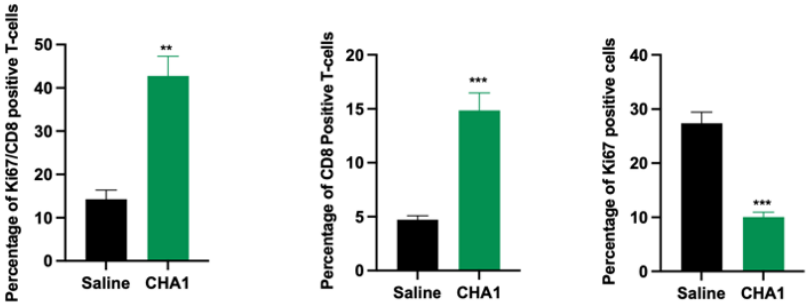

C

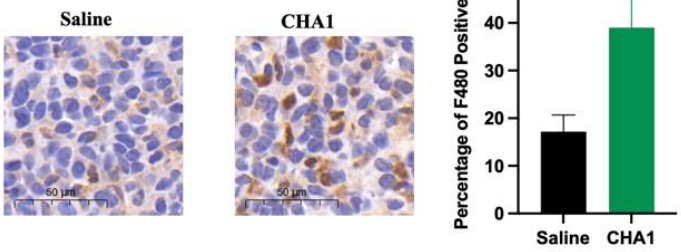

D

CD8$^+$ T-cell staining
CHA1 QOD treatment

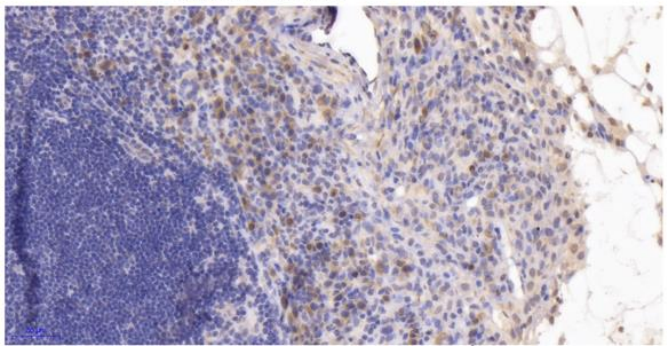

E

F480$^+$ macrophage staining
CHA1 QOD treatment

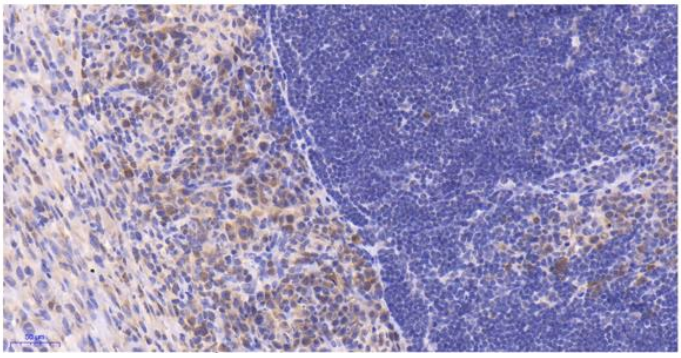

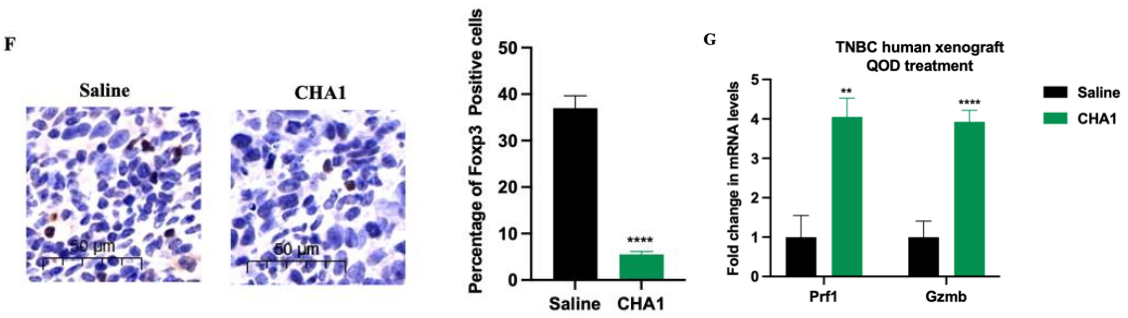

Figure 3.9. CHA1 Treatment Increased Infiltration of IFNγ-secreting Cytotoxic T-cells and Macrophages and Decreased Infiltration of Immune-suppressor Treg Cells into Tumor Microenvironment in TNBC Syngeneic Mouse Model. A) IHC of $CD8^+$ T-cells indicated increased the percentage of $CD8^+$ cytotoxic T-cells after CHA1 QOD in TNBC syngeneic model. Different sections of treated and untreated tumors were stained with anti-CD8 antibody. Representative immunostaining section with quantification of the percentage of $CD8^+$ T-cells in untreated tumors and treated tumors (n= 5 mice/group). **B)** Immunofluorescent of co-staining of $Ki67^+CD8^+$T-cells indicated increased the percentage of active IFNγ-secreting $Ki67^+CD8^+$ cytotoxic T-cells after CHA1 QOD in TNBC syngeneic model. Different sections of different treated and untreated tumors were stained with anti-CD8 and anti-Ki67 antibody. Representative immunofluorescence staining section of $Ki67^+$ $CD8^+$ T-cells, $CD8^+$ T-cells and $Ki67^+$ tumor cells with quantification in untreated and treated tumors (n= 4 mice/group). **C)** IHC of $F480^+$ cells indicated increased the percentage of $F480^+$ macrophages after CHA1 QOD in TNBC syngeneic model. Different sections of different treated and untreated tumors were stained with anti-F480 antibody. Representative immunostaining section with quantification of the percentage of $F480^+$ cells in control tumors and treated tumors (n= 5 mice/group). **D-E)** IHC of **D)** $CD8^+$ T-cells and **E)** $F480^+$ macrophages revealed the presence of lymphoid structure after CHA1 QOD in TNBC syngeneic model. **F)** IHC of $Foxp3^+$ T-cells indicated decreased the percentage of $Foxp3^+$ Treg after CHA1 QOD in TNBC syngeneic model. Different sections of different treated and untreated tumors were stained with anti-Foxp3 antibody. Representative immunostaining section with quantification of the percentage of $Foxp3^+$ T-cells in untreated and treated tumors (n= 4 mice/group). **G)** CHA1 QOD treatment in TNBC human xenograft induced the gene expression of mouse Prf-1 and Gzmb, suggesting activation of NK cells. The gene expression was measured by qRT-PCR in saline and CHA1 treated tumors (n=4-5). Unpaired two-tailed t-test was used for the comparison between two groups. * $P < 0.05$, ** $P < 0.05$, *** $P < 0.005$, **** $P < 0.001$. qRT-PCR experiment was done in triplicates in three independent experiments. Data were represented as mean ± SEM.

We further defined how CHA1 might alter the tumor T cell population by examining its effect on PD-1 and PD-L1 expression. The PD-L1-PD-1 interaction is thought to be a mechanism protecting against autoimmunity by inhibiting proinflammatory $CD8^+$ T-cells [198]. Further, elevation of PD-L1 is one characteristic of

hot tumors, which are more successfully treated with ICIs therapy [199]. Consistent with the elevation of $CD8^+$ T-cells in CHA1-treated tumors, the expression of PD-1, a marker of T-cell exhaustion, declined significantly following CHA1 treatment in syngeneic model (Figure 3.10B, 3-10C) [200].

Another influence on the tumor immune environment is the expression of PD-L1 and PD-L2 ligands on antigen-presenting cells, non-lymphoid tissues and tumor cells [201]. The expression of PD-L1 and PD-L2 mRNA was tested in control and CHA1-treated tumors in human and syngeneic models (Figure 3.10A-3-10C). After CHA1 treatment, the gene expression of PD-L1 was increased, while there was no significant change in the expression of PD-L2. The induction of PD-L1 in TNBC human xenograft tumors after CHA1 indicated tumor-intrinsic change mediated by CHA1 (Figure 3.10A). The induction effect of CHA1 was also more significant than using each drug individually (Figure 3.10D). CHA1-upregulated PD-L1 expression was also examined by staining, confirming an increase in PD-L1 positive cells in the CHA1-treated group in human and syngeneic models (Figure 3.10E, 3.10F). Staining of PD-L1 in different tumor sections after EGCG, DAC and CHA1 treatment in TNBC human xenograft both recapitulated the observation CHA1 induced PD-L1, but also demonstrated again the synergy of combining both drugs (Figure 3.10E). Furthermore, the level of STAT3 phosphorylation was positively correlated with mRNA levels of PD-L1 in our human xenograft (Figure 3.10G), indicating IFN regulation of PD-L1 expression as previously reported [108, 202].

The second immune checkpoint pathway that is targeted to enhance antitumor immunity is cytotoxic T-lymphocyte-associated antigen 4 (CTLA-4). CTLA-4 can be

expressed by $CD8^+$ T-cells, $CD4^+$ T-cells, and Treg [201]. CTLA-4 expression was tested in saline and in CHA1 treated tumors. The expression profile was not altered after treatment in human xenograft model (Figure 3.10A). This result was expected since our human xenograft model lacked T-cells. However, the syngeneic mouse model showed that CHA1 treatment decreased the transcription of CTLA-4, which is one of markers of T-cell exhaustion (Figure 3.10B, 3.10C) [200]. Exhausted T-cells become hyporesponsive and they lack their effector function (loss of IFN-γ production) [203]. One of the strategies to enhance T-cell response is targeting PD-1 pathway or co-inhibitory receptor such as CTLA-4 [203]. Together, the downregulation of T-cells exhaustion markers, PD-1 and CTLA-4 and the increase in IFNγ-secreting $Ki67^+$ $CD8^+$ T-cells suggested that CHA1 promotes cytotoxic T-cells activation and enhances their function which is important for ICIs efficacy.

Recent evidence suggested that upregulation of PD-L1 expression was not the only biomarker to the response into ICIs. It has been claimed that the response to ICIs arises in the tumor with high expression of dendritic cell and $CD8^+$ T cell-associated genes, which is called T cell ”inflamed” phenotype (Figure 3.10H) [204, 205]. In addition to PD-L1 induction, CHA1 was effective in induction of T-cell inflamed gene signature in syngeneic model (Figure 3.10I, 3.10J). In addition, CHA1 upregulated Psmb10, which is one of T-cell inflamed gene signature, in syngeneic mouse model (Figure 3.7E). Furthermore, our data demonstrated that CHA1 upregulated HLA-DRB1 (Figure 3.7C) which is MHC-II gene that linked to T-cell inflamed signature, in human xenograft, indicating CHA1 manipulated the tumor cells themselves to express genes indicative of T-cells activation. Thus, CHA1 increased the chance of successful response to ICIs. In

addition, there was a positive correlation between PD-L1 and CHA1 T-cell inflamed genes in our syngeneic and human xenograft model (Figure 3.10K, 3.10L). We also showed that PD-L1 expression was positively correlated with CHA1 T-cell inflamed genes in an invasive breast cancer patient dataset retrieved from TCGA (Figure 3.10M). Thus, CHA1 was effective in induction of gene signature rather than PD-L1 to increase the chance of successful response of ICIs.

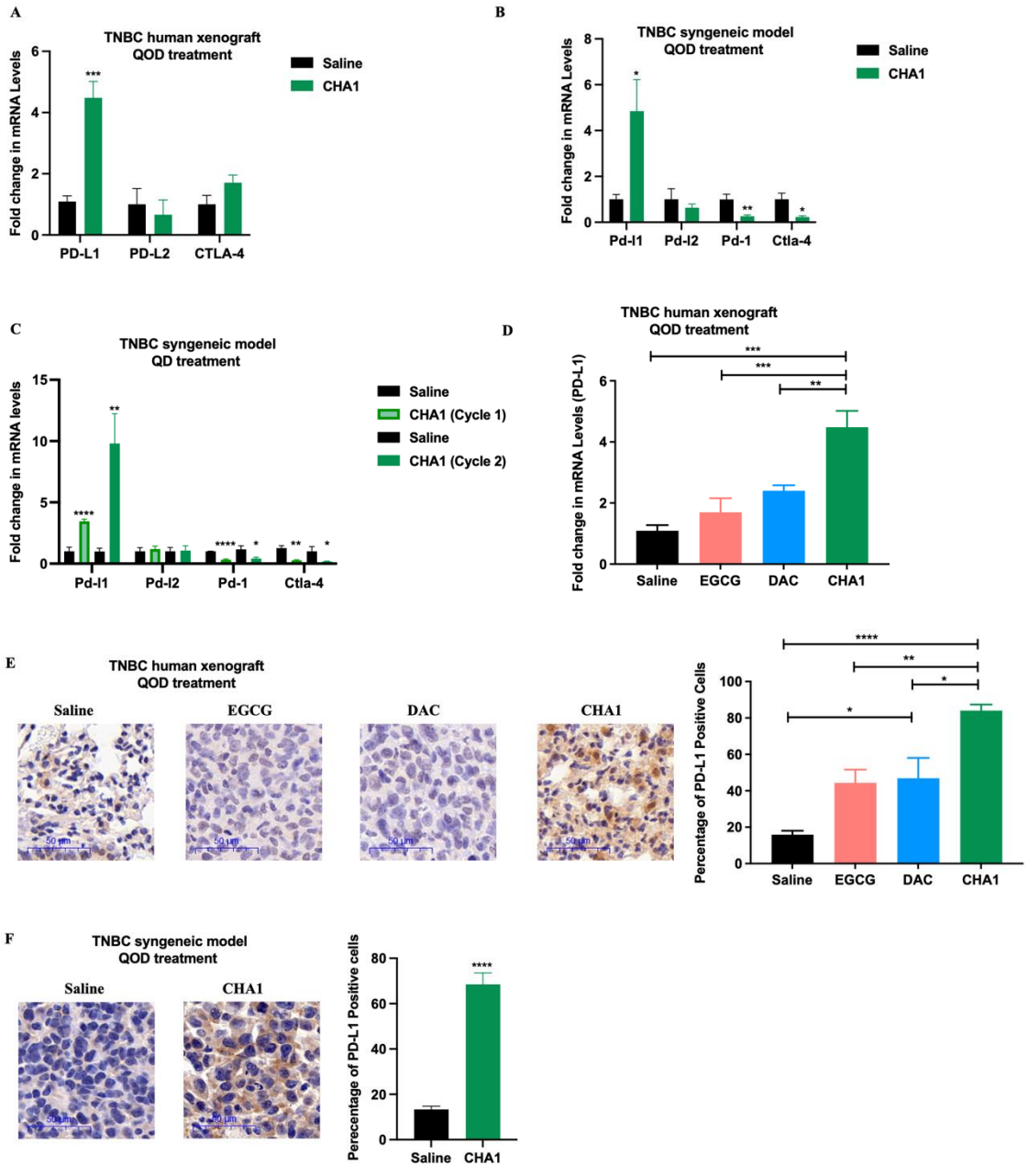

G

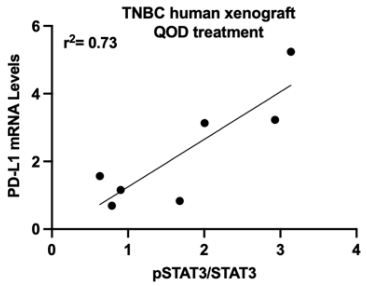

H

Published T-cell inflamed signature
CCL2
CCL3
CCL4
CCL5
CD27
CD276
CD4
CD8A
CMKLR1
CTLA4
CXCL10
CXCL9
CXCR6
EOMES
FOXP3
GZMB
GZMK
HLA-DMA
HLA-DMB
HLA-DOA
HLA-DOB
HLA-DQA1
HLA-DRB1
HLA-E
ICOS
IDO1
IFNG
IRF1
LAG3
NKG7
PD-L1
PD-L2
PRF1
PSMB10
STAT1
TIGIT
TNF

Overlap genes
Ccl4
Ccl5
Cd4
Cd8a
Cxcl10
Cxcl9
Gzmb
HLA-DRB1
Icos
Ido1
Ifng
Lag3
PDL-1, Pdl-1
Prf-1
Psmb10
Stat1
Tigit

hypergeometric p-value = 7.2e-46

CHA1 gene signature
Ccl4
Ccl5
Cd4
CD74
Cd8a
Ctla-4
Cxcl10
Cxcl9
Gzmb
HAL-DRB1
HLA-B
HLA-DRB5
ICAM-1
Icos
Ido1
IFI27, Ifi27
IFIT1, Ifit1
IFIT2
IFIT3, Ifit3
Ifng
ISG20
Lag3
OAS1, Oas1a, Oas1b, Oas1g
OAS2
OAS3, Oas3
OASL, Oasl1, Oasl2
Pd-1
PD-L1, Pd-l1
Prf-1
Psmb10
PSMB9
Stat1
Tigit
VCAM

I

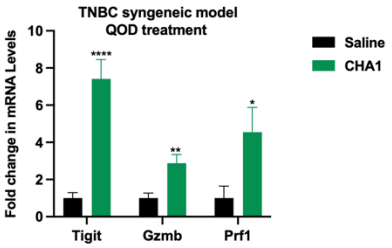

J

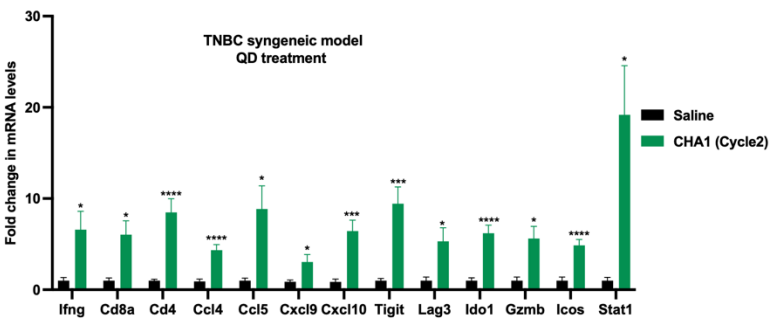

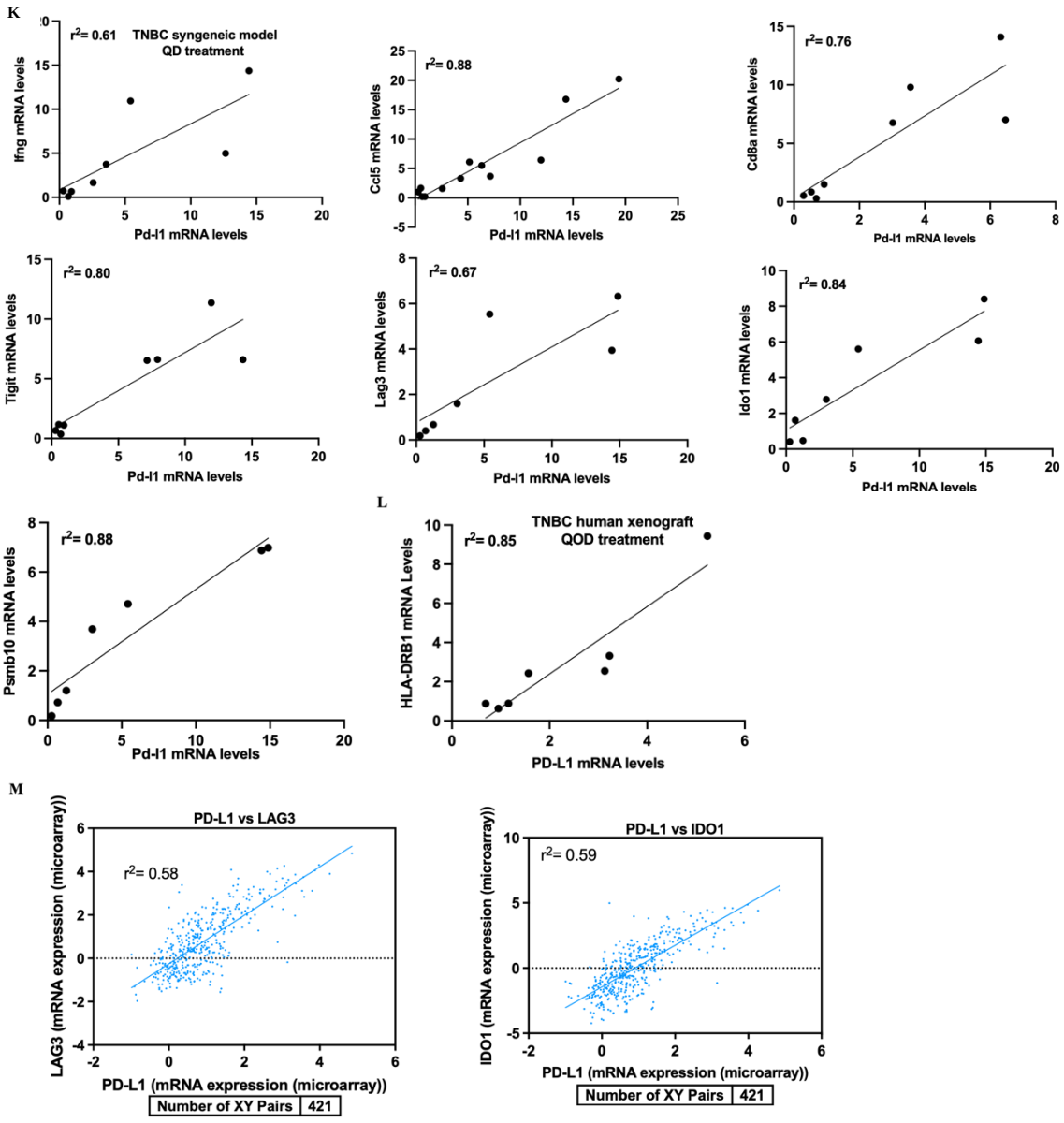

Figure 3.10. CHA1 Induced PD-L1 Expression and T-cell Inflamed Signature in TNBC Human Xenograft and TNBC Syngeneic Model. A) CHA1 QOD treatment in human xenograft increased the gene expression of PD-L1 and did not change the gene expression of PD-L2 and CTLA-4. **B-C)** CHA1 QOD and CHA1 QD treatment in TNBC syngeneic model induced the gene expression of Pd-l1, did not change the gene expression of pd-l2 and decreased the gene expression of Pd-1 and Ctla-4. The gene expression was measured by qRT-PCR in saline and CHA1 treated tumors (human xenograft QOD, n=4-6 mice, syngeneic QOD, n=5-6, syngeneic QD cycle 1, n=3-4, syngeneic QD cycle 2, n=5-7). D) CHA1 QOD treatment in TNBC human xenograft elevated the gene expression of PD-L1. DAC QOD treatment also induced the expression of PD-L1; however, the PD-L1-induction level was higher after CHA1 treatment (n=4-5). **E)** IHC of PDL-1^{+} cells demonstrated increased the protein levels of PD-L1 after CHA1 QOD treatment in TNBC human xenograft. Different sections of different control,

EGCG, DAC, and CHA1 treated tumors were stained with anti-PD-L1 antibody. Representative immunostaining section with quantification of the percentage of PD-$L1^+$ cells in control tumors and treated tumors (n= 4 mice/group). **F)** IHC of PD-$L1^+$ cells revealed increased the protein levels of PD-L1 after CHA1 QOD treatment in TNBC syngeneic mouse. Different sections of different treated and untreated tumors were stained with anti-PDL-1 antibody. Representative immunostaining section with quantification of the percentage of PDL-1^+ cells in control tumors and treated tumors (n= 4 mice/group). **G)** STAT3 phosphorylation status (Figure 3.8A) was positively correlated with mRNA levels of PD-L1(Figure 3.10A) after CHA1 QOD treatment in TNBC human xenograft tumors. r^2 value was calculated using GraphPad Prism**. H)** Overlapping genes between the published T-cell inflamed signature associated with anti-PD-1/anti-PD-L1 response and CHA1 gene signature. There were 17 genes overlapped between the two signatures (hypergeometric p-value = 7.7 e-46). **I-J)** CHA1 QOD and CHA1 QD treatment upregulated the expression of T-cell inflamed gene signature in TNBC syngeneic mouse model. The gene expression was tested after CHA1 QOD (n=5) and CHA1 QD cycle 2 (n=5-7) treatment in TNBC syngeneic model. **K)** Pd-l1 mRNA levels were positively correlated with mRNA levels of Ifng, Cd8a, Ccl5, Tigit, Lag3, Ido1, and Psmb10 after CHA1 QD treatment in TNBC syngeneic mouse model. Figure 3.7E, Figure 3.10A, Figure 3.10J, and Figure 3.12I was used to generate the data. r2 value was calculated using GraphPad Prism. **L)** PD-L1 mRNA level (Figure 3.10A) was positively correlated with mRNA level of HLA-DRB1 (Figure 3.7C) after CHA1 QOD treated TNBC human xenograft tumors. **M)** The co-expression data was obtained from cBioPortal for Cancer Genomics "TCGA, Cell 2015 " [163] (refer to materials and methods). PD-L1 expression was positively correlated with CHA1 T-cell inflamed gene including LAG3 and IDO1 in invasive breast cancer patients. r^2 value was calculated using GraphPad Prism. Linear regression analysis was performed using Pearson r values. Unpaired two-tailed t-test was used for the comparison between two groups. Adjusted one-way ANOVA was used for multiple comparison. * $P < 0.05$, ** $P < 0.05$, *** $P < 0.005$, **** $P < 0.001$. qRT-PCR experiments were done in triplicate in three independent experiments. Data were represented as mean ± SEM.

3.7. CHA1 Gene Signature Predicted Better Prognosis

We further investigated the CHA1 gene signature in the METABRIC invasive breast cancer patient dataset. To achieve this, the patient dataset was classified into two groups based on mRNA expression of CHA1 T-cell inflamed gene signature: patients with high expression of PD-L1, CD8A, CCL5, TIGIT, LAG3 IDO1, and GZMB profile and patients with low/no alteration of PD-L1, CD8A, CCL5, TIGIT, LAG3, IDO1, and GZMB expression profile. We found that invasive breast cancer and TNBC patients with CHA1 T-cell inflamed gene signature-enriched had better prognosis and prolonged

survival (Figure 3.11A, 3.11B). Furthermore, analysis of TCGA and METBRIC invasive breast cancer patients' dataset demonstrated that CHA1 gene signature including PD-L1, TIGIT, HLA-B, HLA-DRB1, OAS2, IFI27 and HBP1 could predict favorable outcome in invasive breast cancer patients (Figure 3.11C-3.11I).

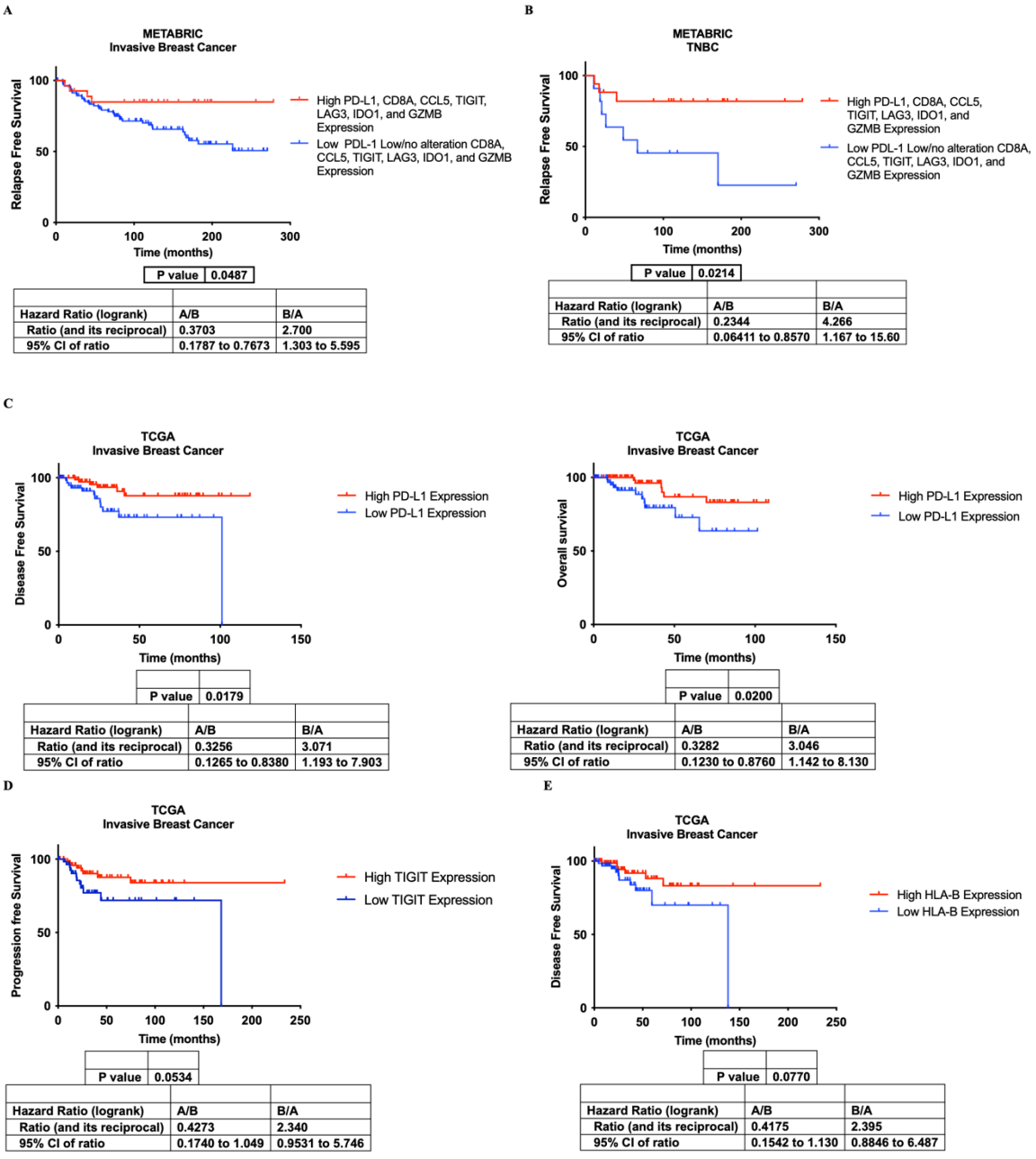

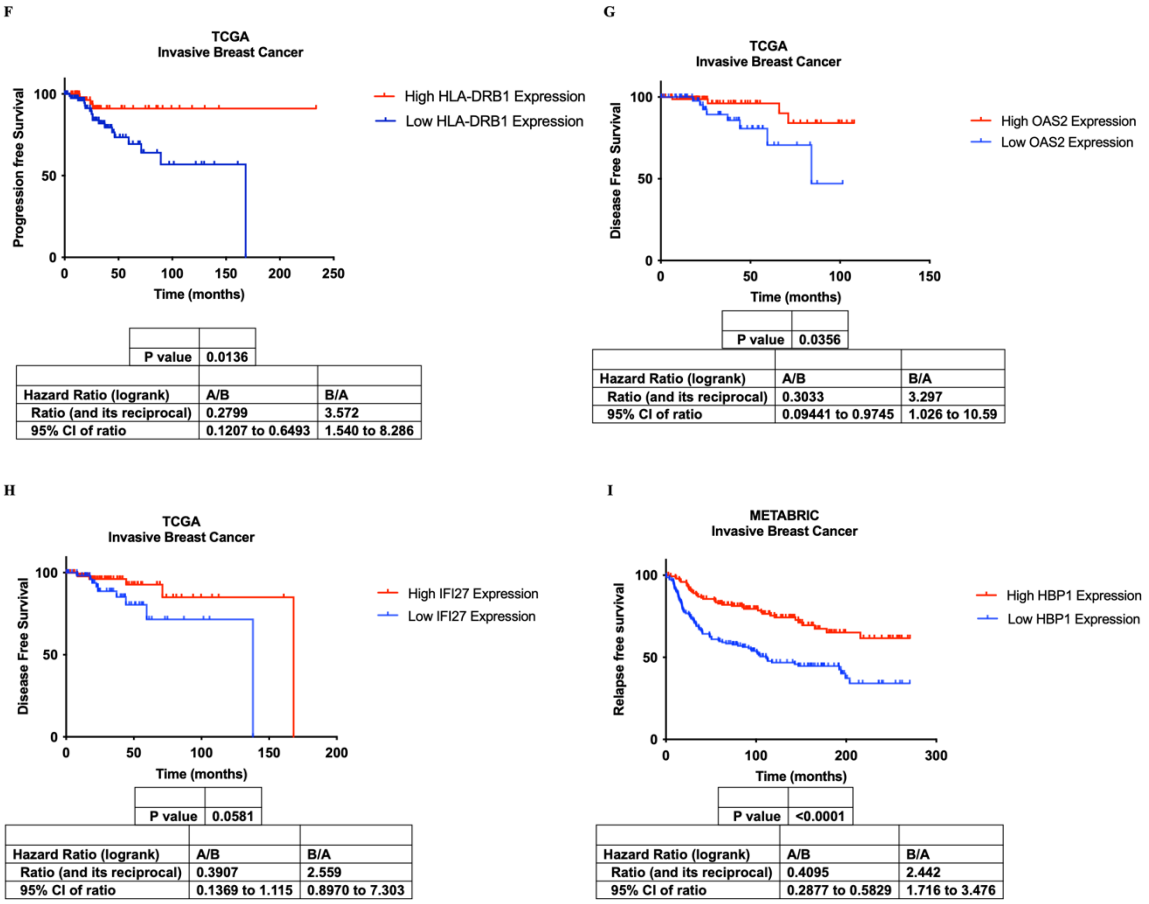

Figure 3.11. CHA1 Gene Signature Associated with Improved Prognosis in Invasive Breast Cancer Patients and TNBC Patients. A-B) Invasive breast cancer patients and TNBC patients with high expression of CHA1 T-cell inflamed gene signature include PD-L1, CD8A, CCL5, TIGIT, LAG3, IDO1, and GZMB had a prolonged relapse free survival. **C-I)** Invasive breast cancer patients with high expression of CHA1 gene signature include PD-L1, TIGIT, HLA-B, HLA-DRB1, OAS2, IFI27 and HBP1 had a prolonged survival. cBioPortal for Cancer Genomics was used to extract the data. The survival data for (A, B, I) was obtained from "METABRIC, Nature 2012 & Nat Commun 2016 (n=2509)" [160-162], for (D, F) was obtained from "TCGA, PanCancer Atlas (n=1084)" and for (C, E, G-I) was obtained from "TCGA, Cell 2015 (n=818)" [163]. mRNA expression relative to all samples with z-score threshold of 1.3 was used to extract the data. Kaplan-Meier survival curve with the hazard ratio (HR), 95% confidence intervals (CIs) and log-rank *P*-value was used for survival analysis.

3.8. CHA1 Collaborated with Immune Checkpoint Inhibitor Anti-PD-L1 in TNBC Syngeneic Mouse Model

The substantial data demonstrating CHA1 reprogramed both the tumor and the TME further suggested that CHA1 could be used in combination with ICIs. The 4T1

immune competent TNBC model is unfortunately limited in the number of ICIs drugs that can be used. As previously shown, 4T1 tumors had a significant and deleterious effect on the hematopoietic system resulting in splenomegaly and granulocytosis [206]. In addition, it has been reported that repeated dose of anti-PD-L1/anti-PD-1 in 4T-1 tumor-bearing-Balb/c mice caused hypersensitivity reaction [206, 207]. However, and even with that limitation, CHA1 worked synergistically with anti-PD-L1 in reducing both tumor volume and tumor weight (Figure 3.12B). In addition, CHA1+ anti-PD-L1 tumor displayed a sign of necrosis (Figure 3.12D). Interestingly, CHA1 did not work with anti-PD-1 or anti-CTLA-4 (Figure 3.12E, 3.12F). Again, we could not administer more than 2 doses due the limitation of the 4T-1.

We then asked how the addition of CHA1 to anti-PD-L1 could affect the TME. IF staining of $Ki67^{+}CD8^{+}$ T-cells was performed (Figure 3.12G). CHA1 and CHA1+ anti-PD-L1 significantly increased $Ki67^{+}$ $CD8^{+}$ cytotoxic T-cells, indicating activation of the proliferation of IFNγ-secreting T-cell. In addition, IHC staining of PD-L1 was performed (Figure 3.12H). CHA1 and CHA1+ anti-PD-L1 significantly increased PD-L1 positive cells. To further analyze the mechanistic interaction between CHA1 and anti-PD-L1 at the molecular level, the expression of several genes associated with T-cell inflamed TME (Pd-l1, Ifng, Cd8a, Cd4, Ccl4, Ccl5, Cxcl9, Cxcl10 and Tigit), Wnt inhibitors (sFrp1 and Hbp1), MHC-I (β2m, H2d) , MHC-II (H2Aa, H2Ab1), and ISGs (Oas3, Ifit3) was examined in the 4 treatment groups: control, anti-PD-L1, CHA1, CHA1 + anti-PD-L1 (Figure 3.12I-3.12L). The effect was dominated by CHA1. CHA1, and CHA1+ anti-PD-L1 significantly induced the expression of these genes, suggesting that addition of CHA1 into anti-PD-L1 enhanced the responsiveness to anti-PD-L1 through activation of CHA1

gene signature associated with intra-tumor and T-cell immune response and inhibition of Wnt signaling. In addition, our data also showed that CHA1+ anti-PD-L1 associated with prolonged survival compared to saline and anti-PD-L1 group in our TNBC syngeneic mouse model (Figure 3.12M).

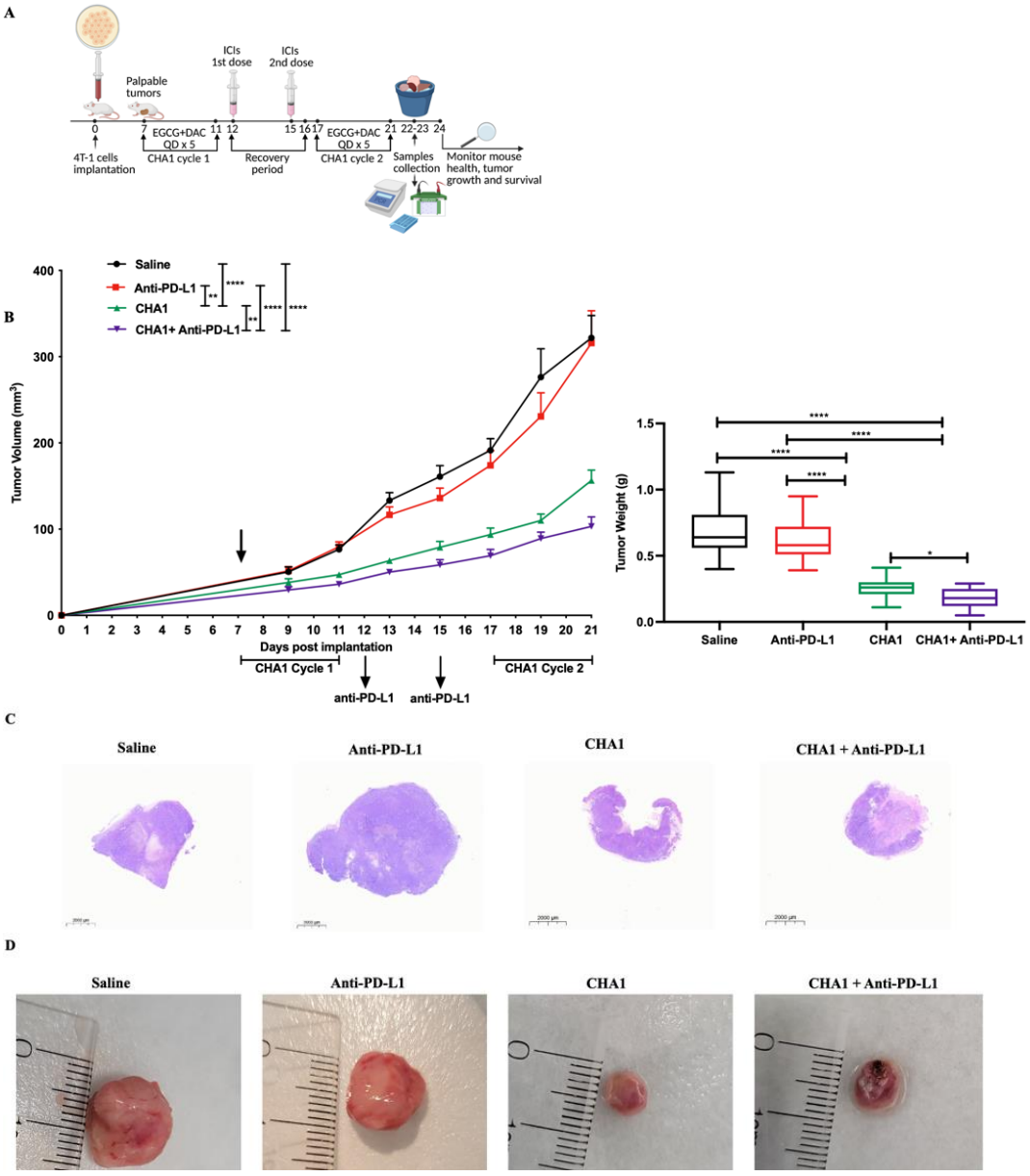

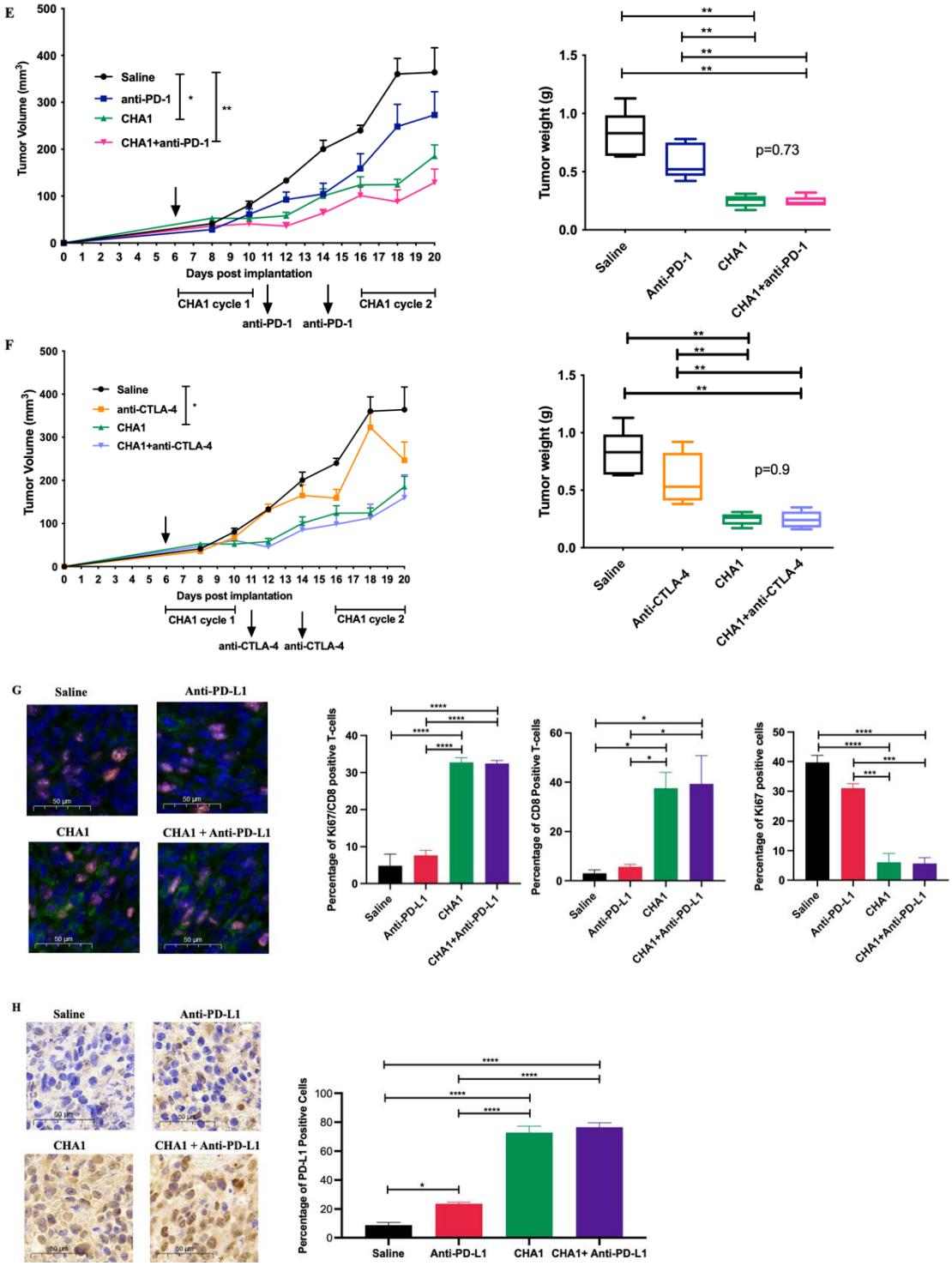
E
Tumor Volume (mm3)
Saline
anti-PD-1
CHA1
CHA1+anti-PD-1
Days post implantation
CHA1 cycle 1
CHA1 cycle 2
anti-PD-1 anti-PD-1
Tumor weight (g)
p=0.73
Saline
Anti-PD-1
CHA1
CHA1+anti-PD-1
F
Tumor Volume (mm3)
Saline
anti-CTLA-4
CHA1
CHA1+anti-CTLA-4
Days post implantation
CHA1 cycle 1
CHA1 cycle 2
anti-CTLA-4 anti-CTLA-4
Tumor weight (g)
p=0.9
Saline
Anti-CTLA-4
CHA1
CHA1+anti-CTLA-4
G
Saline
Anti-PD-L1
CHA1
CHA1 + Anti-PD-L1
Percentage of Ki67/CD8 positive T-cells
Percentage of CD8 Positive T-cells
Percentage of Ki67 positive cells
Saline
Anti-PD-L1
CHA1
CHA1+Anti-PD-L1
H
Saline
Anti-PD-L1
CHA1
CHA1 + Anti-PD-L1
Percentage of PD-L1 Positive Cells
Saline
Anti-PD-L1
CHA1
CHA1+ Anti-PD-L1

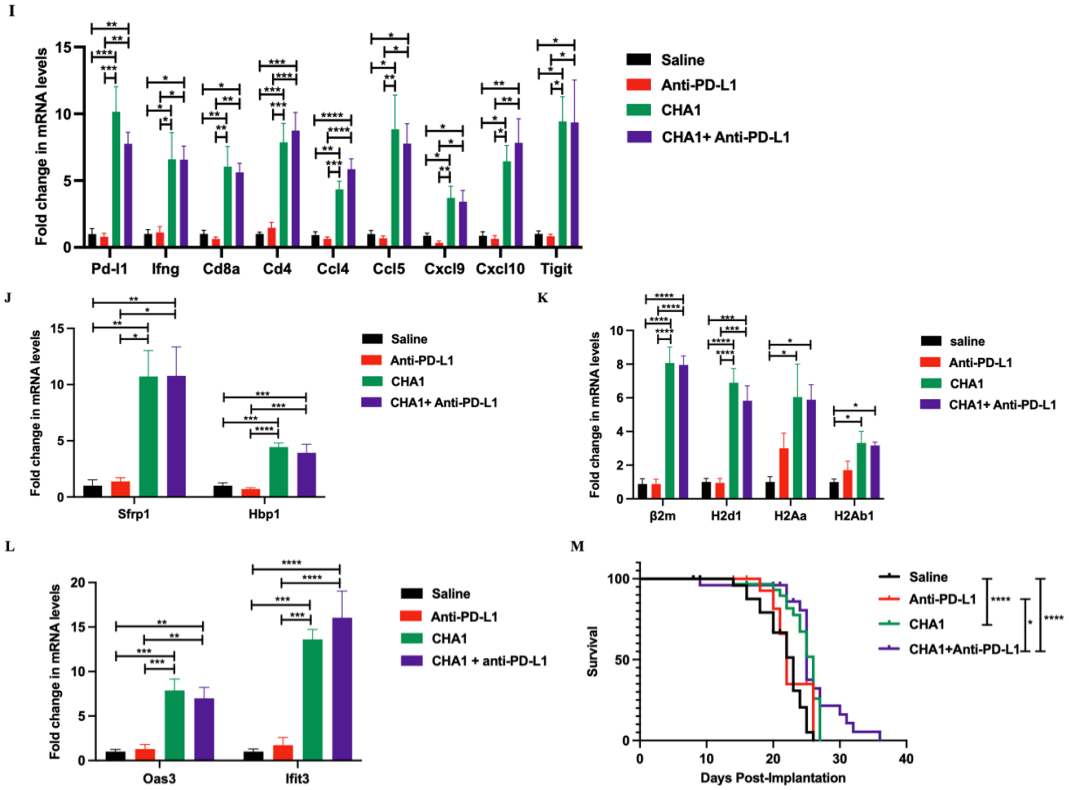

Figure 3.12. CHA1 Enhanced the Response to Anti-PD-L1 but not to Anti-PD-1 or Anti-CTLA-4 in TNBC Syngeneic Mouse Model. A) Study design of CHA1 treatment in combination with ICIs. The CHA QD treatment timeline was followed as in figure 3.4E. The 4-T1 cells were implanted orthotopically into Balb/c mice. Mice were treated with saline, ICIs, CHA1, CHA1+ICIs for the indicated time. Tumor volume was measured with calipers. Tumors were weighted at the end of the experiment. Anti-PD-L1 or anti-PD-1 or anti-CTLA-4 (100 µg/mouse) was administrated on day 12 and day 15 during recovery period. **B)** CHA1 sensitized the tumors to anti-PD-L1. CHA1 treatment with anti-PD-L1 suppressed the tumor growth and reduced the tumor weight (n=15-23). **C)** H&E staining of saline, anti-PD-L1, CHA1, and CHA1+ anti-PD-L1. **D)** Picture of tumors dissected at the end of the experiment of the 4 treatment groups: saline, anti-PD-L1, CHA1, and CHA1+ anti-PD-L1. Tumor treated with CHA1+ anti-PD-L1 had a necrotic area. **E-F)** CHA1 did not work with **E)** anti-PD-1 and **F)** anti-CTLA-4 (n=5mice/group). **G)** Immunofluorescent of co-staining of $Ki67^+$ $CD8^+$T-cells showed that CHA1 and CHA1 + anti-PD-L1 treatment increased the percentage of infiltration of actively proliferating IFNγ-secreting cytotoxic $CD8^+$ T-cells. Different sections of different treated and untreated tumors were stained with anti-CD8 and anti-Ki67 antibody. Representative Immunofluorescence staining section with quantification of the percentage of $Ki67^+$ $CD8^+$ T-cells, $CD8^+$ T-cells and $Ki67^+$ tumor cells in untreated tumors and treated tumors (n= 3 mice/group). **H)** IHC of $PD\text{-}L1^+$ cells in showed that anti-PD-L1, CHA1 and CHA1+ anti-PD-L1 treatment increased the expression of PD-L1. Different sections of different treated and untreated tumors were stained with anti-PD-L1 antibody. Representative immunostaining section with quantification of the percentage of $PD\text{-}L1^+$ cells in untreated tumors and treated tumors (n= 3 mice/group). **I-L)** The

combination of CHA1 and anti-PD-L1 enhanced the immune response to anti-PD-L1 through **I)** upregulation of CHA1 T- cell inflamed genes, **J)** induction of the gene expression of Wnt inhibitors (sFrp1 and Hbp1), **K)** increase the gene expression of MHC-I (β2m, H2d), MHC-II (H2Aa, H2Ab1), and **L)** upregulation of ISGs (Oas3, Ifit3). The gene expression was tested by qRT-PCR after saline, anti-PD-L1, CHA1, CHA1+ anti-PD-L1 treatment (n= 5-8 mice/group). **M)** CHA1+ anti-PD-L1 prolonged the survival of 4T1- tumor-bearing mice compared to control (P<0.0001, HR=2.8, 95%CI=1.4-5.6) and anti-PD-L1 (P=0.02, HR=1.8, 95%CI=0.9-3.6). At least 12 mice were treated with saline, anti-PD-L1, CHA1, and CHA1+ anti-PD-L1 for the indicated time following Figure 3.12A regimen. The results were combination of two different studies. Mann-Whitney U-test was used for tumor volume and tumor weight comparison. Adjusted one-way ANOVA was used for multiple comparison. Kaplan-Meier survival curve with the hazard ratio (HR), 95% confidence intervals (CIs) and log-rank P-value was used for survival analysis (refer to materials and methods). * $P < 0.05$, ** $P < 0.05$, *** $P < 0.005$, **** $P < 0.001$. qRT-PCR experiments were done in triplicates in three independent experiments. Data were represented as mean ± SEM.

3.9. Graphical Summary of CHA1 functions

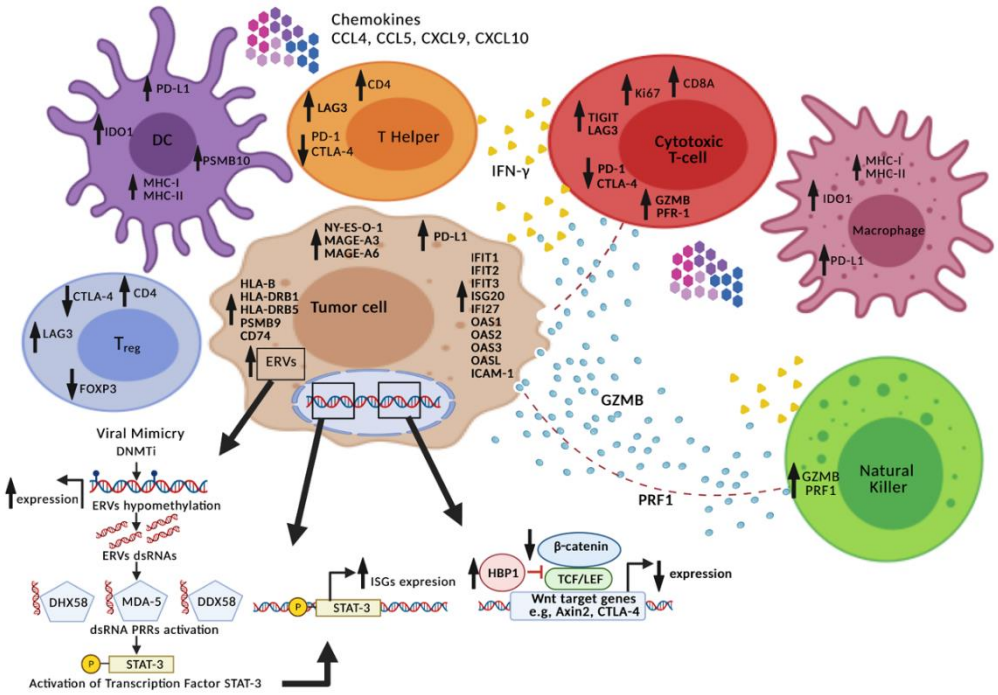

Figure 3.13. CHA1 Gene Signature. CHA1 can convert cold tumors into hot tumors by altering key signaling pathways and cellular processes and reprogramed a tumor cell to have antigen presentation properties, upregulate PD-L1, increase effector immune cells infiltration, decrease immune suppressor cells infiltration, and induce T-cell inflamed signature. Thus, CHA1 could be an ideal collaborative agent to enhance immune checkpoint inhibitors (ICIs) response. CHA1 suppressed Wnt/β-catenin pathway, which is a tumor intrinsic factor that play important role to determine the response into ICIs, by

induction of Wnt inhibitor including HBP1 and sFRP1. CHA1 also activated IFNα/β and IFNγ pathways, that correlated with successful ICIs treatment, and upregulated interferon stimulated genes (ISGs). One possible mechanism was through activation of viral mimicry. Also, CHA1 induced CTAs on tumor cells that can result in increased immune recognition of tumor cells and therefore, activation of T-cells to secrete IFNγ. In addition, CHA1 increased the infiltration of activated cytotoxic IFNγ-secreting $Ki67^+$ $CD8^+$ T-cells. The production of IFNγ by activated cytotoxic T-cells, and other cells such as T-helper cells and natural killer (NK) cells resulted in stimulation of key downstream signaling molecules. IFNγ can upregulate the expression of MHC-I, MHC-II and other components of the immunoproteasome and antigen-presenting machinery. Activation of antigen presentation is important for T-cells activation, resulting in tumor cells elimination. Thus, antigen presenting cells (APCs) such as dendritic cells (DC), macrophages and tumor cells can present the antigen to cytotoxic $CD8^+$ T-cells via MHC-I or to T-helper cells via MHC-II. One important effect of CHA1 was induction of antigen machinery in APCs including tumor cells. Furthermore, CHA1 induced the expression of chemokines such as CCL4, CCL5, CXCL9, and CXCL10 that function to recruit additional cytotoxic $CD8^+$ T cells. Moreover, CHA1 upregulated perforin (PRF1), and granzymes (GZMB). Active $CD8^+$ T cells and NK cells can secrete PRF1 and GZMB which play important role in apoptosis. Furthermore, CHA1 upregulated the expression of T-cell inflamed signature. One of the functions of IFN-γ is induction of a host of checkpoints, such as PD-L1, on the surface of macrophages, DCs and tumor cells. In addition to upregulation of PD-L1, other checkpoint molecules including TIGIT, LAG3, and IDO1 can also be homeostatically upregulated by T cell activation and IFN-γ signaling in order to restrain the antitumor immune response. In addition, CHA1 downregulated T-cell exhaustion markers including PD-1 and CTLA-4 which is a Wnt target gene and decreased the infiltration of immune suppressor $FOXP3^+$Treg. Overall, CHA1 function through an array of effector molecules to induce a T-cell inflamed tumor microenvironment (TME) that crucial for ICIs effectiveness.

3.10. Author Contributions

Mariam Alamoudi performed Figure 3.1, 3.3A, 3.3B, 3.4-3.13 and Table 3.1-3.7. Mollie Chipman participated in Figure 3.6 A, 3.6 D, 3.6E, 3.6G, 3.7C, 3.7G, 3.8D, 3.8E and 3.10A. Maricel Castener and Helen Uong performed Figure 3.2, 3.3B-3.3F. Francesca Deleso-Frechette participated in Figure 3.5B, 3.7C, 3.7D, 3.7F-H, 3.7J, 3.8E-F, 3.8H, 3.8J, 3.9A, 3.9C, 3.10A-B, and 3.10D, 3.10F. Kaiqi Li participated in Figure 3.3B-3.3C, 3.4D, 3.5F, 3.5I, 3.8A-C, 3.9A-C, and 3.10F. Rui Zhang participated in 3.4D, 3.5B, 3.5I, 3.7D, 3.8B, 3.8F,3.8J, 3.9A, 3.9C-G, 3.10A-B, and 3.10F. Zixu Wang participated in 3.4D, 3.5B, 3.5I, 3.7D, 3.8B, 3.8F, 3.8J, 3.9A, 3.9C-G, 3.10A-B, and 3.10F. George

Triantafillou participated in Figure 3.4F-G, 3.5C, 3.5G, 3.8G, 3.10C, 3.10I, 3.12B, 3.12D-F, and 3.12 M. Roaya Alqurashi and Ahlam Bogis participated in Figure 3.4F-G, 3.12B, 3.12D-F, and 3.12M. Kyle Gillani participated in Figure 3.7C, 3.7F, 3.7J, and 3.8H. Christopher Herbosa participated in Figure 3.7E, 3.8G, 3.9B, 3.9F, 3.10C, 3.10E, and 3.10I-J. Corinne Carland participated in Figure 3.7A, 3.8D, and 3.8E. Eileen Liu participated in Figure 3.7J, 3.8F, 3.8H, and 3.10F. Anise Applebaum participated in Figure 3.8E. Salwa Hafez and Ashley Besch participated in Figure 3.6A and 3.6D. Mohammed Alshagawi participated in Figure 3.5B, 3.12K, and 3.12M. AJ Lee participated in Figure 3.5C and 3.10C. Ismail Shaker and Lamma Hassan participated in Figure 3.7C and 3.8E. Eric Paulson participated in Figure 3.3B-F, 3.4B, 3.6A, and 3.6D.

Chapter 4: Discussion

4.1. Discussion

While immune check point inhibitors (ICIs) are game-changing treatments that activate the local immune environment to destroy tumors, they work on tumor types that express machinery to engage the resident immune system, termed “hot” tumors. However, the vast majority (>75%) of tumors respond poorly to ICIs and are termed “cold” for immune system engagement [107, 208]. An important challenge is discovering strategies to convert tumors from “cold” to “hot”’ i.e., to engage the local immune environment, increasing tumor responsiveness to ICIs. Triple negative breast cancer (TNBC) is one of the cancers that has limited treatment options and uneven ICI efficacy [107, 208-212].

One of the biochemical mechanisms associated with cold tumors and resistance to ICIs is elevated Wnt signaling. As discussed previously, it has been difficult to inhibit Wnt signaling therapeutically, with few compounds having been tested in clinical trials. In this study, we elaborate a new therapeutic strategy for inhibiting Wnt signaling, altering the tumor microenvironment, and improving immunotherapy for TNBC and possibly other cancers. Our goal was to thoughtfully consider strategies and minimize the side-effects for the patient. The compound combination elaborated here (EGCG and DAC) have well known safety profiles and no effects on tumors when used independently, but when used together (CHA1) have far greater effects, which appear to be the sum of the treatment’s impact on multiple pathways. The initial design of CHA1 treatment was to inhibit Wnt signaling as a means of inhibiting tumor growth, which

which was successful in our work here. Intriguingly, the unbiased analysis of our RNA-seq from the human xenograft model, while further confirming the inhibition of Wnt signaling, also revealed greater functionality for CHA1 action.

It has been reported that aberrant epigenetic alterations play important role in breast cancer development and progression [213]. Previous work demonstrated that there was a negative correlation between histone lysine specific demethylase 1 (LSD1) expression and the expression of chemokines such as CCL5, CXCL9 and CXCL9 that increased recruitment of $CD8^+$ T cell and PD-L1 [213]. High number of T-cell infiltration into tumor sites is critical for ICIs efficacy [108-110]. They suggested that the resistance to anti-PD-1was contributed to silence the gene expression of effector T cell chemokines. Their work showed that LSD1 inhibitor enhanced $CD8^+$ T cell trafficking into TME by reinduction of these chemokines [213]. In addition, the combination of anti-PD-1 with LSD1 inhibitor suppressed the tumor growth and enhanced the response to anti-PD-1 in mice bearing TNBC xenograft tumors [213]. This raises the question of whether combining ICIs with other approaches to target epigenetic modifications could augment the response to ICIs.

It has been demonstrated that the expression of Th1-associated chemokines such as CXCL9 and CXCL10, MHC molecules, and PD-L1 are epigenetically silenced by DNMT [107]. One of the mechanistic function of CHA1 is suppression of DNMT1 [135, 140, 149]. As consequences of CHA1-epigenetic modification, careful analyses of CHA1 for tumor-intrinsic and overall function demonstrated a far broader alteration of the tumor and its microenvironment. CHA1 treatment resulted in activation of immune-related pathways, including stimulation of the IFN pathway via viral mimicry, induction of

antigen presentation machinery including MHC-I and MHC-II and upregulation of a T-cell inflamed gene signature including increased the expression of PD-L1 and chemokines such as CCL4, CCL5, CXCL9, and CXCL10 that recruits more $CD8^+$ T cells to tumor sites. Concomitantly, CHA1 treatment increased tumor infiltration of active IFNγ-secreting $Ki67^+$ $CD8^+$ T-cells, $F480^+$ macrophages and decreased infiltration of $FOXP3^+$ Treg. The tumor reprogramming by CHA1 combinational therapy suggested that it may act synergistically with ICIs and indeed, CHA1 in conjunction with anti-PD-L1 was significantly suppressed tumor growth compared to CHA1.

Many TNBC tumors have a common phenotype of hyperactive Wnt signaling [214]. Activation of Wnt signaling has been linked to breast cancer cell growth and to recurrence of the disease [41, 42]. β-catenin levels are elevated by Wnt signaling, which is thought to contribute to the poor prognosis of patients with TNC [215]. The data from both human xenograft and syngeneic model revealed that CHA1 reduced β-catenin protein levels and AXIN2, a Wnt target gene. As predicted, we showed significant induction of HBP1 and sFRP1 in both TNBC human xenograft and syngeneic model in both QOD and QD cycles regimens. The data from human xenograft suggested that both drugs were required to inhibit Wnt target gene AXIN2. Several studies reported EGCG suppressed Wnt signaling in colon cancer cells, lung cancer stem cells and breast cancer cells [56, 216, 217]. However, previous work showed that DAC monotherapy was not able to downregulate Wnt target genes in AML cell lines and mouse model [218].

Wnt signaling has been linked to resistance to ICIs in melanoma [108]. High Wnt signaling resulted in decreased T-cell infiltration into tumor sites which is critical for ICI efficacy [108-110]. The second reason for failure of ICI therapy in melanoma was a

dysfunctional JAK/STAT/IFN pathway [108]. Furthermore, mutations in the interferon receptor pathway was linked to resistance to anti-CTLA-4 or anti-PD-1 in metastatic melanoma patients [219]. Activation of IFN signaling resulted in promoting innate and adaptive immune response [58]. In addition, active IFN signaling was required for proper anti-tumor immune response and ICIs efficacy, and for activation of tumor antigen presentation [108]. In addition, IFN activation induced PD-L1 expression [108]. It has been reported that PD-L1 was regulated by JAK/STATs/IFN pathway [202]. GSEA analysis of the RNA-seq indicated activation of IFNα/β and IFNγ pathways after CHA1. Our data showed that CHA1 increased phosphorylation status of STAT3 in both human and syngeneic models, indicating stimulation of IFNα/β and IFNγ pathways [58]. Looking at downstream targets, CHA1 treatment markedly increased the expression of IFN stimulated genes (ISGs).

We investigated the possible source of IFN stimulation, and a major possibility was induction of viral mimicry via alteration of the epigenome. Several reports from studies of DNMTi suggested that part of its efficacy lies in the hypomethylation of ERVs [220]. Previous work reported that DNMT is enhanced the efficacy of anti-CTLA4 in melanoma by triggering IFN response via viral mimicry [220]. Therefore, we examined whether CHA1 induced human ERVs and muERVL-1. Indeed, human ERVs and muERVL-1 were induced by CHA1.

Immune recognition of cancer plays a critical role in cancer immunotherapy [91, 92]. Thus, a critical aspect for successful cancer immunotherapy treatment relies on development of strategies to increase expression of tumor specific antigen expression, enhance T cells function, and upregulate MHC molecules [91, 92]. All these factors act

together to facilitate tumor cell recognition by immune system and promote an immune response against tumor antigens [91, 92]. Numerous types of immunogenic tumor antigens have been identified including cancer testis antigens (CTAs) [221]. The expression of CTAs (e.g., MAGE and NY-ESO-1) are restricted to solid tumors and to immune-privileged sites such as the testis, the placenta, and during fetal development [221]. Malignant cells evade immune recognition by epigenetic modifications and other changes of some key immune stimulatory molecules. The expression of CTAs, MHC-I and MHC-II are exclusively regulated by DNA methylation [191, 222-224]. In cancer, the transcription of these genes is often silenced by hypermethylation. Demethylating agents such as DAC can reactivate these methylation-silenced genes [191, 222-224]. Our data showed that CHA1 induced MHCI, MHCII, and CTAs in human xenograft and syngeneic models. The upregulation of MHC-I and MHC-II in human xenograft revealed that CHA1 manipulated the tumor cells to become antigen presenting cells (APCs), indicating enhance tumor visibility by immune system. In addition, CHA1 upregulated β2-microglobulin (β_2M) expression which is a component of MHC-I. One of ICIs-resistance mechanism is mediated by downregulation of the MHC-I antigen presentation pathway, such as MHC-I molecules and β_2M expression [92, 96]. Several studies reported that downregulation of β_2M expression can lead to the loss of MHC-I expression on the cell surface, resulting in impaired antigen presentation to cytotoxic $CD8^+$ T cells [92, 96]. Therefore, the lack of functional MHC-I antigen presentation can lead to decrease immune recognition of tumor cells and impair eradication of the tumor cells by cytotoxic $CD8^+$ T cells. Furthermore, our data demonstrated that CHA1 induced MHC-II in tumor cells, indicating upregulation of tsMHC-II. In addition, several studies found

that there was a positive correlation between tsMHC-II expression and improved patient outcomes in different types of cancer, including TNBC [91, 100-103]. It has been demonstrated that upregulation of tsMHC-II expression was positively correlated with improved progression-free (PFS) and overall survival (OS) in melanoma and classic Hodgkin lymphoma patients who received anti-PD-1/anti-PD-L1 [91, 100, 101]. In addition, it has been reported that tsMHC-II expression with lymph node metastases following adjuvant radiotherapy and/or chemotherapy was positively correlated with improved disease-free survival (DFS) in TNBC patients [102]. Moreover, there was a significant correlation between improved PFS and the expression of several genes of MHC-II pathway including CIITA, CD74, HLA-DPA1, HLA-DPB1, HLA-DPB2, HLA-DQA1, HLA-DRB1, HLA-DRB5, and HLA-DRB6 as well as CIITA or CD74 alone in TNBC patients [103]. Furthermore, it has been reported that the induction of tsMHC-II expression was associated with the infiltration of $CD4^+$ T helper and $CD8^+$ cytotoxic T cell, absence of lymphovascular invasion, increased formation of tertiary lymphoid structures, stimulation of IFNγ-stimulated gene including PD-L1 and upregulation of IFNγ, IL2, and IL12 expression which are Th1 cytokines [91, 102]. Importantly, tsMHC-II could be used as a prognostic clinical biomarker of T-cell inflamed tumor since MHC-II expression is upregulated by IFNγ [91]. Also, our data from TCGA showed that high expression of HLA-B (MHC-I) and HLA-DRB1 (MHC-II) was associated with increased survival in patients with invasive breast carcinoma.

Our work showed that CHA1 induced the expression of CTAs. CTAs are one important sources of antigens on the tumor cell surface. Since CTAs are highly immunogenic and can elicit potent integrated natural humoral and cellular responses, they

are targets for cancer vaccine and adoptive T cell immunotherapy, including CAR-T [83, 84]. Importantly, the induction of CTAs was tumor-specific which is important for future clinical application [83].

Multiple factors play important roles in determine the responsiveness to immunotherapy. Some factors derived from tumor cells or from within the tumor micro- or macro-environment, including neoantigen load, diversity of the immune infiltrate, expression of immune checkpoints, and the enrichment of prognostic immune gene signatures. Turning cold non-inflamed tumor into hot inflamed tumor is critical for successful ICIs therapy. An effective response to ICIs has been correlated with inflamed tumor that is characterized by infiltration of T cells, the presence of IFNγ in tumor microenvironment and the expression of PD-L1 [194]. Conversely, there is a lack of therapeutic efficacy response to ICIs in non-inflamed tumor [195]. One approach to achieve a durable clinical response in patient with cold tumor is the use of collaborative agents to create immunogenic tumor microenvironment [199].

Treatment of TNBC with ICIs has recently gained significant attention. Despite the fact that breast tumors, in general, are considered not highly immunogenic tumor, TNBC is considered the more immunogenic hot subtype [225]. It has been reported TNBC has a higher level of lymphocyte infiltration, suggesting that TNBC patients may benefit from immunotherapy [225]. However, objective response rates (ORR) of ICIs as monotherapy in metastatic TNBC was variable and did not exceed 24% [226]. A recent study classified TNBC based on spatial immune cell contextures in relation to patient prognosis and response to anti-PD-1 as well as pathways of T cell evasion into excluded, ignored and inflamed [227]. The inflamed phenotype showed a favorable response to

ICIs. The other two types (ignored and excluded) was resistance to ICIs [227]. The ignored phenotype was characterized by low densities of $CD8^+$ T cells and activation of Wnt with up regulation of Wnt target genes as well as activation of the PPARγ pathway [227]. Intrinsic Wnt/β-catenin pathway has also been linked to disfavor T cells inflamed microenvironment in melanoma [109]. Furthermore, it has been shown that Wnt pathway can create T cell exclusion in bladder cancer and melanoma [112, 228]. One of the mechanism of cDC1 recruitment failure in melanoma was associated with Wnt activation [112]. It has been reported that suppression of Wnt/β-catenin pathway can lead to infiltration of $CD8^+$ T cells and increase in IFNγ associated gene targets in syngeneic mouse models of B16F10 melanoma, 4T1 mammary carcinoma, Neuro2A neuroblastoma, and Renca (renal adenocarcinoma) [194]. Furthermore, the response rate was increased with subsequent combination with ICIs [194]. Hence, CHA1 by inhibiting Wnt could convert excluded phenotype into inflamed one, therefore, enhance ICIs response in ignored TNBC.

In March 2019, anti-PD-L1 received accelerated approval to be used in recurrent or unresectable PD-L1 positive metastatic TNBC [116]. However, Roche (the company who made anti-PD-L1) voluntarily withdrew the indication of TNBC in 2021 [118]. In November 2020, FDA granted accelerated approval to anti-PD-1 in metastatic TNBC who locally recurrent or unresectable disease and whose tumors expressed PD-L1. The status of PD-L1 expression determined the patient eligibility for ICIs treatment, indicating that PD-L1 expression is critical for treatment efficacy. PD-L1 is a surrogate biomarker used in clinical trials to predict the effectiveness of ICIs [204]. One of the important findings in our study is the induction of PD-L1 in human xenograft and

syngeneic mouse models. Our results showed increase the gene expression of PD-L1 as well as the protein levels which validated by immunostaining. The result from human xenograft indicated upregulation of PD-L1 in tumor cells.

Recent evidence suggested that upregulation of PD-L1 expression was not the only biomarker to the response into ICIs. Several clinical trials reported that T-cell inflamed gene signature was associated with increased the response with ICIs [204]. Our data showed that in addition to PD-L1, CHA1 induced the expression of T-cell inflamed signature. It has been reported that this gene signature was associated with prolonged patient survival [204]. This was consistent with our data in invasive and TNBC patients as we showed that CHA1 T-cell inflamed gene signature was associated with improved patient outcome. In addition, our data from TCGA indicated CHA1 ISGs signature such as IFIT2 and OAS2 was associated with increased survival in patients with invasive breast carcinoma.

It is well established that the response to ICIs is mainly dependent on the density of pre-existing tumor-infiltrating $CD8^+$ T cells [203]. T-cells exhaustion characterized by lack of T-cells response and progression loss of their effector function (loss of IFN-γ production) [203]. One of the reasons of the progressive loss of T cell function in cancer is the induction and maintenance of T cell hyporesponsiveness by the special immunosuppressive TME [203]. In hot tumors, the failure of ICIs therapy is due mainly T-cells dysfunction. However, in cold tumors, lack of pre-existing immune response results from low immunogenicity and failed T cell priming [203]. Together, these imply the rationality of combination immune-activating therapy with ICIs. One of the important findings in our work was downregulation of PD-1 and CTLA-4 expression after CHA1

treatment, which are markers of T-cell exhaustion [200]. One possible explanation of reduction in mRNA levels of CTLA-4 was the suppressive function of CHA1 on Wnt signaling since CTLA-4 is a Wnt target gene [229].

Our finding demonstrated that CHA1 treatment could sensitize tumor cells to ICIs by creating immunogenic hot TME via inhibition of Wnt/β-catenin and changing the immune response within the tumor and within TME. CHA1 treatment reprogramed tumor cells by boosting host immune responses through enhancement of antigen presentation, activation of IFN response, induction of PD-L1 and T-cell inflamed signature, repression of T-cells exhaustion markers and increase the intra-tumoral infiltration of effector immune cells, particularly IFNγ-secreting $CD8^{+}Ki67^{+}$ T cells. Thus, CHA1 could be an ideal combination with ICIs. Our data indicated that CHA1 enhanced the anti-tumor response of anti-PDL-1 and the addition of CHA1 into anti-PD-L1 increased the survival rate in our TNBC syngeneic model.

The result of the study could offer a new hope of TNBC patients, especially those whose disease does not respond to ICIs. In addition, CHA1 could be a promising collaborative agent to improve ICIs in ICIs refractory cancer such as melanoma and colorectal cancer.

4.2. Summary of Thesis Results

TNBC is an aggressive type of breast cancer that does not express ER or PR and does not have overexpressed HER2 [1, 3, 7]. Brain metastasis is the most common complication of TNBC [13]. Wnt signaling pathway was identified as a potentially therapeutic target of TNBC [34-36]. Activated Wnt signaling is associated with resistance to ICIs in many cancers [108]. Here, we approached inhibition of Wnt signaling as a

tumor treatment by using our novel drug combination, CHA1, which is a combination of an active ingredient of green tea EGCG and a DNMT1i DAC, to reactivate multiple Wnt inhibitors. The effect of CHA1 was tested in TNBC human xenograft model and in TNBC syngeneic model. This approach was successful at inducing HBP1 and sFRP1 and inhibiting TNBC tumor growth. Inhibition of Wnt signaling was required for the efficacy of the drug combination as knockdown of sFRP1 or HBP1 was sufficient to abrogate tumor growth inhibition. We also observed elevated antigen presentation machinery including MHC-I and MHC-II expression and increased IFN signaling as well as induction of viral mimicry. Concomitant with these changes, we observed the drug combination altered the tumor microenvironment, resulting in increased tumor infiltration of IFNγ–secreting $Ki67^{+}CD8^{+}$ T-cells and macrophages as well as decreased in $FOXP\text{-}3^{+}$ Treg infiltration. Furthermore, CHA1 downregulated PD-1 and CTLA-4, markers of T-cell exhaustion. CHA1 also upregulated PD-L1 which is a biomarker of ICIs respond. In addition, CHA1 was effective in induction of T-cell inflamed gene signature beyond PD-L1. All the mechanistic targets identified required the combination of both drugs for maximum function. Either drug alone was either ineffective or only partially effective. Our finding suggests that CHA1 could re-program the tumor from “cold” i.e. immunologically silent, into a “hot” tumor with significant immune cell infiltration, indicating that CHA1 could be a good candidate as collaborative agent with ICIs. Our work in TNBC syngeneic model demonstrated that CHA1 sensitized TNBC tumors to anti-PD-L1 response and CHA1+ anti-PD-L1 treatment associated with higher survival rate compared to control and anti-PD-L1. Finally, analysis of TCGA and METABRIC

dataset indicated that the CHA1 gene signature was positively correlated with improved patient outcome.

4.3. Study Limitations

One of the big limitations of the study is the cell lines, 4-T1, that used for TNBC syngeneic model. 4T-1 murine mammary carcinoma is widely used as a TNBC syngeneic model, although there are some drawbacks of this model. It has been reported that 4T-1 tumor-bearing mice developed leukemoid reactions. The characteristics of leukemoid reaction include bone marrow hyperplasia, granulocytosis, and splenomegaly due granulocytic hyperplasia. Furthermore, it has been shown that 4T-1 tumor-bearing mice expressed high levels of myeloid colony-stimulating factors G-CSF and GM-CSF which could be contributed to this paraneoplastic syndrome [206]. We noticed similar effect in our 4T-1 syngeneic model. Control and anti-PD-L1 treated 4T-1 tumors had a splenomegaly. On the other hand, CHA1 and CHA1+ anti-PD-L1 groups did not have any spleen enlargement.

The second limitation of 4-T1 model is that we could not administer more than 2 doses of anti-PD-L1. We lost more than 60 % of the mice after the third doe of anti-PD-L1. It has been reported that repeated administration of anti-PD-L1 and anti-PD-1 resulted in fatal hypersensitivity reaction in 4T-1 tumor-bearing mice, however, this reaction was not observed in non-tumor bearing mice or Renca and B16-tumor bearing mice, suggesting this hypersensitivity reaction is specific to 4T-1 tumor-bearing mice [207]. The highly myeloproliferative properties of 4T-1 model suggested the existence of a primed TME for hypersensitivity reactions [206]. One of the reasons of fatal hypersensitivity reactions is an accumulation of neutrophils within the lungs and

accumulation of IgG1 antibodies in serum. Furthermore, administration of neutrophil depletion (anti-Gr-1) resulted in improved survival of anti-PD-1 treated mice. In addition, treatment with ganetespib, an inhibitor of the molecular chaperone heat shock protein 90 (HSP90), that used to suppress the migration of neutrophils into lungs protected the mice and prevented the accumulation of neutrophils and IgG1 after anti-PD-1 treatment, suggesting the role of neutrophils in development the hypersensitivity reaction [207].

The study limitations prevented us from conducting a well-design survival study due to the death of the mice before they reached tumor endpoint. However, we were able to study the effectiveness of CHA1 in combination with anti-PD-L1. Alternatively, EMT-6 TNBC syngeneic model could be used. Both 4T-1 and EMT-6 are mouse TNBC cell lines that can be orthotopically implanted into Balb/c mice. EMT-6 is less aggressive and less invasive compared to 4T-1. Importantly, the hypersensitivity reaction that occurred after repeated administration of anti-PD-1/anti-PD-L1 has not been reported with EMT-6 tumor bearing mice [207]. Moreover, future study of the effect of CHA1 in different mouse models such as melanoma and colorectal syngeneic mouse model could be another alternative.

4.4. Future Directions

4.4.1. Clinical Translation of CHA1 and CHA1 + anti-PD-L1 for TNBC Patients

Our works demonstrated that CHA1 had anti-tumor effect in TNBC human xenograft and in TNBC syngeneic model. In addition, CHA1 sensitized the tumor to anti-tumor effect of anti-PD-L1. CHA1 could be a promising therapeutic option to improve anti-PD-L1 response in TNBC patients. The next step is to translate CHA1+anti-PD-L1 into a Phase I clinical trial. EGCG, in a dose equivalent of 4-8 cups per day, has been

widely studied in human clinical trials with no appreciable side effects have been reported [56]. It has been reported that the side effects associated with single oral administration of EGCG (200, 400, 600, and 800 mg) into healthy individual were well tolerated [169]. Some participants experienced mild headaches and fatigue [169]. However, liver toxicity has been reported with high dose of EGCG at 800 mg twice a day for 6 months [230]. Normal liver function has been restored after EGCG discontinuation [231]. DAC is FDA-approved, and its side effects are well-documented which include neutropenia, nausea, and myelosuppression [232]. DAC side effects are manageable with careful monitoring of patients' complete blood and platelet counts [232].

The doses we used for either EGCG or DAC in our study are attainable in human with manageable side effects [166-178]. In our TNBC syngeneic model, we configured the dosing schedule of CHA1 to conform with the FDA approved regimen of DAC (20 mg/m^2 by continuous I.V. infusion over 1 hour daily for 5 days). The treatment cycle can be repeated every 4 weeks or after hematological recovery (absolute neutrophil count (ANC) at least 1,000/μL and platelets at least 50,000/μL). The minimum duration of treatment is 4 cycles. [232]. Our dosing regimen did not cause any undesirable side effects. The clinical translational applications of CHA1 will start with conducting Phase I clinical trials of CHA1. The study will be an EGCG dose escalation study with a fixed DAC dose (20 mg/m^2 I.V. infusion daily for 5 days, FDA approved dose). The first primary endpoints will be to determine the maximum tolerated dose (MTD), that can be in combination with anti-PD-L1, as well as dose-limiting toxicity (DLTs). After we determine the MTD of CHA1, anti-PD-L1, atezolizumab, at the dose of 800 mg IV infusion on days 1 and 8 of a 28-day cycle will be added to the regimen (NCT02425891). The second primary endpoint will be to determine the safety and tolerability of CHA1+ anti-PD-L1. Liver function

tests, complete blood and platelet counts will be monitored during and after treatment protocol. In addition, irAEs of anti-PD-L1 will be monitored. PK parameters will also be determined. The plasma and the cerebrospinal fluids (CSF) of CHA1 will be measured. The secondary end point is to assess the efficacy and clinical benefits such as complete (CR) or partial (PR) remission, progression-free survival (PFS), and overall survival (OS). In addition, PD-L1 levels in tumor biopsy can be used as a surrogate biomarker for treatment efficacy.

4.4.2. Clinical Translation of CHA1 and CHA1 + anti-PD-L1 for TNBC Patients with Brain Metastasis

One of the common locations for cancer metastases is the brain, with up to 46% of TNBC patients developing brain metastases [16]. 50% of metastases related death are due brain metastases [14]. Since the treatments for brain metastases must be able to cross the blood-brain barrier (BBB), their treatment options are limited, leading to a median survival rate of up to 5 months once diagnosed [16]. The development of treatments of brain metastases are challenging since patients with brain metastases are commonly excluded from clinical trials, therefore, the treatment options are restricted to surgery or whole brain radiation therapy (WBRT) [233]. Both DAC and EGCG can cross the BBB [153, 234, 235], making CHA1 treatment a promising not only for TNBC patients but also for TNBC patients with brain metastases. In addition, our data showed that CHA1 reduced brain and overall metastases in TNBC human xenograft. Moreover, previous work in the lab demonstrated that CHA1 decreased the numbers of seizures in chronic seizure mouse model.

Part of clinical translational of CHA1 + anti-PD-L1 is to include TNBC patients with brain metastases in Phase I clinical trials. The reduction in the metastases can be assessed by contrast-enhanced magnetic resonance imaging (MRI) [233]. In addition, circulating tumor cells (CTCs) can be used to determine clinical efficacy (refer to section 4.4.5).

4.4.3. Pharmacokinetic Study of CHA1

The PK profile of EGCG and DAC have been widely studied [166-178]. However, the PK of CHA1 has not been characterized. It is important to conduct PK study of CHA1 in the preclinical model. The aim of this experiment is to inform us the effective concentrations and accurate dosing recommendations for human patients and therefore, reduce side effects associated with the treatment. Tumor-bearing mice will receive a single dose of either DAC or EGCG, or CHA1 as we intend to administer in patients (QD cycles regimen). Then, blood samples will be collected at different time points. The plasma levels will be determined by HPLC. C_{max}, AUC, $t_{1/2}$, and other pharmacokinetic parameters will be determined. In addition, the level of CHA1 in cerebrospinal fluid will be measured since both drugs cross the BBB [153, 234, 235]. After we conduct the PK study in preclinical model, the next step is to study PK profile of CHA1 in Phase I clinical trial.

4.4.4. Development of Oral Formulation Works Synergistically with ICIs

Hypomethylating agents (HMAs) such as decitabine (DAC) and azacytidine (AZA) have been approved by FDA as parental therapies for treatment of myelodysplastic syndromes (MDS) [138]. In addition, HMAs were also used for acute myeloid leukemia (AML) and chronic myelomonocytic leukemia (CMML) [138].

Development of oral formulation of HMAs has gained a significant interest to minimize the burden of parenteral therapies and to improve patient-adherence. One of the challenges to the development of HMAs oral analogs is to overcome the rapid metabolism of agents by the enzyme cytidine deaminase (CDA), which is expressed in the GI tract and in the liver and is involved in first-pass metabolism [236]. In July 2020, FDA approved an oral DAC in combination with cedazuridine, CDA inhibitor (CDAi) [138]. Furthermore, in September 2020, FDA approved an oral AZA as a maintenance treatment for AML [138]. Both DAC and AZA are incorporated into DNA and inhibit DNMT, resulting in hypomethylation and reactivation of silenced genes such as tumor suppressor genes and genes involved in cell cycle control like p16, p15, and p57 [135]. The main difference in their mechanism of action is that 80-90% of the AZA is incorporated into RNA, leading to defect in the processing of tRNA and rRNAs and inhibition of protein synthesis [135, 237]. There were no direct randomized clinical trials performed to compare between DAC and AZA in term of clinical efficacy and safety. Several indirect systemic reviews and network meta-analysis was conducted to compare the parental formulations of the two agents [238, 239]. The conclusion from these retrospective studies demonstrated that both drugs improved the overall response rate (ORR) and the overall survival (OS) compared to conventional care regimens (CCR). Furthermore, AZA treatment was associated with higher rate of complete remission with incomplete blood count recovery (CRi) compared to CCR [239]. Indirect head-to-head comparisons showed that DAC was superior to AZA in term of complete remission (CR) [239]. In addition, patients who received DAC experienced higher rate of hematological adverse effects compared to AZA [239]. Moreover, indirect comparison showed that

AZA improved overall survival compared to DAC [238]. However, these indirect comparisons cannot provide a reliable answer to confirm the superiority of either agents. In addition to low certainty of the evidence, there are many limitations of these indirect comparison include the limited number of included trials, heterogeneity between the different studies, and network consistency [239]. Further direct head-to-head randomized clinical trials are required, particularly a clinical study to compare between the oral formulations of the two agents. In the meantime, the selections of either drugs should be based on patient's preferences, the severity of the disease, the availability and the cost of the drugs.

HMAs did not work in solid tumors [139]. Despite their effectiveness in MDS and AML patients, HMAs monotherapy treatment is associated with unsatisfied outcomes including low rate of complete remission [240, 241]. Several approaches have been used to potentiate HMAs effects by combining with investigational drugs, however, have failed in clinical trials, except for combinations with the BCL2 inhibitor venetoclax [241]. Our approach was to combine EGCG (DNMTi and HDACi) and DAC (DNMTi) that both have known well tolerated adverse events. We showed that the combination of both EGCG and DAC was required to inhibit tumor growth in our TNBC human xenograft. We also showed that CHA1 eradicated tumor cells in 4T-1 TNBC syngeneic model. Previous work reported that DAC at dose similar to our dose did not suppress the tumor growth of 4T-1 TNBC syngeneic model [242]. In addition, EGCG at higher dose than we used had no effect on the tumor growth of 4T-1 TNBC syngeneic model [243]. In addition to suppression tumor growth, our data showed that both drugs are needed for

maximum inhibition of Wnt pathway, re-induction of antigen presentation, particularly MHC-II, stimulation of JAK/STAT/IFN pathway, and upregulation of PD-L1 expression.

One of the approaches to enhance the response to ICIs in solid tumors is the use of collaborative agents such as HMAs [139]. In our study, we demonstrated that CHA1, a combination of EGCG and DAC, sensitized the tumor to anti-PD-L1 response in TNBC syngeneic model. The FDA approval of oral AZA and oral DAC + cedazuridine (CDAi) gave the potential to ease of administration and convenience associated with oral agents. I would like to study the efficacy of AZA or DAC + CDAi as substitute of DAC in combination with EGCG in TNBC syngeneic model. I also would like to study the effect of the new combination with ICIs. If the study demonstrates successful results, it will open a new hope for TNBC. In addition, the fact that combination drugs can administrate orally will reduce the infusion burden, decrease regimen complexity, and improve patient adherence.

4.4.5. Study The Effect of CHA1 and CHA1 + anti-PD-L1 on Circulating Tumor Cells

Circulating tumor cells (CTCs), that are derived from the primary tumors and are escaped into the blood circulation, are important source of metastasis [244]. CTCs detection is an emerging clinical test to identify early and rare metastatic events and metastatic progression [244]. CTCs are considered as a liquid biopsy that can be detected in the peripheral blood of cancer patients [244]. It is also useful to monitor patient prognosis and treatment response [245, 246]. It has been reported that the detection of CTCs in cancer patients was inversely correlated with disease progression and treatment outcome [246]. In addition, the presence of CTCs in breast cancer has been associated

with poor prognosis [247]. Therefore, CTCs can be used as a surrogate prognostic biomarker to measure the clinical response. CellSearch® is the only FDA-approved clinical test for enumeration of CTCs [244]. It is a semi-automated qualitative immunomagnetic-capture immunofluorescent detection image analysis test. CTCs can be identified using epithelial markers (EpCAM and cytokeratins (CK) 8, 18, and/or 19 that are expressed by CTCs) and leukocyte marker (CD45) [244]. CTCs are $EpCAM^{+}$ / $CK^{+}/CD45^{-}$ [244].

I would like to study the effect of CHA1 and CHA1+anti-PD-L1 on CTCs using the MDA-MB-231 TNBC human xenograft pre-clinical model. I will examine whether CHA1, and CHA1 + anti-PD-L1 treatment decreases metastasis by reducing CTCs. CTCs isolation via fluorescence-activated cell sorting analysis (FACS) will be used [248]. Peripheral blood will be collected from control mice and CHA1, and CHA1+anti-PD-L treated mice in EDTA tubes. CTC levels will be sorted based on EpCAM/CK/CD45 status. One sample will be left unstained and used as a negative control. This experiment, if successful, would suggest that measuring CTCs levels in patients could be a predictive biomarker for treatment efficacy and could be applied to Phase I clinical trial to evaluate the efficacy of CHA1 and CHA1 + anti-PD-L1, particularly for TNBC patients with brain metastasis.

4.4.6. Single Cell RNA-sequencing of CHA1 and CHA1 + anti-PD-L1

Unlike next-generation sequencing (NGS) which is used to study tumor heterogenicity and to assess any biological changes evolved in tumor cells after treatment, Single-cell RNA sequencing (scRNA-seq) can be applied to study the gene expression of bulk tumors at single-cell resolution [249]. scRNA-seq is a powerful

technology that can provide a detailed landscape about entire tumor ecosystem and the mechanism of intra-tumoral and inter-tumoral signaling interactions [250]. One of the advantages of scRNA-seq that it can provide a clear insight into TME at single-cell levels and classify immune cell populations in the TME as well as identify the functional status of immune cells [249]. Immune system displays heterogenicity and scRNA-seq reveals there are different kinds of tumor-infiltrating immune cells into TME including innate immune cells like dendritic cells (DCs), immature dendritic cells (iDCs), activated dendritic cells (aDCs), eosinophils and neutrophils, mast cells, macrophages, natural killer cells (NK) and adaptive immune cells like $CD4^+$ T helper cells like Th1 and Th2, $CD4^+$ $FOXP3^+$ regulatory T cells (Treg), $CD8^+$ cytotoxic T cells, and effector memory T cells (Tem), etc [249, 251, 252]. It has been reported that tumors infiltrated with $CD8^+$ cytotoxic T-cells has a favorable response to ICIs and better prognosis, while tumors infiltrated with Treg became irresponsive to ICIs [253]. scRNA-seq can also provide an analysis of immune-related gene signature [249]. scRNA-seq can be used to discover the mechanism of drug resistance mediated by specific immune cells [249]. This is important to understand why some patients are not sensitive to anti-CTLA-4 and anti-PD-1/PD-L1 treatment [249]. scRNA-seq analysis of ICIs-sensitive and ICIs-resistance glioblastoma patients who received anti-PD-1 therapy revealed that ICIs-resistance samples were enriched with a specific group of $CD73^{hi}$ macrophages which resulted in immune suppression TME and disfavor T cell infiltration [254]. Furthermore, scRNA-seq analysis of 11 breast cancer patients demonstrated that there was high infiltration of T lymphocytes, B lymphocytes, and macrophages. Furthermore, the T cells exhibited an

exhausted phenotype and macrophages were polarized into M2, indicating immunosuppressive of TME [255].

I would like to perform scRNA-seq for the 4 treatments groups: saline, anti-PD-L1, CHA1, CHA1 + anti-PD-L1. I would like to examine the effect of CHA1 on the immune cell subtypes and determine the functional and the activity status of the immune cells. I also want to identify the significant TME-related alterations mediated by CHA1 that resulted in improvement of the anti-tumor activity of anti-PD-L1. I also would like to conduct scRNA-seq for the 4 treatment groups in metastatic tumors to see whether there is any difference on immune cell subtypes, functions, and activity and to see whether TME shapes differently in the metastatic tumors. This unbiases analysis will provide a detailed picture of TME landscape after CHA1 and CHA1 + anti-PD-L1 and it will tell us how CHA1 mediated inflamed hot TME and how the treatment reprograms TME in the primary tumor and metastatic tumors. It will also identify which immune cell is critically important to CHA1 function.

4.4.7. Epigenetic Mapping of Breast Cancer and Breast Cancer Metastasis after CHA1 and CHA1 + anti-PD-L1

Aberrant epigenetic modifications play an important role in tumorigenesis via silencing of tumor suppressor genes or induction of oncogenes [256]. Epigenetic modifications are involved in regulation of different biological responses of cancer cells such as proliferation, apoptosis, senescence, and metastasis [257]. Epigenetic modifications can also regulate cancer cells functions and oncogenic transformation [258]. Epigenetic modifications include DNA methylation, histone modification, chromatin remodeling and the effects of noncoding RNA [257]. Generally, methylation

of DNA CpG islands, hypoacetylation and/or hypermethylation of histones caused gene repression [257].

DNA methylation involved a transfer of a methyl group to the cytosine of DNA CpG islands by DNA methyltransferases (DNMTs), resulting in silencing of the gene [257]. The gene expression of methylated gene can be reactivated by demethylation [257]. Abnormal DNA methylations are common in cancer cells [257]. It has been reported that the expression of key tumor suppressor genes such as p16, P53 and BRCA1 are repressed by DNA methylation [259, 260].

Histone modification is a form of epigenetic modification that is mediated by histone acetyltransferases (HATs), histone deacetylases (HDACs), histone methyltransferases (HMTs) and histone demethylases (HDMs) [257]. It has been reported that HDACs can cause silencing of tumor suppressor genes via hypoacetylation of their promoters [257]. Furthermore, treatment with HDAC inhibitor was effective to reverse hypoacetylation of the promoter of p21 and restore its expression, resulting in an antitumor effect [261]. HMTs also plays a major role in regulating the gene expression. Methylation at H3K9, H3K27, and H4K20 resulted in repression of gene expression while methylation of H3K4, H3K36, and H3K79 was associated with induction of gene expression [262].

It is important to study the effect of epigenetic related noncoding RNAs (ncRNAs) such as microRNAs (miRNAs) [257]. miRNAs play a significant role in regulation of mRNA translation [257]. The regions where miRNAs target located are frequently carcinogenic-associated regions [263]. miRNAs can be classified into tumor-promoting oncogenic miRNAs like miR-155, miR-21, and miR-17-92 that are induced

and tumor-suppressing miRNAs like miR-15-16 that are repressed during carcinogenesis [264]. Recent study showed that circulating miRNAs can be detected in the peripheral blood and can be used as predictive biomarkers for cancer [265].

Alterations in epigenetic landscape has been linked to the etiology of breast cancer and breast cancer metastasis [266]. The breast cancer initiation and the process of metastatic progression not only induced by mutations of tumor-suppressor genes or oncogenes but also induced by epigenetic modifications [266]. It has been showed that BRCA1 mRNA expression was inactivated by hypermethylation. Furthermore, a meta-analysis revealed that hypermethylation of BRCA1 has been positively correlated with the risk of development of highly aggressive breast cancer and metastases [267]. EMT, which also plays a critical role in breast cancer metastases, is epigenetically regulated [266, 268]. It has been reported that the promoter of epithelial transmembrane protein E-cadherin was methylated in TNBC, resulting in its repression. Hypermethylation of E-cadherin has been associated with metastatic progression [269]. Moreover, suppression of the mRNA expression of the genes involved in stem cell properties has been detected in the samples of TNBC primary tumors and it has been associated with clinically aggressive TNBC phenotype [270]. Furthermore, it has been found that HDAC1 has been associated with breast cancer cells growth and migration [271]. In addition, overexpression of HDAC1 and HDAC7 in breast cancer cells plays a critical role in maintain CSC phenotype [272]. Furthermore, HDAC8 overexpression has been linked to clinicopathological features of TNBC, indicating its diagnostic role [273]. Several miRNAs like miRNA-22 and miRNA-10b have been contributed to the development of drug resistance in breast cancer [274, 275].

In our study, we used CHA1, which is a combination of EGCG and decitabine. Decitabine is an epigenetic drug that works by inhibition of DNMT, resulting in reactivating the gene expression [257]. In addition, EGCG has been found to stabilize the mRNA of HBP1, which is a transcriptional repressor of DNMT [56, 149]. HBP1 is a direct target of miR-155 [276]. It has been reported that miR-155 oncogenic function in colorectal cancer is contributed to its repression of HBP1 expression [276]. Furthermore, in addition to DAC, EGCG can inhibit DNMT activity and restored the expression of methylation-silenced genes [148]. In addition, EGCG has been shown to have HDAC inhibition activity [277]. I would like to study the effect of CHA1 on the methylation of the entire genome by using whole-genome bisulfite sequencing (WGBS). I also would like to study the effect of CHA1 on histone modification by conducting chromatin immunoprecipitation-deep sequencing (ChIP-Seq). Furthermore, I would like to study the effect of CHA1 on miRNAs by microRNA-sequencing (miRNA-sequencing). The study will be performed on untreated and CHA1-treated TNBC tumors. I also would like to perform this experiment on metastatic tumors dissected from untreated and CHA1 treated mice. I want to discover which CHA1-induced epigenetic modifications have a significant role in the disease progression. I would like to identify which tumor-suppressor genes and/or oncogene are epigenetically regulated by CHA1 and are involved in initiation and progression of the tumors and metastases development. I also would like to see which histone modifications are altered after CHA1 treatment. In addition, I would like to examine miRNAs expression and modifications after CHA1. Furthermore, I would like to learn how the epigenetic modifications induced by CHA1 contributed to the reduction in metastases. I will compare CHA1-induced epigenetic

signature of primary tumors and CHA1-induced epigenetic signature of metastatic tumors with epigenetic signature of untreated tumors and untreated metastases. I want to find if there are any differences between CHA1-treated primary tumors, CHA1-treated metastases, and untreated ones in term of epigenetic alterations, particularly, the alterations in Wnt, EMT and CSCs formation. Moreover, it has been reported that TME is epigenetically regulated [139]. I would like to discover the epigenic modifications induced by CHA1 that reprogrammed the TME in CHA1-treated tumors and CHA1-treated metastases and how these modifications altered the metastases progression. Lastly, I would like to perform the same epigenetic mapping study in primary tumor and metastatic tumors after anti-PD-L1 and CHA1 + anti-PD-L1.

This epigenetic mapping study will provide a precise answer about the exact mechanism of CHA1 as an epigenetic drug. In addition, this study can identify potential biomarkers that can be used for diagnosis and monitor disease progression. Furthermore, the study can detect important epigenetic driver of metastases that can be used as an early biomarker to identify metastatic events. Finally, this study can help to identify a pharmacological target that can be applied for future research.

4.4.8. Study The Effect of Targeting EMT in Combination with CHA1

The use of ICIs in solid tumor is a hopeful therapeutic option for many patients. Despite the initial success and remarkable results, most patients developed resistance to ICIs. Molecular characterization of ICIs-refractory cancers indicates that resistant cancers showed acquisition of epithelial-mesenchymal transition (EMT) and upregulation of Wnt signaling [49, 50, 278]. Tumors of TNBC patients display properties of EMT and Wnt activation which results in occurrence of cancer-stem cells like properties [30, 278].

Furthermore, Wnt signaling activation is inversely correlated with the epithelial transmembrane protein E-cadherin, indicating upregulation of Wnt in cancer cells result in EMT [32, 36]. Several studies demonstrated that aberrant activation of intrinsic Wnt/β-catenin pathway can mediate T-cell exclusion TME in bladder cancer and melanoma [112, 228]. In addition, it has also been reported that Wnt/β-catenin pathway creates non-T-cells inflamed (cold) TME in melanoma [109]. It has been reported that EMT drives tumor cells growth and metastasis not only by alterations of cancer cell properties, but also by alteration of TME landscape [279]. Activation of EMT status in cancer cells is associated with immune suppression TME. Epithelial tumor cells showed high infiltration of $CD8^+$ cytotoxic T-cells which is characterization of hot TME, indicating that epithelial tumor cells more responsive to ICIs [278]. On the other hand, mesenchymal tumor cells displayed immune suppression cold TME and infiltration of immune suppressive cells (Treg) [278]. The pathway behind development of this suppressive effect involved PD-L1 regulation via EMT regulators (the transcription factor Zinc finger E-box-binding homeobox 1 (ZEB1) and miR200 family) [280]. Furthermore, EMT has been associated with increased infiltration of tumor-associated macrophages (TAMs) into TME via induction of CCL2, therefore, development of ICIs resistance [281, 282]. Furthermore, EMT has been linked to switch the status of cancer cells from epithelial neutrophil-enriched to mesenchymal M2 macrophage-enriched [278].

It has been reported that EMT is epigenetically regulated [268]. Lysine-specific demethylase 1 (LSD1) plays important role in EMT regulation [283]. EMT is characterized by transcriptional silencing of E-cadherin mediated by EMT-inducing transcription factors (EMT-TFs) including Snail, Slug and ZEB1 [33, 284, 285]. LSD1

that is recruited by Snail represses E-cadherin in breast cancer. In addition, LSD1 has been implicated in regulation of EMT, induction of CSCs-like properties, tumor growth and drug-resistance in breast cancer mouse model [283]. Moreover, the combination of pharmacological inhibitor of LSD1, pargyline, with chemotherapy in pre-clinical breast cancer mouse model resulted in reduced the tumor growth, suppressed the mesenchymal phenotypes, and increased infiltration of M1 macrophage into TME [283]. It has been reported that the combination of LSD1 inhibitors with anti-PD-1 in TNBC xenograft model resulted in increased the efficacy of anti-PD-1, suppressed the tumor growth and metastases as well as increased infiltration of cytotoxic $CD8^+$ T cell into TME [213].

Targeting multiple pathways in cancer is an effective tool to eradicate cancer cells and overcome drugs resistance. Several studies demonstrated that EMT and Wnt play a significant role in mediating ICIs resistance and creating cold tumor TME [49, 50, 109, 112, 228, 278, 279]. Previous works showed that LSD1 inhibitor abrogated EMT signature and mediated hot TME [213, 283]. In addition, it has been reported that silencing of the promoter of epithelial marker gene E-cadherin, CDH1, through DNMTs. Furthermore, DNA methylation is involved in regulation the expression of EMT-transcription factors including TWIST1/2, ZEB1/2, and SNAI1/2 [286].

Our work demonstrated that CHA1 downregulated Wnt signaling and reprogramed the TME to exhibit hot status. Furthermore, both CHA1 and LSD1 inhibitor act epigenetically. However, CHA1 targets DNA methylation while LSD1 inhibitor targets histone modification [257]. I would like to examine whether the addition of LSD1 inhibitor augments the tumor inhibitory activity of CHA1. The study will be performed in EMT6-tumor bearing TNBC syngeneic mouse model to avoid the limitations of 4T-1

syngeneic model [206, 207]. I will evaluate the effect of the new combination on tumor growth. Our work showed that CHA1 induced the protein expression of E-cadherin. The expression of several markers of EMT such as E-cadherin, Snail, vimentin, and ZEB1 will be tested. Also, the effect on Wnt signaling will be examined. Since both Wnt and EMT involved in formation of CSCs, the expression of stem-cell marker will be tested. In addition, I will look at the effect of the combination drugs on metastases. I would like to study the effect of CHA1 + LSD1 inhibitor on TME landscape. Our work showed that CHA1 was effective in combination with anti-PD-L1, however, CHA1 did not work with anti-PD-1 or anti-CTLA-4. Previous study showed that LSD1 inhibitor enhanced the anti-tumor activity of anti-PD-1 [213]. So, I would like to study the effect of CHA1 + LSD1 inhibitor in combination with anti-PD-L1, anti-PD-1 and anti-CTLA-4, and examine whether the new treatment combination sensitizes the tumors to the ICIs and improves the survival. If the result of the study is promising, the new combination treatment could be a potential therapeutic option for TNBC patients and particularly for ICIs-refractory TNBC patients.

4.4.9. Study The Effect of CHA1 in ICIs-non-responding Tumors

Melanoma responds poorly to chemotherapy. However, in 2011, anti-CTLA-4, ipilimumab, was the first FDA-approved immune checkpoint inhibitor for patients with metastatic melanoma [287]. Furthermore, in 2014, anti-PD-1, pembrolizumab and nivolumab, were also approved for advanced melanoma [287]. Unfortunately, despite the significant improvement in the clinical outcome after treatment with ICIs in metastatic melanoma, the majority of patients did not respond to ICIs [111]. In ICIs-responding patients, infiltrating of $CD8^+$ cytotoxic T cells, a characteristic of T cell-inflamed TME, is

essential for ICIs response and it can be used to predict the response to ICI [111]. Aberrant activation of Wnt signaling is one of the mechanism that mediates resistance to ICIs in melanoma [108-111]. Stimulation of Wnt signaling has been associated with decreased T-cell infiltration into TME [108-111]. It has been reported that the combination of RNAi-mediated β-catenin inhibition with ICIs sensitized non-inflamed tumors and increased the response to ICIs in syngeneic mouse models of B16F10 melanoma, 4T1 mammary carcinoma, Neuro2A neuroblastoma, and renca renal adenocarcinoma [194].

Another tumor that poorly responds to ICIs is colorectal cancer [111]. It has been reported that activation of the Wnt/β-catenin signaling pathway was positively correlated with the absence of T-cell infiltration in colorectal cancer patients [288]. Furthermore, immunohistochemical analysis of 155 colorectal cancer tissues revealed that there was a significant reduction of $CD8^+$ T-cell infiltration in the tumors that highly expressed β-catenin [288]. This finding highlighted that Wnt/β-catenin signaling pathway could be the driver of colorectal cancer resistance to ICIs.

Targeting Wnt/β-catenin signaling could be a potential strategy to prime ICI-nonresponding melanoma and colorectal cancer to ICIs. Since CHA1 demonstrated inhibitory effect on Wnt and improved the response to anti-PD-L1 in TNBC syngeneic model, I would like to study the effect of CHA1 in melanoma and colorectal syngeneic mouse model and examine whether CHA1 sensitize these tumors to ICIs. If CHA1 promotes the anti-tumor effect of ICIs in melanoma and colorectal cancer, it will open a new hope for ICIs-refractory patients.

4.4.10. Study The Effect of CHA1 in Combination with Anti-angiogenesis

Cancer cells can promote immune suppression in TME, leading to restrain the efficacy of ICI. One of the resistance mechanisms to ICIs is mediated by angiogenesis [289]. Angiogenesis results in formation of malfunctional tumor vessels that serves as physical barrier for infiltration of effector immune cells into TME [289]. Several studies reported that combination of anti-angiogenesis and ICIs is an effective strategy to normalize aberrant vascular-immune crosstalk and potentiate ICI efficacy [289]. Therefore, FDA granted approval for the combination of anti-angiogenesis with ICIs in patients with kidney, liver, lung, or uterine cancer [289].

The growth of tumor cells requires sufficient oxygen and nutrients supply from the blood vessels. However, tumor cells grow rapidly and exceed their blood supply from the existing vasculature, leading to development of hypoxia in TME [289]. Hypoxia promotes immunosuppressive mechanisms in TME by activation of the angiogenic master switch, hypoxia-inducible factor-1 (HIF-1), and upregulation of vascular endothelial growth factor (VEGF) in tumors [289]. VEGF functions as a powerful immunosuppressive factor in innate and adaptive anti-tumor immunity. VEGF is the major driver of tumor angiogenesis by promoting the proliferation and survival of endothelial cells (ECs) and the formation of malformed and malfunctional neovessels within the tumor [289]. Tumor endothelial cells display immunosuppressive characteristics, such as upregulation of PD-L1 expression, resulting in inactivation of T-cells. In addition, VEGF suppresses the maturation of dendritic cell (DC), which in turn interferes with T cell priming by impaired antigen presentation. Furthermore, VEGF promotes polarizing tumor-associated macrophages (TAMs) to immunosuppressive M2-

like phenotype. Moreover, VEGF increase infiltration of immune suppressor Treg cells into TME [289].

Wnt components are expressed in endothelial cells and implicated in many aspects of angiogenesis involving upregulation of VEGF and its blockade reduced microvessel density and VEGF [52, 53]. In addition, several studies reported that aberrant Wnt signaling activation has been associated with resistance to ICIs and reduced the numbers of T-cell infiltration into TME [108-110]. Furthermore, epigenetic modifications including DNA methylation regulate the expression of key genes critical for angiogenesis promotion such as VEGF, its receptors (VEGFR1/Flt1, VEGFR2/KDR and VEGFR3/Flt4) and endothelial nitric oxide synthase (eNOS) [290]. These genes play essential role not only in regulation of endothelial cells, but also in supporting the growth of different types of solid tumors and leukemias, resulting in the growth of the cancer cells.

Targeting multiple pathways in cancer could be a viable strategy to overcome ICIs resistance. The use of axitinib which is VEGFR1, 2, and 3 inhibitor [289] in combination of CHA1 that suppresses Wnt signaling and acts epigenetically by DNMT inhibition could be a potential therapeutic to augment ICIs response and overcome the resistance. So, I would like to study the effect of combination of axitinib with CHA1 in in EMT6-tumor bearing TNBC syngeneic mouse model to avoid the limitations of 4T-1 syngeneic model [206, 207]. In addition, the effect of the new combination will be evaluated on tumor growth. The protein and gene expression of VEGF will be tested. Furthermore, the effect of CHA1 + axitinib on TME landscape will be tested. Our work showed that CHA1 sensitized the tumor to anti-PD-L1, however, CHA1 did not work

with anti-PD-1 or anti-CTLA-4. So, I would like to study the effect of CHA1 + axitinib in combination with anti-PD-L1, anti-PD-1 and anti-CTLA-4, and examine whether the new treatment combination improves the response to the ICIs and prolongs the survival. The result of this study could provide a promising therapeutic option for TNBC patient and particularly for ICIs-refractory TNBC patients.

4.4.11. Study The Effect of CHA1 in Combination with Adoptive T Cell Immunotherapy

The expression of cancer testis antigens (CTAs), NY-ESO-1, MAGE-A3, and MAGE-A6, were significantly elevated after CHA1 treatment. The induction of CTAs after CHA1 was due to DNMT inhibition since CTAs expressions were epigenetically regulated [76]. Induction of CTAs, which are highly immunogenic, could promote T cells infiltration and facilitate tumor lysis by cytotoxic T lymphocytes (CTLs) [191]. Eliciting CTLs response to target a tumor specific antigen is a critical component in successful immunotherapy [191]. Since CTAs have restricted expression in adult somatic tissues and immunogenic nature, these CTAs could be potential targets of cancer vaccine therapy and adoptive T cell immunotherapy including chimeric antigen receptor T cells (CAR T) and engineered T cell receptor (TCR) therapy [84].

NY-ESO-1 is the most promising CTA for immune-based therapy since its tumor expression is associated with the induction of an immune response in a wide range of cancer types [84, 291]. NY-ESO-1 has been reported to induce humoral immune responses. Serum NY-ESO-1 autoantibodies were detected in patients with esophageal, colorectal, lung, breast, prostate, gastric, and hepatocellular cancer [292]. In addition, humoral and cellular responses against NY-ESO-1 were detected in a metastatic

melanoma patient with a high-titer antibody response [293]. HLA-A2, MHC-1, restricted epitopes in NY-ESO-1 that can be recognized by $CD8^+$ cytotoxic T cells were identified [293]. Furthermore, HLA-DRB1*0401 and HLA-DP4, MHC-II, restricted epitopes in NY-ESO-1 which can be recognized by $CD4^+$ T cells were detected [294, 295].

It has been demonstrated that the combination of NY-ESO-1 vaccine with DAC as an addition to the second-line chemotherapy doxorubicin can result in induction of humoral and $CD8^+$ T cell responses against NY-ESO-1in patients with relapsed epithelial ovarian cancer [296]. Furthermore, the study reported stable disease in 50% of patients (5/10).

The clinical trials of NY-ESO-1 cancer vaccines have proven induction of both humoral and cellular responses after vaccination; however, the clinical benefit of this approach was limited since few complete responses have been obtained [291]. Therefore, the focus has changed toward the development of engineered T cells against NY-ESO-1. Adoptive T cell therapy with HLA-A2 restricted NY-ESO-1transduced $CD8^+$ T cells was evaluated in treatment-refractory melanoma and synovial cell sarcoma patients [297]. The study reported improved the clinical response rates and overall survival [297].

Several clinical trials are currently ongoing to study the safety and efficacy of NY-ESO-1 specific or multi-tumor-associated antigen (TAA) TCR-transduced T cells in a range of advanced solid tumors (NCT03047811, NCT02457650, NCT02869217, NCT02366546) including breast cancer (NCT03093350) [291]. Moreover, the safety and efficacy of NY-ESO-1 or multi TAA transduced T cell therapy in combination with other modalities including the demethylating agent DAC and AZA (NCT03017131, NCT01333046) are currently under investigation [291]. It has been demonstrated that

pretreatment with DAC upregulated NY-ESO-1 followed by engineered TCR therapy resulted in an efficient trafficking of NY-ESO-1-specific T cells towards tumor cells leading to prolonged survival in mice [298].

Several challenges have been associated with adoptive T cell immunotherapy. One of the limitations is the cost of the treatment [299]. Cytokine release syndrome (CRS) is a common side effect [83, 300]. It is characterized by the release of number of inflammatory cytokines such as IL-6, TNF-α, and IFNγ by activated T cells leading to high fever, hypotension, and hypoxia. CRS can potentially result in organ failure and death in most severe cases. This toxicity is short-lived since highly activated T cells have short survival in vivo and currently best addressed by supportive care [300].

Taken together, I would like to study the effect of combining CHA1 with NY-ESO-1 specific or multi-TAA (MAGE-A3, MAGE-A6, NY-ESO-1) TCR therapy in humanized murine model of TNBC. The humoral and cellular response will be tested. The tumor growth will be monitored. This study could provide a hope for TNBC patients whose cancers refractory to ICIs and chemotherapy as well as TNBC patient with recurrent disease that no-responding to treatment since they have no treatment options.

Chapter 5: References

1. Medina, M.A., et al., *Triple-Negative Breast Cancer: A Review of Conventional and Advanced Therapeutic Strategies.* International journal of environmental research and public health, 2020. **17**(6): p. 2078.
2. Sung, H., et al., *Global Cancer Statistics 2020: GLOBOCAN Estimates of Incidence and Mortality Worldwide for 36 Cancers in 185 Countries.* CA: A Cancer Journal for Clinicians, 2021. **71**(3): p. 209-249.
3. Li, C.-J., et al., *Pathogenesis and Potential Therapeutic Targets for Triple-Negative Breast Cancer.* Cancers, 2021. **13**(12): p. 2978.
4. Gucalp, A. and T.A. Traina, *Triple-negative breast cancer: adjuvant therapeutic options.* Chemother Res Pract, 2011. **2011**: p. 696208.
5. Untch, M., et al., *13th st. Gallen international breast cancer conference 2013: primary therapy of early breast cancer evidence, controversies, consensus - opinion of a german team of experts (zurich 2013).* Breast Care (Basel), 2013. **8**(3): p. 221-9.
6. Inic, Z., et al., *Difference between Luminal A and Luminal B Subtypes According to Ki-67, Tumor Size, and Progesterone Receptor Negativity Providing Prognostic Information.* Clin Med Insights Oncol, 2014. **8**: p. 107-11.
7. Harbeck, N., et al., *Breast cancer.* Nature Reviews Disease Primers, 2019. **5**(1): p. 66.
8. Morris, G.J., et al., *Differences in breast carcinoma characteristics in newly diagnosed African-American and Caucasian patients: a single-institution compilation compared with the National Cancer Institute's Surveillance, Epidemiology, and End Results database.* Cancer, 2007. **110**(4): p. 876-84.
9. Dent, R., et al., *Triple-negative breast cancer: clinical features and patterns of recurrence.* Clin Cancer Res, 2007. **13**(15 Pt 1): p. 4429-34.
10. Lehmann, B.D., et al., *Identification of human triple-negative breast cancer subtypes and preclinical models for selection of targeted therapies.* The Journal of clinical investigation, 2011. **121**(7): p. 2750-2767.
11. Lehmann, B.D., et al., *Refinement of triple-negative breast cancer molecular subtypes: implications for neoadjuvant chemotherapy selection.* PloS one, 2016. **11**(6): p. e0157368.
12. Kim, I.S., et al., *Immuno-subtyping of breast cancer reveals distinct myeloid cell profiles and immunotherapy resistance mechanisms.* Nature cell biology, 2019. **21**(9): p. 1113-1126.
13. Niwińska, A., et al., *Triple-negative breast cancer with brain metastases: a comparison between basal-like and non-basal-like biological subtypes.* Journal of neuro-oncology, 2011. **105**(3): p. 547-553.
14. Eichler, A.F., et al., *The biology of brain metastases-translation to new therapies.* Nat Rev Clin Oncol, 2011. **8**(6): p. 344-56.
15. Nayak, L., E.Q. Lee, and P.Y. Wen, *Epidemiology of brain metastases.* Curr Oncol Rep, 2012. **14**(1): p. 48-54.
16. Dagogo-Jack, I., et al., *Treatment of brain metastases in the modern genomic era.* Pharmacol Ther, 2017. **170**: p. 64-72.
17. Lin, N.U., J.R. Bellon, and E.P. Winer, *CNS metastases in breast cancer.* J Clin Oncol, 2004. **22**(17): p. 3608-17.

18. Howe, L.R. and A.M. Brown, *Wnt signaling and breast cancer.* Cancer Biol Ther, 2004. **3**(1): p. 36-41.
19. MacDonald, B.T., K. Tamai, and X. He, *Wnt/beta-catenin signaling: components, mechanisms, and diseases.* Dev Cell, 2009. **17**(1): p. 9-26.
20. Luo, J., et al., *Wnt signaling and human diseases: what are the therapeutic implications?* Lab Invest, 2007. **87**(2): p. 97-103.
21. Yang, K., et al., *The evolving roles of canonical WNT signaling in stem cells and tumorigenesis: implications in targeted cancer therapies.* Lab Invest, 2016. **96**(2): p. 116-36.
22. Holland, J.D., et al., *Wnt signaling in stem and cancer stem cells.* Curr Opin Cell Biol, 2013. **25**(2): p. 254-64.
23. Jang, G.B., et al., *Wnt/beta-Catenin Small-Molecule Inhibitor CWP232228 Preferentially Inhibits the Growth of Breast Cancer Stem-like Cells.* Cancer Res, 2015. **75**(8): p. 1691-702.
24. Ye, X. and R.A. Weinberg, *Epithelial-Mesenchymal Plasticity: A Central Regulator of Cancer Progression.* Trends Cell Biol, 2015. **25**(11): p. 675-686.
25. Takebe, N., R.Q. Warren, and S.P. Ivy, *Breast cancer growth and metastasis: interplay between cancer stem cells, embryonic signaling pathways and epithelial-to-mesenchymal transition.* Breast Cancer Res, 2011. **13**(3): p. 211.
26. Batlle, E. and H. Clevers, *Cancer stem cells revisited.* Nature Medicine, 2017. **23**(10): p. 1124-1134.
27. Yang, L., et al., *LGR5 Promotes Breast Cancer Progression and Maintains Stem-Like Cells Through Activation of Wnt/β-Catenin Signaling.* Stem Cells, 2015. **33**(10): p. 2913-24.
28. Fillmore, C.M. and C. Kuperwasser, *Human breast cancer cell lines contain stem-like cells that self-renew, give rise to phenotypically diverse progeny and survive chemotherapy.* Breast Cancer Res, 2008. **10**(2): p. R25.
29. Gómez-Miragaya, J., et al., *Resistance to taxanes in triple-negative breast cancer associates with the dynamics of a CD49f+ tumor-initiating population.* Stem cell reports, 2017. **8**(5): p. 1392-1407.
30. Kotiyal, S. and S. Bhattacharya, *Breast cancer stem cells, EMT and therapeutic targets.* Biochem Biophys Res Commun, 2014. **453**(1): p. 112-6.
31. Dave, B., et al., *Epithelial-mesenchymal transition, cancer stem cells and treatment resistance.* Breast Cancer Res, 2012. **14**(1): p. 202.
32. Thiery, J.P., *Epithelial-mesenchymal transitions in tumour progression.* Nat Rev Cancer, 2002. **2**(6): p. 442-54.
33. Kalluri, R. and R.A. Weinberg, *The basics of epithelial-mesenchymal transition.* J Clin Invest, 2009. **119**(6): p. 1420-8.
34. Tepass, U., et al., *Cadherins in embryonic and neural morphogenesis.* Nat Rev Mol Cell Biol, 2000. **1**(2): p. 91-100.
35. Nelson, W.J. and R. Nusse, *Convergence of Wnt, beta-catenin, and cadherin pathways.* Science, 2004. **303**(5663): p. 1483-7.
36. Kim, K., Z. Lu, and E.D. Hay, *Direct evidence for a role of beta-catenin/LEF-1 signaling pathway in induction of EMT.* Cell Biol Int, 2002. **26**(5): p. 463-76.

37. Xu, L., et al., *Lgr5 in cancer biology: functional identification of Lgr5 in cancer progression and potential opportunities for novel therapy.* Stem Cell Research & Therapy, 2019. **10**(1): p. 219.
38. Seshagiri, S., et al., *Recurrent R-spondin fusions in colon cancer.* Nature, 2012. **488**(7413): p. 660-664.
39. Storm, E.E., et al., *Targeting PTPRK-RSPO3 colon tumours promotes differentiation and loss of stem-cell function.* Nature, 2016. **529**(7584): p. 97-100.
40. Kim, M.J., Y. Huang, and J.I. Park, *Targeting Wnt Signaling for Gastrointestinal Cancer Therapy: Present and Evolving Views.* Cancers (Basel), 2020. **12**(12).
41. King, T.D., M.J. Suto, and Y. Li, *The Wnt/beta-catenin signaling pathway: a potential therapeutic target in the treatment of triple negative breast cancer.* J Cell Biochem, 2012. **113**(1): p. 13-8.
42. Yang, L., et al., *FZD7 has a critical role in cell proliferation in triple negative breast cancer.* Oncogene, 2011. **30**(43): p. 4437-46.
43. Ueno, N.T. and D. Zhang, *Targeting EGFR in Triple Negative Breast Cancer.* J Cancer, 2011. **2**: p. 324-328.
44. van de Wetering, M., et al., *Mutant E-cadherin breast cancer cells do not display constitutive Wnt signaling.* Cancer Res, 2001. **61**(1): p. 278-84.
45. Bao, R., et al., *Inhibition of tankyrases induces Axin stabilization and blocks Wnt signalling in breast cancer cells.* PLoS One, 2012. **7**(11): p. e48670.
46. Veeck, J., et al., *Aberrant methylation of the Wnt antagonist SFRP1 in breast cancer is associated with unfavourable prognosis.* Oncogene, 2006. **25**(24): p. 3479-88.
47. Klopocki, E., et al., *Loss of SFRP1 is associated with breast cancer progression and poor prognosis in early stage tumors.* Int J Oncol, 2004. **25**(3): p. 641-9.
48. Matsuda, Y., et al., *WNT signaling enhances breast cancer cell motility and blockade of the WNT pathway by sFRP1 suppresses MDA-MB-231 xenograft growth.* Breast Cancer Res, 2009. **11**(3): p. R32.
49. Khramtsov, A.I., et al., *Wnt/beta-catenin pathway activation is enriched in basal-like breast cancers and predicts poor outcome.* Am J Pathol, 2010. **176**(6): p. 2911-20.
50. Lin, S.Y., et al., *Beta-catenin, a novel prognostic marker for breast cancer: its roles in cyclin D1 expression and cancer progression.* Proceedings of the National Academy of Sciences of the United States of America, 2000. **97**(8): p. 4262-4266.
51. Dey, N., et al., *Wnt signaling in triple negative breast cancer is associated with metastasis.* BMC Cancer, 2013. **13**(1): p. 537.
52. Dejana, E., *The role of wnt signaling in physiological and pathological angiogenesis.* Circ Res, 2010. **107**(8): p. 943-52.
53. Hu, J., et al., *Blockade of Wnt signaling inhibits angiogenesis and tumor growth in hepatocellular carcinoma.* Cancer Res, 2009. **69**(17): p. 6951-9.
54. Bilir, B., O. Kucuk, and C.S. Moreno, *Wnt signaling blockage inhibits cell proliferation and migration, and induces apoptosis in triple-negative breast cancer cells.* J Transl Med, 2013. **11**: p. 280.
55. Jang, G.B., et al., *Blockade of Wnt/beta-catenin signaling suppresses breast cancer metastasis by inhibiting CSC-like phenotype.* Sci Rep, 2015. **5**: p. 12465.

56. Kim, J., et al., *Suppression of Wnt signaling by the green tea compound (-)-epigallocatechin 3-gallate (EGCG) in invasive breast cancer cells. Requirement of the transcriptional repressor HBP1.* J Biol Chem, 2006. **281**(16): p. 10865-75.
57. Li, Y., W.P. Hively, and H.E. Varmus, *Use of MMTV-Wnt-1 transgenic mice for studying the genetic basis of breast cancer.* Oncogene, 2000. **19**(8): p. 1002-9.
58. Parker, B.S., J. Rautela, and P.J. Hertzog, *Antitumour actions of interferons: implications for cancer therapy.* Nature Reviews Cancer, 2016. **16**(3): p. 131-144.
59. Cheon, H., J. Yang, and G.R. Stark, *The functions of signal transducers and activators of transcriptions 1 and 3 as cytokine-inducible proteins.* J Interferon Cytokine Res, 2011. **31**(1): p. 33-40.
60. Platanias, L.C., *Mechanisms of type-I- and type-II-interferon-mediated signalling.* Nat Rev Immunol, 2005. **5**(5): p. 375-86.
61. Porritt, R.A. and P.J. Hertzog, *Dynamic control of type I IFN signalling by an integrated network of negative regulators.* Trends Immunol, 2015. **36**(3): p. 150-60.
62. Balkwill, F., D. Watling, and J. Taylor-Papadimitriou, *Inhibition by lymphoblastoid interferon of growth of cells derived from the human breast.* Int J Cancer, 1978. **22**(3): p. 258-65.
63. Hobeika, A.C., P.S. Subramaniam, and H.M. Johnson, *IFNalpha induces the expression of the cyclin-dependent kinase inhibitor p21 in human prostate cancer cells.* Oncogene, 1997. **14**(10): p. 1165-70.
64. Bernardo, A.R., et al., *Synergy between RA and TLR3 promotes type I IFN-dependent apoptosis through upregulation of TRAIL pathway in breast cancer cells.* Cell Death Dis, 2013. **4**(1): p. e479.
65. Gresser, I., et al., *Injection of mice with antibody to interferon enhances the growth of transplantable murine tumors.* J Exp Med, 1983. **158**(6): p. 2095-107.
66. Deonarain, R., et al., *Critical roles for IFN-beta in lymphoid development, myelopoiesis, and tumor development: links to tumor necrosis factor alpha.* Proc Natl Acad Sci U S A, 2003. **100**(23): p. 13453-8.
67. Pulaski, B.A., M.J. Smyth, and S. Ostrand-Rosenberg, *Interferon-γ-dependent Phagocytic Cells Are a Critical Component of Innate Immunity against Metastatic Mammary Carcinoma.* Cancer Research, 2002. **62**(15): p. 4406-4412.
68. Bidwell, B.N., et al., *Silencing of Irf7 pathways in breast cancer cells promotes bone metastasis through immune escape.* Nat Med, 2012. **18**(8): p. 1224-31.
69. Ni, L. and J. Lu, *Interferon gamma in cancer immunotherapy.* Cancer Med, 2018. **7**(9): p. 4509-4516.
70. Higgs, B.W., et al., *Interferon Gamma Messenger RNA Signature in Tumor Biopsies Predicts Outcomes in Patients with Non-Small Cell Lung Carcinoma or Urothelial Cancer Treated with Durvalumab.* Clin Cancer Res, 2018. **24**(16): p. 3857-3866.
71. Karachaliou, N., et al., *Interferon gamma, an important marker of response to immune checkpoint blockade in non-small cell lung cancer and melanoma patients.* Ther Adv Med Oncol, 2018. **10**: p. 1758834017749748.
72. Chen, R., C.A. Ishak, and D.D. De Carvalho, *Endogenous Retroelements and the Viral Mimicry Response in Cancer Therapy and Cellular Homeostasis.* Cancer Discovery, 2021. **11**(11): p. 2707-2725.

73. Chiappinelli, K.B., et al., *Inhibiting DNA Methylation Causes an Interferon Response in Cancer via dsRNA Including Endogenous Retroviruses.* Cell, 2016. **164**(5): p. 1073.
74. Roulois, D., et al., *DNA-Demethylating Agents Target Colorectal Cancer Cells by Inducing Viral Mimicry by Endogenous Transcripts.* Cell, 2015. **162**(5): p. 961-73.
75. Jansz, N. and G.J. Faulkner, *Endogenous retroviruses in the origins and treatment of cancer.* Genome Biology, 2021. **22**(1): p. 147.
76. Jones, P.A., et al., *Epigenetic therapy in immune-oncology.* Nature Reviews Cancer, 2019. **19**(3): p. 151-161.
77. Janin, M. and M. Esteller, *Epigenetic Awakening of Viral Mimicry in Cancer.* Cancer Discovery, 2020. **10**(9): p. 1258-1260.
78. Cañadas, I., et al., *Tumor innate immunity primed by specific interferon-stimulated endogenous retroviruses.* Nat Med, 2018. **24**(8): p. 1143-1150.
79. Laumont, C.M., et al., *Noncoding regions are the main source of targetable tumor-specific antigens.* Sci Transl Med, 2018. **10**(470).
80. Cherkasova, E., et al., *Detection of an Immunogenic HERV-E Envelope with Selective Expression in Clear Cell Kidney Cancer.* Cancer Res, 2016. **76**(8): p. 2177-85.
81. Wieczorek, M., et al., *Major Histocompatibility Complex (MHC) Class I and MHC Class II Proteins: Conformational Plasticity in Antigen Presentation.* Frontiers in Immunology, 2017. **8**.
82. Neefjes, J., et al., *Towards a systems understanding of MHC class I and MHC class II antigen presentation.* Nature Reviews Immunology, 2011. **11**(12): p. 823-836.
83. Meng, X., et al., *A novel era of cancer/testis antigen in cancer immunotherapy.* International Immunopharmacology, 2021. **98**: p. 107889.
84. Raza, A., et al., *Unleashing the immune response to NY-ESO-1 cancer testis antigen as a potential target for cancer immunotherapy.* Journal of Translational Medicine, 2020. **18**(1): p. 140.
85. Chen, Y.T., et al., *Multiple cancer/testis antigens are preferentially expressed in hormone-receptor negative and high-grade breast cancers.* PLoS One, 2011. **6**(3): p. e17876.
86. Caballero, O.L. and Y.T. Chen, *Cancer/testis (CT) antigens: potential targets for immunotherapy.* Cancer Sci, 2009. **100**(11): p. 2014-21.
87. Cheever, M.A., et al., *The Prioritization of Cancer Antigens: A National Cancer Institute Pilot Project for the Acceleration of Translational Research.* Clinical Cancer Research, 2009. **15**(17): p. 5323-5337.
88. Chiappinelli, K.B., et al., *Combining Epigenetic and Immunotherapy to Combat Cancer.* Cancer Res, 2016. **76**(7): p. 1683-9.
89. Chou, J., et al., *Epigenetic modulation to enable antigen-specific T-cell therapy of colorectal cancer.* J Immunother, 2012. **35**(2): p. 131-41.
90. Srivastava, P., et al., *Induction of cancer testis antigen expression in circulating acute myeloid leukemia blasts following hypomethylating agent monotherapy.* Oncotarget, 2016. **7**(11): p. 12840-56.

91. Axelrod, M.L., et al., *Biological Consequences of MHC-II Expression by Tumor Cells in Cancer.* Clin Cancer Res, 2019. **25**(8): p. 2392-2402.
92. Dhatchinamoorthy, K., J.D. Colbert, and K.L. Rock, *Cancer Immune Evasion Through Loss of MHC Class I Antigen Presentation.* Frontiers in Immunology, 2021. **12**(469).
93. Carretero, R., et al., *Analysis of HLA class I expression in progressing and regressing metastatic melanoma lesions after immunotherapy.* Immunogenetics, 2008. **60**(8): p. 439.
94. Carretero, R., et al., *Regression of melanoma metastases after immunotherapy is associated with activation of antigen presentation and interferon-mediated rejection genes.* Int J Cancer, 2012. **131**(2): p. 387-95.
95. Wang, E., A. Worschech, and F.M. Marincola, *The immunologic constant of rejection.* Trends in Immunology, 2008. **29**(6): p. 256-262.
96. Garrido, F., et al., *The urgent need to recover MHC class I in cancers for effective immunotherapy.* Current Opinion in Immunology, 2016. **39**: p. 44-51.
97. Matsumoto, H., et al., *Increased CD4 and CD8-positive T cell infiltrate signifies good prognosis in a subset of triple-negative breast cancer.* Breast Cancer Res Treat, 2016. **156**(2): p. 237-47.
98. Homet Moreno, B., et al., *Response to Programmed Cell Death-1 Blockade in a Murine Melanoma Syngeneic Model Requires Costimulation, CD4, and CD8 T Cells.* Cancer Immunology Research, 2016. **4**(10): p. 845-857.
99. Linnemann, C., et al., *High-throughput epitope discovery reveals frequent recognition of neo-antigens by CD4+ T cells in human melanoma.* Nat Med, 2015. **21**(1): p. 81-5.
100. Johnson, D.B., et al., *Melanoma-specific MHC-II expression represents a tumour-autonomous phenotype and predicts response to anti-PD-1/PD-L1 therapy.* Nat Commun, 2016. **7**: p. 10582.
101. Roemer, M.G.M., et al., *Major Histocompatibility Complex Class II and Programmed Death Ligand 1 Expression Predict Outcome After Programmed Death 1 Blockade in Classic Hodgkin Lymphoma.* J Clin Oncol, 2018. **36**(10): p. 942-950.
102. Park, I.A., et al., *Expression of the MHC class II in triple-negative breast cancer is associated with tumor-infiltrating lymphocytes and interferon signaling.* PLoS One, 2017. **12**(8): p. e0182786.
103. Forero, A., et al., *Expression of the MHC Class II Pathway in Triple-Negative Breast Cancer Tumor Cells Is Associated with a Good Prognosis and Infiltrating Lymphocytes.* Cancer Immunol Res, 2016. **4**(5): p. 390-9.
104. Jin, M.-Z. and W.-L. Jin, *The updated landscape of tumor microenvironment and drug repurposing.* Signal Transduction and Targeted Therapy, 2020. **5**(1): p. 166.
105. Giraldo, N.A., et al., *The clinical role of the TME in solid cancer.* British Journal of Cancer, 2019. **120**(1): p. 45-53.
106. Galon, J. and D. Bruni, *Approaches to treat immune hot, altered and cold tumours with combination immunotherapies.* Nature Reviews Drug Discovery, 2019. **18**(3): p. 197-218.

107. Nagarsheth, N., M.S. Wicha, and W. Zou, *Chemokines in the cancer microenvironment and their relevance in cancer immunotherapy.* Nat Rev Immunol, 2017. **17**(9): p. 559-572.
108. Sharma, P., et al., *Primary, Adaptive, and Acquired Resistance to Cancer Immunotherapy.* Cell, 2017. **168**(4): p. 707-723.
109. Spranger, S., R. Bao, and T.F. Gajewski, *Melanoma-intrinsic beta-catenin signalling prevents anti-tumour immunity.* Nature, 2015. **523**(7559): p. 231-5.
110. Spranger, S. and T.F. Gajewski, *Impact of oncogenic pathways on evasion of antitumour immune responses.* Nat Rev Cancer, 2018. **18**(3): p. 139-147.
111. Li, X., et al., *WNT/β-Catenin Signaling Pathway Regulating T Cell-Inflammation in the Tumor Microenvironment.* Front Immunol, 2019. **10**: p. 2293.
112. Spranger, S., R. Bao, and T.F. Gajewski, *Melanoma-intrinsic β-catenin signalling prevents anti-tumour immunity.* Nature, 2015. **523**(7559): p. 231-5.
113. Ramos-Casals, M., et al., *Immune-related adverse events of checkpoint inhibitors.* Nature Reviews Disease Primers, 2020. **6**(1): p. 38.
114. Wright, J.J., A.C. Powers, and D.B. Johnson, *Endocrine toxicities of immune checkpoint inhibitors.* Nature Reviews Endocrinology, 2021. **17**(7): p. 389-399.
115. Kubli, S.P., et al., *Beyond immune checkpoint blockade: emerging immunological strategies.* Nature Reviews Drug Discovery, 2021. **20**(12): p. 899-919.
116. Schmid, P., et al., *Atezolizumab and Nab-Paclitaxel in Advanced Triple-Negative Breast Cancer.* New England Journal of Medicine, 2018. **379**(22): p. 2108-2121.
117. Emens, L.A., et al., *LBA16 IMpassion130: Final OS analysis from the pivotal phase III study of atezolizumab + nab-paclitaxel vs placebo + nab-paclitaxel in previously untreated locally advanced or metastatic triple-negative breast cancer.* Annals of Oncology, 2020. **31**: p. S1148-S1148.
118. *Roche provides update on Tecentriq US indication for PD-L1-positive, metastatic triple-negative breast cancer*. 2021 [cited 2021 27 August]; Available from: https://www.roche.com/media/releases/med-cor-2021-08-27.htm.
119. Cortes, J., et al., *Pembrolizumab plus chemotherapy versus placebo plus chemotherapy for previously untreated locally recurrent inoperable or metastatic triple-negative breast cancer (KEYNOTE-355): a randomised, placebo-controlled, double-blind, phase 3 clinical trial.* Lancet, 2020. **396**(10265): p. 1817-1828.
120. Cortes, J., et al., *LBA16 KEYNOTE-355: Final results from a randomized, double-blind phase III study of first-line pembrolizumab + chemotherapy vs placebo + chemotherapy for metastatic TNBC.* Annals of Oncology, 2021. **32**: p. S1289-S1290.
121. Schmid, P., et al., *Pembrolizumab for Early Triple-Negative Breast Cancer.* New England Journal of Medicine, 2020. **382**(9): p. 810-821.
122. Schmid, P., et al., *VP7-2021: KEYNOTE-522: Phase III study of neoadjuvant pembrolizumab + chemotherapy vs. placebo + chemotherapy, followed by adjuvant pembrolizumab vs. placebo for early-stage TNBC.* Annals of Oncology, 2021. **32**(9): p. 1198-1200.
123. Rady, I., et al., *Cancer preventive and therapeutic effects of EGCG, the major polyphenol in green tea.* Egyptian Journal of Basic and Applied Sciences, 2018. **5**(1): p. 1-23.

124. Namal Senanayake, S.P.J., *Green tea extract: Chemistry, antioxidant properties and food applications – A review.* Journal of Functional Foods, 2013. **5**(4): p. 1529-1541.
125. Hayakawa, S., et al., *Anti-Cancer Effects of Green Tea Epigallocatchin-3-Gallate and Coffee Chlorogenic Acid.* Molecules, 2020. **25**(19).
126. Chen, D., et al., *EGCG, green tea polyphenols and their synthetic analogs and prodrugs for human cancer prevention and treatment.* Adv Clin Chem, 2011. **53**: p. 155-77.
127. Bimonte, S., et al., *Current shreds of evidence on the anticancer role of EGCG in triple negative breast cancer: an update of the current state of knowledge.* Infectious Agents and Cancer, 2020. **15**(1): p. 2.
128. Zan, L., et al., *Epigallocatechin gallate (EGCG) suppresses growth and tumorigenicity in breast cancer cells by downregulation of miR-25.* Bioengineered, 2019. **10**(1): p. 374-382.
129. Fu, J.D., et al., *Effects of EGCG on proliferation and apoptosis of gastric cancer SGC7901 cells via down-regulation of HIF-1α and VEGF under a hypoxic state.* Eur Rev Med Pharmacol Sci, 2019. **23**(1): p. 155-161.
130. Gu, J.W., et al., *EGCG, a major green tea catechin suppresses breast tumor angiogenesis and growth via inhibiting the activation of HIF-1α and NFκB, and VEGF expression.* Vasc Cell, 2013. **5**(1): p. 9.
131. Braicu, C., et al., *Epigallocatechin-3-Gallate (EGCG) inhibits cell proliferation and migratory behaviour of triple negative breast cancer cells.* J Nanosci Nanotechnol, 2013. **13**(1): p. 632-7.
132. Hong, O.Y., et al., *Epigallocatechin gallate inhibits the growth of MDA-MB-231 breast cancer cells via inactivation of the β-catenin signaling pathway.* Oncol Lett, 2017. **14**(1): p. 441-446.
133. Pal, D., et al., *Epigallocatechin gallate in combination with eugenol or amarogentin shows synergistic chemotherapeutic potential in cervical cancer cell line.* J Cell Physiol, 2018. **234**(1): p. 825-836.
134. Khan, M.A., et al., *(-)-Epigallocatechin-3-gallate reverses the expression of various tumor-suppressor genes by inhibiting DNA methyltransferases and histone deacetylases in human cervical cancer cells.* Oncol Rep, 2015. **33**(4): p. 1976-1984.
135. Amatori, S., et al., *DNA demethylating antineoplastic strategies: a comparative point of view.* Genes Cancer, 2010. **1**(3): p. 197-209.
136. Yu, J., et al., *DNA methyltransferase expression in triple-negative breast cancer predicts sensitivity to decitabine.* J Clin Invest, 2018. **128**(6): p. 2376-2388.
137. Karahoca, M. and R.L. Momparler, *Pharmacokinetic and pharmacodynamic analysis of 5-aza-2'-deoxycytidine (decitabine) in the design of its dose-schedule for cancer therapy.* Clin Epigenetics, 2013. **5**(1): p. 3.
138. Patel, A.A., et al., *Cedazuridine/decitabine: from preclinical to clinical development in myeloid malignancies.* Blood Advances, 2021. **5**(8): p. 2264-2271.
139. Morel, D., et al., *Combining epigenetic drugs with other therapies for solid tumours — past lessons and future promise.* Nature Reviews Clinical Oncology, 2020. **17**(2): p. 91-107.

140. Oki, Y., E. Aoki, and J.-P.J. Issa, *Decitabine—Bedside to bench.* Critical Reviews in Oncology/Hematology, 2007. **61**(2): p. 140-152.
141. Huang, K.C., et al., *Decitabine Augments Chemotherapy-Induced PD-L1 Upregulation for PD-L1 Blockade in Colorectal Cancer.* Cancers (Basel), 2020. **12**(2).
142. Paulson, K.E., et al., *Alterations of the HBP1 transcriptional repressor are associated with invasive breast cancer.* Cancer Res, 2007. **67**(13): p. 6136-45.
143. Sampson, E.M., et al., *Negative regulation of the Wnt-beta-catenin pathway by the transcriptional repressor HBP1.* Embo j, 2001. **20**(16): p. 4500-11.
144. Li, M.-J., et al., *Green tea compounds in breast cancer prevention and treatment.* World journal of clinical oncology, 2014. **5**(3): p. 520-528.
145. Sun, C.L., et al., *Green tea, black tea and breast cancer risk: a meta-analysis of epidemiological studies.* Carcinogenesis, 2006. **27**(7): p. 1310-5.
146. Stuart, E.C., M.J. Scandlyn, and R.J. Rosengren, *Role of epigallocatechin gallate (EGCG) in the treatment of breast and prostate cancer.* Life Sciences, 2006. **79**(25): p. 2329-2336.
147. Mereles, D. and W. Hunstein, *Epigallocatechin-3-gallate (EGCG) for Clinical Trials: More Pitfalls than Promises?* International Journal of Molecular Sciences, 2011. **12**(9).
148. Fang, M.Z., et al., *Tea polyphenol (-)-epigallocatechin-3-gallate inhibits DNA methyltransferase and reactivates methylation-silenced genes in cancer cell lines.* Cancer Res, 2003. **63**(22): p. 7563-70.
149. Pan, K., et al., *HBP1-mediated transcriptional regulation of DNA methyltransferase 1 and its impact on cell senescence.* Mol Cell Biol, 2013. **33**(5): p. 887-903.
150. Quan, H., et al., *Hepatitis C virus core protein epigenetically silences SFRP1 and enhances HCC aggressiveness by inducing epithelial-mesenchymal transition.* Oncogene, 2014. **33**(22): p. 2826-35.
151. Dees, C., et al., *The Wnt antagonists DKK1 and SFRP1 are downregulated by promoter hypermethylation in systemic sclerosis.* Ann Rheum Dis, 2014. **73**(6): p. 1232-9.
152. Wang, Y., et al., *Green tea epigallocatechin-3-gallate (EGCG) promotes neural progenitor cell proliferation and sonic hedgehog pathway activation during adult hippocampal neurogenesis.* Mol Nutr Food Res, 2012. **56**(8): p. 1292-303.
153. Suganuma, M., et al., *Green tea and cancer chemoprevention.* Mutat Res, 1999. **428**(1-2): p. 339-44.
154. Leone, G., et al., *Epigenetic treatment of myelodysplastic syndromes and acute myeloid leukemias.* Current medicinal chemistry, 2008. **15**(13): p. 1274-1287.
155. Reddy, K.B., *Triple-negative breast cancers: an updated review on treatment options.* Curr Oncol, 2011. **18**(4): p. e173-9.
156. Allred, D.C., et al., *Prognostic and predictive factors in breast cancer by immunohistochemical analysis.* Mod Pathol, 1998. **11**(2): p. 155-68.
157. Liberzon, A., et al., *Molecular signatures database (MSigDB) 3.0.* Bioinformatics, 2011. **27**(12): p. 1739-40.

158. Cerami, E., et al., *The cBio cancer genomics portal: an open platform for exploring multidimensional cancer genomics data.* Cancer Discov, 2012. **2**(5): p. 401-4.
159. Gao, J., et al., *Integrative analysis of complex cancer genomics and clinical profiles using the cBioPortal.* Sci Signal, 2013. **6**(269): p. pl1.
160. Curtis, C., et al., *The genomic and transcriptomic architecture of 2,000 breast tumours reveals novel subgroups.* Nature, 2012. **486**(7403): p. 346-52.
161. Pereira, B., et al., *The somatic mutation profiles of 2,433 breast cancers refines their genomic and transcriptomic landscapes.* Nat Commun, 2016. **7**: p. 11479.
162. Rueda, O.M., et al., *Dynamics of breast-cancer relapse reveal late-recurring ER-positive genomic subgroups.* Nature, 2019. **567**(7748): p. 399-404.
163. Ciriello, G., et al., *Comprehensive Molecular Portraits of Invasive Lobular Breast Cancer.* Cell, 2015. **163**(2): p. 506-19.
164. Zeng, L., J.M.P. Holly, and C.M. Perks, *Effects of Physiological Levels of the Green Tea Extract Epigallocatechin-3-Gallate on Breast Cancer Cells.* Frontiers in Endocrinology, 2014. **5**.
165. Öz, S., et al., *Quantitative determination of decitabine incorporation into DNA and its effect on mutation rates in human cancer cells.* Nucleic Acids Res, 2014. **42**(19): p. e152.
166. Lambert, J.D., et al., *Epigallocatechin-3-gallate is absorbed but extensively glucuronidated following oral administration to mice.* J Nutr, 2003. **133**(12): p. 4172-7.
167. Lambert, J.D., et al., *Dose-dependent levels of epigallocatechin-3-gallate in human colon cancer cells and mouse plasma and tissues.* Drug Metabolism and Disposition, 2006. **34**(1): p. 8-11.
168. Kim, S., et al., *Plasma and tissue levels of tea catechins in rats and mice during chronic consumption of green tea polyphenols.* Nutr Cancer, 2000. **37**(1): p. 41-8.
169. Chow, H.H., et al., *Phase I pharmacokinetic study of tea polyphenols following single-dose administration of epigallocatechin gallate and polyphenon E.* Cancer Epidemiol Biomarkers Prev, 2001. **10**(1): p. 53-8.
170. Suganuma, M., et al., *Wide distribution of [3H](-)-epigallocatechin gallate, a cancer preventive tea polyphenol, in mouse tissue.* Carcinogenesis, 1998. **19**(10): p. 1771-6.
171. Chow, H.H., et al., *Effects of dosing condition on the oral bioavailability of green tea catechins after single-dose administration of Polyphenon E in healthy individuals.* Clin Cancer Res, 2005. **11**(12): p. 4627-33.
172. Chow, H.H., et al., *Pharmacokinetics and safety of green tea polyphenols after multiple-dose administration of epigallocatechin gallate and polyphenon E in healthy individuals.* Clin Cancer Res, 2003. **9**(9): p. 3312-9.
173. Lemaire, M., et al., *Inhibition of cytidine deaminase by zebularine enhances the antineoplastic action of 5-aza-2'-deoxycytidine.* Cancer Chemother Pharmacol, 2009. **63**(3): p. 411-6.
174. Lemaire, M., et al., *Importance of dose-schedule of 5-aza-2'-deoxycytidine for epigenetic therapy of cancer.* BMC Cancer, 2008. **8**(1): p. 128.

175. van Groeningen, C.J., et al., *Phase I and pharmacokinetic study of 5-aza-2'-deoxycytidine (NSC 127716) in cancer patients.* Cancer Res, 1986. **46**(9): p. 4831-6.
176. Schrump, D.S., et al., *Phase I study of decitabine-mediated gene expression in patients with cancers involving the lungs, esophagus, or pleura.* Clin Cancer Res, 2006. **12**(19): p. 5777-85.
177. Wijermans, P., et al., *Low-dose 5-aza-2'-deoxycytidine, a DNA hypomethylating agent, for the treatment of high-risk myelodysplastic syndrome: a multicenter phase II study in elderly patients.* J Clin Oncol, 2000. **18**(5): p. 956-62.
178. Terse, P., et al., *Subchronic oral toxicity study of decitabine in combination with tetrahydrouridine in CD-1 mice.* Int J Toxicol, 2014. **33**(2): p. 75-85.
179. Smith, J.L., et al., *A MicroRNA Screen Identifies the Wnt Signaling Pathway as a Regulator of the Interferon Response during Flavivirus Infection.* Journal of virology, 2017. **91**(8): p. e02388-16.
180. Yang, P., et al., *The cytosolic nucleic acid sensor LRRFIP1 mediates the production of type I interferon via a β-catenin-dependent pathway.* Nature Immunology, 2010. **11**: p. 487.
181. Qin, Y., et al., *TRIM9 short isoform preferentially promotes DNA and RNA virus-induced production of type I interferon by recruiting GSK3β to TBK1.* Cell research, 2016. **26**(5): p. 613-628.
182. McCarthy, D.J. and G.K. Smyth, *Testing significance relative to a fold-change threshold is a TREAT.* Bioinformatics, 2009. **25**(6): p. 765-71.
183. Dalman, M.R., et al., *Fold change and p-value cutoffs significantly alter microarray interpretations.* BMC Bioinformatics, 2012. **13**(2): p. S11.
184. Axelrod, M.L., et al., *Biological Consequences of MHC-II Expression by Tumor Cells in Cancer.* Clinical Cancer Research, 2019. **25**(8): p. 2392-2402.
185. Forero, A., et al., *Expression of the MHC Class II Pathway in Triple-Negative Breast Cancer Tumor Cells Is Associated with a Good Prognosis and Infiltrating Lymphocytes.* Cancer Immunology Research, 2016. **4**(5): p. 390-399.
186. Park, I.A., et al., *Expression of the MHC class II in triple-negative breast cancer is associated with tumor-infiltrating lymphocytes and interferon signaling.* PLOS ONE, 2017. **12**(8): p. e0182786.
187. Roemer, M.G.M., et al., *Major Histocompatibility Complex Class II and Programmed Death Ligand 1 Expression Predict Outcome After Programmed Death 1 Blockade in Classic Hodgkin Lymphoma.* Journal of clinical oncology : official journal of the American Society of Clinical Oncology, 2018. **36**(10): p. 942-950.
188. Rodig, S.J., et al., *MHC proteins confer differential sensitivity to CTLA-4 and PD-1 blockade in untreated metastatic melanoma.* Science Translational Medicine, 2018. **10**(450): p. eaar3342.
189. Fortin, J.S., M. Cloutier, and J. Thibodeau, *Exposing the Specific Roles of the Invariant Chain Isoforms in Shaping the MHC Class II Peptidome.* Front Immunol, 2013. **4**: p. 443.
190. Ferrington, D.A. and D.S. Gregerson, *Immunoproteasomes: structure, function, and antigen presentation.* Prog Mol Biol Transl Sci, 2012. **109**: p. 75-112.

191. Li, B., et al., *Induction of a specific CD8+ T-cell response to cancer/testis antigens by demethylating pre-treatment against osteosarcoma.* Oncotarget, 2014. **5**(21): p. 10791-802.
192. Raza, A., et al., *Unleashing the immune response to NY-ESO-1 cancer testis antigen as a potential target for cancer immunotherapy.* J Transl Med, 2020. **18**(1): p. 140.
193. Goel, S., et al., *CDK4/6 inhibition triggers anti-tumour immunity.* Nature, 2017. **548**: p. 471.
194. Ganesh, S., et al., *RNAi-Mediated beta-Catenin Inhibition Promotes T Cell Infiltration and Antitumor Activity in Combination with Immune Checkpoint Blockade.* Mol Ther, 2018. **26**(11): p. 2567-2579.
195. J. Luke, J., et al., *WNT/β-catenin Pathway Activation Correlates with Immune Exclusion across Human Cancers*. 2019. clincanres.1942.2018.
196. Kalathil, S.G., et al., *Augmentation of IFN-γ+ CD8+ T cell responses correlates with survival of HCC patients on sorafenib therapy.* JCI Insight, 2019. **4**(15).
197. Trapani, J.A. and M.J. Smyth, *Functional significance of the perforin/granzyme cell death pathway.* Nat Rev Immunol, 2002. **2**(10): p. 735-47.
198. Zitvogel, L. and G. Kroemer, *Targeting PD-1/PD-L1 interactions for cancer immunotherapy.* Oncoimmunology, 2012. **1**(8): p. 1223-1225.
199. Sharma, P. and J.P. Allison, *The future of immune checkpoint therapy.* Science, 2015. **348**(6230): p. 56-61.
200. Sakuishi, K., et al., *Targeting Tim-3 and PD-1 pathways to reverse T cell exhaustion and restore anti-tumor immunity.* J Exp Med, 2010. **207**(10): p. 2187-94.
201. Seidel, J.A., A. Otsuka, and K. Kabashima, *Anti-PD-1 and Anti-CTLA-4 Therapies in Cancer: Mechanisms of Action, Efficacy, and Limitations.* Front Oncol, 2018. **8**: p. 86.
202. Garcia-Diaz, A., et al., *Interferon Receptor Signaling Pathways Regulating PD-L1 and PD-L2 Expression.* Cell Rep, 2017. **19**(6): p. 1189-1201.
203. Jiang, W., et al., *Exhausted CD8+T Cells in the Tumor Immune Microenvironment: New Pathways to Therapy.* Frontiers in Immunology, 2021. **11**(3739).
204. Ayers, M., et al., *IFN-γ–related mRNA profile predicts clinical response to PD-1 blockade.* The Journal of Clinical Investigation, 2017. **127**(8): p. 2930-2940.
205. Trujillo, J.A., et al., *T Cell-Inflamed versus Non-T Cell-Inflamed Tumors: A Conceptual Framework for Cancer Immunotherapy Drug Development and Combination Therapy Selection.* Cancer Immunol Res, 2018. **6**(9): p. 990-1000.
206. DuPre, S.A. and K.W. Hunter, Jr., *Murine mammary carcinoma 4T1 induces a leukemoid reaction with splenomegaly: association with tumor-derived growth factors.* Exp Mol Pathol, 2007. **82**(1): p. 12-24.
207. Mall, C., et al., *Repeated PD-1/PD-L1 monoclonal antibody administration induces fatal xenogeneic hypersensitivity reactions in a murine model of breast cancer.* Oncoimmunology, 2016. **5**(2): p. e1075114.
208. Ju, X., et al., *Regulation of PD-L1 expression in cancer and clinical implications in immunotherapy.* Am J Cancer Res, 2020. **10**(1): p. 1-11.

209. Wang, X. and M. Li, *Correlate tumor mutation burden with immune signatures in human cancers.* BMC Immunology, 2019. **20**(1): p. 4.
210. Tolba, M.F. and H.A. Omar, *Immunotherapy, an evolving approach for the management of triple negative breast cancer: Converting non-responders to responders.* Crit Rev Oncol Hematol, 2018. **122**: p. 202-207.
211. Emens, L.A., *Breast Cancer Immunotherapy: Facts and Hopes.* Clin Cancer Res, 2018. **24**(3): p. 511-520.
212. Savas, P. and S. Loi, *Expanding the Role for Immunotherapy in Triple-Negative Breast Cancer.* Cancer Cell, 2020. **37**(5): p. 623-624.
213. Qin, Y., et al., *Inhibition of histone lysine-specific demethylase 1 elicits breast tumor immunity and enhances antitumor efficacy of immune checkpoint blockade.* Oncogene, 2019. **38**(3): p. 390-405.
214. Anastas, J.N. and R.T. Moon, *WNT signalling pathways as therapeutic targets in cancer.* Nat Rev Cancer, 2013. **13**(1): p. 11-26.
215. Lin, S.Y., et al., *Beta-catenin, a novel prognostic marker for breast cancer: its roles in cyclin D1 expression and cancer progression.* Proc Natl Acad Sci U S A, 2000. **97**(8): p. 4262-6.
216. Zhu, J., et al., *Wnt/β-catenin pathway mediates (-)-Epigallocatechin-3-gallate (EGCG) inhibition of lung cancer stem cells.* Biochem Biophys Res Commun, 2017. **482**(1): p. 15-21.
217. Oh, S., et al., *Green tea polyphenol EGCG suppresses Wnt/β-catenin signaling by promoting GSK-3β- and PP2A-independent β-catenin phosphorylation/degradation.* BioFactors (Oxford, England), 2014. **40**(6): p. 586-595.
218. Li, K., et al., *Sequential combination of decitabine and idarubicin synergistically enhances anti-leukemia effect followed by demethylating Wnt pathway inhibitor promoters and downregulating Wnt pathway nuclear target.* Journal of Translational Medicine, 2014. **12**(1): p. 167.
219. Gao, J., et al., *Loss of IFN-gamma Pathway Genes in Tumor Cells as a Mechanism of Resistance to Anti-CTLA-4 Therapy.* Cell, 2016. **167**(2): p. 397-404 e9.
220. Chiappinelli, K.B., et al., *Inhibiting DNA Methylation Causes an Interferon Response in Cancer via dsRNA Including Endogenous Retroviruses.* Cell, 2015. **162**(5): p. 974-86.
221. Chinnasamy, N., et al., *A TCR targeting the HLA-A*0201-restricted epitope of MAGE-A3 recognizes multiple epitopes of the MAGE-A antigen superfamily in several types of cancer.* J Immunol, 2011. **186**(2): p. 685-96.
222. Li, X., et al., *Decitabine: a promising epi-immunotherapeutic agent in solid tumors.* Expert Rev Clin Immunol, 2015. **11**(3): p. 363-75.
223. Majumder, P. and J.M. Boss, *DNA methylation dysregulates and silences the HLA-DQ locus by altering chromatin architecture.* Genes Immun, 2011. **12**(4): p. 291-9.
224. Campoli, M. and S. Ferrone, *HLA antigen changes in malignant cells: epigenetic mechanisms and biologic significance.* Oncogene, 2008. **27**(45): p. 5869-85.
225. Hammerl, D., et al., *Breast cancer genomics and immuno-oncological markers to guide immune therapies.* Semin Cancer Biol, 2018. **52**(Pt 2): p. 178-188.

226. Kwa, M.J. and S. Adams, *Checkpoint inhibitors in triple-negative breast cancer (TNBC): Where to go from here.* Cancer, 2018. **124**(10): p. 2086-2103.
227. Hammerl, D., et al., *Spatial immunophenotypes predict response to anti-PD1 treatment and capture distinct paths of T cell evasion in triple negative breast cancer.* Nature Communications, 2021. **12**(1): p. 5668.
228. Sweis, R.F., et al., *Molecular Drivers of the Non-T-cell-Inflamed Tumor Microenvironment in Urothelial Bladder Cancer.* Cancer Immunol Res, 2016. **4**(7): p. 563-8.
229. Shah, K.V., et al., *CTLA-4 is a direct target of Wnt/beta-catenin signaling and is expressed in human melanoma tumors.* J Invest Dermatol, 2008. **128**(12): p. 2870-9.
230. Crew, K.D., et al., *Phase IB randomized, double-blinded, placebo-controlled, dose escalation study of polyphenon E in women with hormone receptor-negative breast cancer.* Cancer Prev Res (Phila), 2012. **5**(9): p. 1144-54.
231. Lovera, J., et al., *Polyphenon E, non-futile at neuroprotection in multiple sclerosis but unpredictably hepatotoxic: Phase I single group and phase II randomized placebo-controlled studies.* J Neurol Sci, 2015. **358**(1-2): p. 46-52.
232. Kantarjian, H.M., et al., *Multicenter, randomized, open-label, phase III trial of decitabine versus patient choice, with physician advice, of either supportive care or low-dose cytarabine for the treatment of older patients with newly diagnosed acute myeloid leukemia.* J Clin Oncol, 2012. **30**(21): p. 2670-7.
233. Cohen, J.V. and H.M. Kluger, *Systemic Immunotherapy for the Treatment of Brain Metastases.* Front Oncol, 2016. **6**: p. 49.
234. Natsume, A., et al., *The DNA demethylating agent 5-aza-2'-deoxycytidine activates NY-ESO-1 antigenicity in orthotopic human glioma.* Int J Cancer, 2008. **122**(11): p. 2542-53.
235. Ecke, I., et al., *Antitumor effects of a combined 5-aza-2'deoxycytidine and valproic acid treatment on rhabdomyosarcoma and medulloblastoma in Ptch mutant mice.* Cancer Res, 2009. **69**(3): p. 887-95.
236. Mahfouz, R.Z., et al., *Increased CDA expression/activity in males contributes to decreased cytidine analog half-life and likely contributes to worse outcomes with 5-azacytidine or decitabine therapy.* Clin Cancer Res, 2013. **19**(4): p. 938-48.
237. Hollenbach, P.W., et al., *A comparison of azacitidine and decitabine activities in acute myeloid leukemia cell lines.* PLoS One, 2010. **5**(2): p. e9001.
238. Wen, B., et al., *Indirect comparison of azacitidine and decitabine for the therapy of elderly patients with acute myeloid leukemia: a systematic review and network meta-analysis.* Experimental Hematology & Oncology, 2020. **9**(1): p. 3.
239. Ma, J. and Z. Ge, *Comparison Between Decitabine and Azacitidine for Patients With Acute Myeloid Leukemia and Higher-Risk Myelodysplastic Syndrome: A Systematic Review and Network Meta-Analysis.* Frontiers in Pharmacology, 2021. **12**(1919).
240. Lübbert, M., et al., *Valproate and Retinoic Acid in Combination With Decitabine in Elderly Nonfit Patients With Acute Myeloid Leukemia: Results of a Multicenter, Randomized, 2 × 2, Phase II Trial.* Journal of Clinical Oncology, 2020. **38**(3): p. 257-270.

241. Zavras, P.D., et al., *Clinical Trials Assessing Hypomethylating Agents Combined with Other Therapies: Causes for Failure and Potential Solutions.* Clinical Cancer Research, 2021. **27**(24): p. 6653-6661.
242. Terracina, K.P., et al., *DNA methyltransferase inhibition increases efficacy of adoptive cellular immunotherapy of murine breast cancer.* Cancer Immunol Immunother, 2016. **65**(9): p. 1061-73.
243. Luo, T., et al., *(-)-Epigallocatechin gallate sensitizes breast cancer cells to paclitaxel in a murine model of breast carcinoma.* Breast Cancer Research, 2010. **12**(1): p. R8.
244. Kitz, J., et al., *Circulating Tumor Cell Analysis in Preclinical Mouse Models of Metastasis.* Diagnostics (Basel), 2018. **8**(2).
245. Mu, Z., et al., *Detection and Characterization of Circulating Tumor Associated Cells in Metastatic Breast Cancer.* Int J Mol Sci, 2016. **17**(10).
246. Lee, S.J., et al., *Circulating tumor cells are predictive of poor response to chemotherapy in metastatic gastric cancer.* Int J Biol Markers, 2015. **30**(4): p. e382-6.
247. Magbanua, M.J., et al., *Circulating tumor cell analysis in metastatic triple-negative breast cancers.* Clin Cancer Res, 2015. **21**(5): p. 1098-105.
248. Lopresti, A., et al., *Sensitive and easy screening for circulating tumor cells by flow cytometry*. JCI Insight, 2019. **5**(14).
249. Zhang, Y., et al., *Single-cell RNA sequencing in cancer research.* Journal of Experimental & Clinical Cancer Research, 2021. **40**(1): p. 81.
250. Wu, F., et al., *Single-cell profiling of tumor heterogeneity and the microenvironment in advanced non-small cell lung cancer.* Nature Communications, 2021. **12**(1): p. 2540.
251. Talmadge, J.E., M. Donkor, and E. Scholar, *Inflammatory cell infiltration of tumors: Jekyll or Hyde.* Cancer Metastasis Rev, 2007. **26**(3-4): p. 373-400.
252. Bindea, G., et al., *Spatiotemporal dynamics of intratumoral immune cells reveal the immune landscape in human cancer.* Immunity, 2013. **39**(4): p. 782-95.
253. Fridman, W.H., et al., *The immune contexture in human tumours: impact on clinical outcome.* Nature Reviews Cancer, 2012. **12**(4): p. 298-306.
254. Goswami, S., et al., *Immune profiling of human tumors identifies CD73 as a combinatorial target in glioblastoma.* Nature Medicine, 2020. **26**(1): p. 39-46.
255. Chung, W., et al., *Single-cell RNA-seq enables comprehensive tumour and immune cell profiling in primary breast cancer.* Nature Communications, 2017. **8**(1): p. 15081.
256. Baylin, S.B. and P.A. Jones, *A decade of exploring the cancer epigenome — biological and translational implications.* Nature Reviews Cancer, 2011. **11**(10): p. 726-734.
257. Cheng, Y., et al., *Targeting epigenetic regulators for cancer therapy: mechanisms and advances in clinical trials.* Signal Transduction and Targeted Therapy, 2019. **4**(1): p. 62.
258. Shen, H. and P.W. Laird, *Interplay between the cancer genome and epigenome.* Cell, 2013. **153**(1): p. 38-55.

259. Baylin, S.B. and P.A. Jones, *A decade of exploring the cancer epigenome - biological and translational implications.* Nat Rev Cancer, 2011. **11**(10): p. 726-34.
260. Merlo, A., et al., *5' CpG island methylation is associated with transcriptional silencing of the tumour suppressor p16/CDKN2/MTS1 in human cancers.* Nat Med, 1995. **1**(7): p. 686-92.
261. Ocker, M. and R. Schneider-Stock, *Histone deacetylase inhibitors: signalling towards p21cip1/waf1.* Int J Biochem Cell Biol, 2007. **39**(7-8): p. 1367-74.
262. Völkel, P. and P.O. Angrand, *The control of histone lysine methylation in epigenetic regulation.* Biochimie, 2007. **89**(1): p. 1-20.
263. Calin, G.A., et al., *Human microRNA genes are frequently located at fragile sites and genomic regions involved in cancers.* Proc Natl Acad Sci U S A, 2004. **101**(9): p. 2999-3004.
264. Kasinski, A.L. and F.J. Slack, *Epigenetics and genetics. MicroRNAs en route to the clinic: progress in validating and targeting microRNAs for cancer therapy.* Nat Rev Cancer, 2011. **11**(12): p. 849-64.
265. Andersen, G.B. and J. Tost, *Circulating miRNAs as Biomarker in Cancer.* Recent Results Cancer Res, 2020. **215**: p. 277-298.
266. Zhuang, J., et al., *Perspectives on the Role of Histone Modification in Breast Cancer Progression and the Advanced Technological Tools to Study Epigenetic Determinants of Metastasis.* Front Genet, 2020. **11**: p. 603552.
267. Zhang, L. and X. Long, *Association of BRCA1 promoter methylation with sporadic breast cancers: Evidence from 40 studies.* Scientific Reports, 2015. **5**(1): p. 17869.
268. O'Leary, K., A. Shia, and P. Schmid, *Epigenetic Regulation of EMT in Non-Small Cell Lung Cancer.* Current Cancer Drug Targets, 2018. **18**(1): p. 89-96.
269. Kashiwagi, S., et al., *Significance of E-cadherin expression in triple-negative breast cancer.* Br J Cancer, 2010. **103**(2): p. 249-55.
270. Kagara, N., et al., *Epigenetic regulation of cancer stem cell genes in triple-negative breast cancer.* Am J Pathol, 2012. **181**(1): p. 257-67.
271. Tang, Z., et al., *HDAC1 triggers the proliferation and migration of breast cancer cells via upregulation of interleukin-8.* Biological Chemistry, 2017. **398**(12): p. 1347-1356.
272. Witt, A.E., et al., *Identification of a cancer stem cell-specific function for the histone deacetylases, HDAC1 and HDAC7, in breast and ovarian cancer.* Oncogene, 2017. **36**(12): p. 1707-1720.
273. Menbari, M.N., et al., *Association of HDAC8 Expression with Pathological Findings in Triple Negative and Non-Triple Negative Breast Cancer: Implications for Diagnosis.* Iran Biomed J, 2020. **24**(5): p. 288-94.
274. Ahmad, A., et al., *Functional role of miR-10b in tamoxifen resistance of ER-positive breast cancer cells through down-regulation of HDAC4.* BMC Cancer, 2015. **15**(1): p. 540.
275. Wang, B., et al., *A dual role of miR-22 modulated by RelA/p65 in resensitizing fulvestrant-resistant breast cancer cells to fulvestrant by targeting FOXP1 and HDAC4 and constitutive acetylation of p53 at Lys382.* Oncogenesis, 2018. **7**(7): p. 54.

276. Li, N., et al., *MiR-155 promotes colitis-associated intestinal fibrosis by targeting HBP1/Wnt/β-catenin signalling pathway.* J Cell Mol Med, 2021. **25**(10): p. 4765-4775.
277. Ciesielski, O., M. Biesiekierska, and A. Balcerczyk, *Epigallocatechin-3-gallate (EGCG) Alters Histone Acetylation and Methylation and Impacts Chromatin Architecture Profile in Human Endothelial Cells.* Molecules, 2020. **25**(10).
278. Soundararajan, R., et al., *Targeting the Interplay between Epithelial-to-Mesenchymal-Transition and the Immune System for Effective Immunotherapy.* Cancers (Basel), 2019. **11**(5).
279. Lou, Y., et al., *Epithelial-Mesenchymal Transition Is Associated with a Distinct Tumor Microenvironment Including Elevation of Inflammatory Signals and Multiple Immune Checkpoints in Lung Adenocarcinoma.* Clin Cancer Res, 2016. **22**(14): p. 3630-42.
280. Chen, L., et al., *Metastasis is regulated via microRNA-200/ZEB1 axis control of tumour cell PD-L1 expression and intratumoral immunosuppression.* Nat Commun, 2014. **5**: p. 5241.
281. Low-Marchelli, J.M., et al., *Twist1 induces CCL2 and recruits macrophages to promote angiogenesis.* Cancer Res, 2013. **73**(2): p. 662-71.
282. Hsu, D.S., et al., *Acetylation of snail modulates the cytokinome of cancer cells to enhance the recruitment of macrophages.* Cancer Cell, 2014. **26**(4): p. 534-48.
283. Boulding, T., et al., *LSD1 activation promotes inducible EMT programs and modulates the tumour microenvironment in breast cancer.* Scientific Reports, 2018. **8**(1): p. 73.
284. Cano, A., et al., *The transcription factor snail controls epithelial-mesenchymal transitions by repressing E-cadherin expression.* Nat Cell Biol, 2000. **2**(2): p. 76-83.
285. Lin, T., et al., *Requirement of the histone demethylase LSD1 in Snai1-mediated transcriptional repression during epithelial-mesenchymal transition.* Oncogene, 2010. **29**(35): p. 4896-904.
286. Dong, B., Z. Qiu, and Y. Wu, *Tackle Epithelial-Mesenchymal Transition With Epigenetic Drugs in Cancer.* Frontiers in Pharmacology, 2020. **11**(1889).
287. Koustas, E., et al., *The Resistance Mechanisms of Checkpoint Inhibitors in Solid Tumors.* Biomolecules, 2020. **10**(5).
288. Xue, J., et al., *Intrinsic β-catenin signaling suppresses CD8+ T-cell infiltration in colorectal cancer.* Biomedicine & Pharmacotherapy, 2019. **115**: p. 108921.
289. Lee, W.S., et al., *Combination of anti-angiogenic therapy and immune checkpoint blockade normalizes vascular-immune crosstalk to potentiate cancer immunity.* Experimental & Molecular Medicine, 2020. **52**(9): p. 1475-1485.
290. Pirola, L., O. Ciesielski, and A. Balcerczyk, *The Methylation Status of the Epigenome: Its Emerging Role in the Regulation of Tumor Angiogenesis and Tumor Growth, and Potential for Drug Targeting.* Cancers (Basel), 2018. **10**(8).
291. Thomas, R., et al., *NY-ESO-1 Based Immunotherapy of Cancer: Current Perspectives.* Front Immunol, 2018. **9**: p. 947.
292. Oshima, Y., et al., *NY-ESO-1 autoantibody as a tumor-specific biomarker for esophageal cancer: screening in 1969 patients with various cancers.* Journal of gastroenterology, 2016. **51**(1): p. 30-34.

293. Jäger, E., et al., *Simultaneous humoral and cellular immune response against cancer–testis antigen NY-ESO-1: definition of human histocompatibility leukocyte antigen (HLA)-A2–binding peptide epitopes.* The Journal of experimental medicine, 1998. **187**(2): p. 265-270.
294. Zarour, H.M., et al., *NY-ESO-1 encodes DRB1* 0401-restricted epitopes recognized by melanoma-reactive CD4+ T cells.* Cancer research, 2000. **60**(17): p. 4946-4952.
295. Zeng, G., et al., *CD4+ T cell recognition of MHC class II-restricted epitopes from NY-ESO-1 presented by a prevalent HLA DP4 allele: association with NY-ESO-1 antibody production.* Proceedings of the National Academy of Sciences, 2001. **98**(7): p. 3964-3969.
296. Odunsi, K., et al., *Epigenetic potentiation of NY-ESO-1 vaccine therapy in human ovarian cancer.* Cancer immunology research, 2014. **2**(1): p. 37-49.
297. Robbins, P.F., et al., *Tumor regression in patients with metastatic synovial cell sarcoma and melanoma using genetically engineered lymphocytes reactive with NY-ESO-1.* Journal of Clinical Oncology, 2011. **29**(7): p. 917.
298. Everson, R.G., et al., *Efficacy of systemic adoptive transfer immunotherapy targeting NY-ESO-1 for glioblastoma.* Neuro-oncology, 2015. **18**(3): p. 368-378.
299. Perica, K., et al., *Adoptive T cell immunotherapy for cancer.* Rambam Maimonides Med J, 2015. **6**(1): p. e0004.
300. Yang, J.C., *Toxicities Associated With Adoptive T-Cell Transfer for Cancer.* Cancer J, 2015. **21**(6): p. 506-9.